TITLE: LONG DISTANCE FUNCTIONAL COUPLING ASSOCIATED WITH EEG STATE CHANGES: *THE EXAMINATION OF PHASE AND AMPLITUDE SYNCHRONY OF NEURAL ASSEMBLIES ACROSS HEMISPHERES DURING REM AND NON-REM SLEEP ONSET.*

by

HANS VON GIZYCKI

A dissertation submitted to the Graduate Faculty in Psychology in partial fulfillment of the requirements for the degree of Doctor of Philosophy, The City University of New York

2008

This manuscript has been read and accepted for the
Graduate Faculty in Psychology in satisfaction of the
dissertation requirement for the degree of Doctor of Philosophy.

6/20/2008	Professor Arthur J. Spielman, Ph.D.
Date	Chair of Examining Committee
6/20/2008	Professor Joseph Glick, Ph.D.
Date	Executive Officer

Professor Arthur J. Spielman, Ph.D.

Professor Paul Glovinsky, Ph.D.

Professor Lucas Parra, Ph.D.
Supervision Committee

THE CITY UNIVERSITY OF NEW YORK

Abstract

TITLE: LONG DISTANCE FUNCTIONAL COUPLING ASSOCIATED WITH EEG STATE CHANGES: *THE EXAMINATION OF PHASE AND AMPLITUDE SYNCHRONY OF NEURAL ASSEMBLIES ACROSS HEMISPHERES DURING REM AND NON-REM SLEEP ONSET.*

by

HANS VON GIZYCKI

Adviser: Professor Arthur J. Spielman

Purpose: The innovation and importance of this study is that it assesses the functional relationship between hemispheric synchrony (phase and amplitude) and sleep onset. Our preliminary analysis of the pilot data demonstrates that there is an increase in inter-hemispheric phase synchrony and a decrease in amplitude synchrony during non-REM sleep onset (von Gizycki et al, 2007). The phase synchrony increase during sleep onset supports previous findings in hemispheric coherence research, however, the amplitude synchrony decreases does not. This can be explained by the fact that previous studies that examined hemispheric synchrony used such measures as cross correlation and coherence, and these widely used measures only provide a joint measure of amplitude and phase synchrony, therefore, the unique contribution of hemispheric amplitude at sleep onset could not be detected. We also will examine this effect during sleep onset REM periods in narcoleptic patients where we expect the results to be different than that of non-REM sleep onset. Additionally, prior to the analysis of this human data, I used data from an animal seizure synchrony model (von Gizycki et al, 2006) where hyper-synchrony (elicited epileptic events) is manipulated in order to test and validate phase and amplitude

synchrony measures. Therefore, we will further develop and test our findings that demonstrate that sleep onset produced changes in synchrony of neural assemblies across hemispheres does not just happen in the phase realm but also in the amplitude realm.

Methods: Phase synchrony methods that were employed will be the following, phase synchrony index, synchrony entropy index, and our proprietary method instantaneous phase synchrony distribution. The amplitude synchrony measures were the amplitude synchrony index, and the entropy amplitude index

Results and conclusions: Study 1, validated the synchrony methods with animal data because it was with synchrony methods it was possible to differentiate between two conditions baseline, and pre-seizure. Study 2, demonstrated that during the time course of sleep, there are linear changes and time locked changes in phase synchrony. In addition study 3, demonstrated that for narcoleptics there are synchrony changes that are only observable prior to a sleep onset REM nap during the waking state.

Table of Contents

List of Tables

List of Figures

The purpose of this investigation is to examine changes in the hemispheric synchrony of neural assemblies associated with global state changes. This dissertation is comprised of three logically integrated studies which is comprised of the following: The first is animal research performed in order to validate the methodology using experimental manipulation of the effects not possible in humans, the second study's purpose was to typify the sequence of changes in hemispheric synchrony that take during sleep onset; the function of the third study was to utilize methodology and findings in the sleep onset process in study 2, and typify the sleep onset process of narcoleptics. Therefore this total approach taken in this investigation can be classified as translational research because the findings from the basic research component of this study are applied to the study of a disease in a clinical population.

However, before the three studies that comprise this exposition can be presented an introduction to the whole will be provided that consists of the following: 1) a brief and general introduction to the application of synchrony in neuroscience, and 2) a visual demonstration and description of the synchrony methods will be undertaken, and 3) the rationale for us of synchrony methods will be presented using experimental non-human primate data.

An Introduction to Phase and Amplitude Synchrony

Phase synchrony has become an important paradigm because it reflects long and short distance binding of neural assemblies across the brain. Assessing this effect has been important in the areas of epilepsy and neurocognition research. I utilized this synchrony paradigm as explored in these two research areas because it would provide a novel perspective in the area of sleep and insight into neural mechanisms that are associated with sleep state changes.

Synchrony in neurocognition

The "temporal correlation hypothesis" (Singer, 1999) has been well accepted in the field because this neural synchrony approach has been successful in explaining neuronal integration of anatomically distributed processing. This "binding problem" is thought to be solved by synchronization of neurons into transient oscillatory assemblies (Singer, 1999; Varela et al., 2001, Weiss & Rappelsberger, 2000). One proposed specific perceptual solution to the binding problem is that synchronous neural activity provides a temporal code for grouping together parts of an object (Gray, 1999, Gray et al., 1989, Singer and Gray, 1995). According to this binding by synchrony (BBS) hypothesis, "spatially segregated neurons should exhibit synchronized response episodes if activated by a single stimulus or by stimuli that can be grouped together into a single perceptual object" (Singer, 1997). A good illustration of this point is that coupling of electrical brain activity in the gamma band is considered as the basic mechanism underlying

transient functional coupling of neural assemblies during visual cognitive tasks (von der Malsburg, 1994).

Synchrony in Epilepsy

The synchrony methods that are used in neurocognition originated in epilepsy research. There is a large push forward to develop a seizure prediction measure that is highly sensitive that can detect subtle changes in synchrony prior to a hyper-synchronous event or a seizure (Litt & Echauz, 2002). As expected phase synchronization measures also demonstrate an increase during epileptic seizure activity, as shown for intracortical (e.g., Le Van Quyen et al., 2001) and scalp EEG (e.g., van Putten, 2003). The epilepsy area leads the field in the use and development of these analytical methods. There is a large variety of methods that have been used to assess synchrony such as cross correlation, coherence, wavelet or hilbert based synchronization measures, namely nonlinear interdependences, phase synchronizations, mutual information (Quiroga et al., 2002), global or local synchronization (van Putten, 2003), mean phase coherence (Mormann et al., 2000), and instantaneous phase synchrony distribution (von Gizycki et al., 2007).

However, it is prudent to further develop these synchrony methods and assess their performance in depth using epileptic data, prior to their use in sleep, where there are no hugely obvious EEG landmarks as there are in a seizure. In the analysis of epilepsy you can have at least two very distinct conditions: normal EEG and Seizure EEG, because one is not hyper-synchronous and the other is hyper-synchronous. This is why in study I will further expand the previous pilot synchrony analysis of epileptic animal data in order

to examine in a detailed way their performance. This will be done by comparing the analytical results of several previously used wavelet based measures and one proprietary novel synchrony measure (von Gizycki et al., 2007, Quiroga et al., 2002, Tass 1998) as hyper-synchrony is experimentally manipulated. This approach will provide an in depth understanding of these methods, and will allow me to successfully apply these methods to studies II and III which are sleep protocols. There are a variety of methods in this field (e.g., Quiroga et al., 2002) with no real standard measures; therefore, I have been developing these methods using monkey, rat, and human data in order to refine the use of these methods.

Synchrony in Sleep

Unlike the neurocognitive area these highly developed analytical methods from epilepsy have not yet been applied in the sleep field to assess changes in interhemispheric synchrony. EEG synchronization is associated with sleep onset and sleep depth. However, this effect has been principally demonstrated using the older and very limited coherence and cross-correlation synchrony methods.

There is substantial evidence for the theory that changes in coherence are mediated by the corpus callosum and are associated with sleep. For example, the interhemispheric EEG coherence was decreased in congenitally acallosal infants, children and adults (Kuks et al., 1987; Nielsen et al., 1993; Koeda et al., 1995) and after callosotomy in adults (Montplaisir et al., 1990). It is possible that the corpus callosum contributes to the higher interhemispheric coherence or interhemispheric correlation in the delta and spindle

frequencies that have been found in sleep compared with waking (Corsi-Cabrera et al., 1996; Achermann and Borbely, 1998).

Sleep onset in human is closely linked to EEG slowing. It is well known that the synchronization of thalamically generated activity in delta and spindle-frequencies may arise from an intracortical neuronal network generating synchronous slow oscillations (Steriade et al., 1991; Timofeev and Steriade, 1996). Such low frequency oscillations are a typical feature of normal physiological sleep in the cat (Steriade et al., 2001; Destexhe et al., 1999) and in humans (Achermann and Borbely, 1997; Steriade and Amzica, 1998). Increases in delta and theta power have been closely associated with an increase in interhemispheric coherence (Achermann and Borbely, 1998). Analysis of our pilot data supports these findings (von Gizycki, Cunningham, Spielman & Lombardo, 2007; Please see attached document for conference abstract). However, the analysis of phase and amplitude synchrony give inverse results because phase synchrony increases with sleep onset and amplitude synchrony decreases with sleep onset. This is interesting because the measures that have been used in all previous studies to examine hemispheric synchrony during sleep onset, such as coherence and crosscorrelation, are joint measure of phase and amplitude synchrony (e.g., Corsi-Cabrera et al., 1996; Achermann and Borbely, 1998). Therefore, in study II and III, I re-examine the hemispheric synchrony changes associated with sleep onset using independent phase and amplitude methods.

Description of Methods used for Synchrony Analysis

In papers one to three I give detailed explanations of the synchrony methods used, however, in this introductory section in order to make these methods more accessible to most readers, I give a detailed visual description of the methods used and I minimize the use of technical signal processing terms.

Continuous Wavelet Transform

Preliminary data transformation prior to synchrony analysis was performed as follows: First, EEG signals at 8, 14, 20, 40 and 60 Hz were extracted from the EEG data using a continuous wavelet transform (CWT), applying a first order complex Gaussian wavelet (Matlab Wavelets Toolbox, Mathworks, inc). The CWT is useful for examining the time varying behavior of the frequency spectrum of a finite signal segment, and is mathematically defined as:

$$CWT_x^{\psi}(\tau, s) = \frac{1}{\sqrt{s}} \int x(t)\psi\left(\frac{t-\tau}{s}\right) dt$$

where *x(t)* is the signal segment, *s* is the scale that adjusts the wavelet to a particular frequency (higher scale corresponds to "stretched" lower frequency versions of the wavelet [see figure below]), τ is the window size for the wavelet,

and $\psi(t)$ is the Gaussian wavelet defined as the first derivative of the Gaussian function normalized to have an area of 1:

$$\psi(t) = \frac{-t}{\sqrt{2\pi\sigma^3}} e^{\frac{-t^2}{2\sigma^2}}$$

This approach is really quite simple if it is described visually instead of relying on mathematical nomenclature.

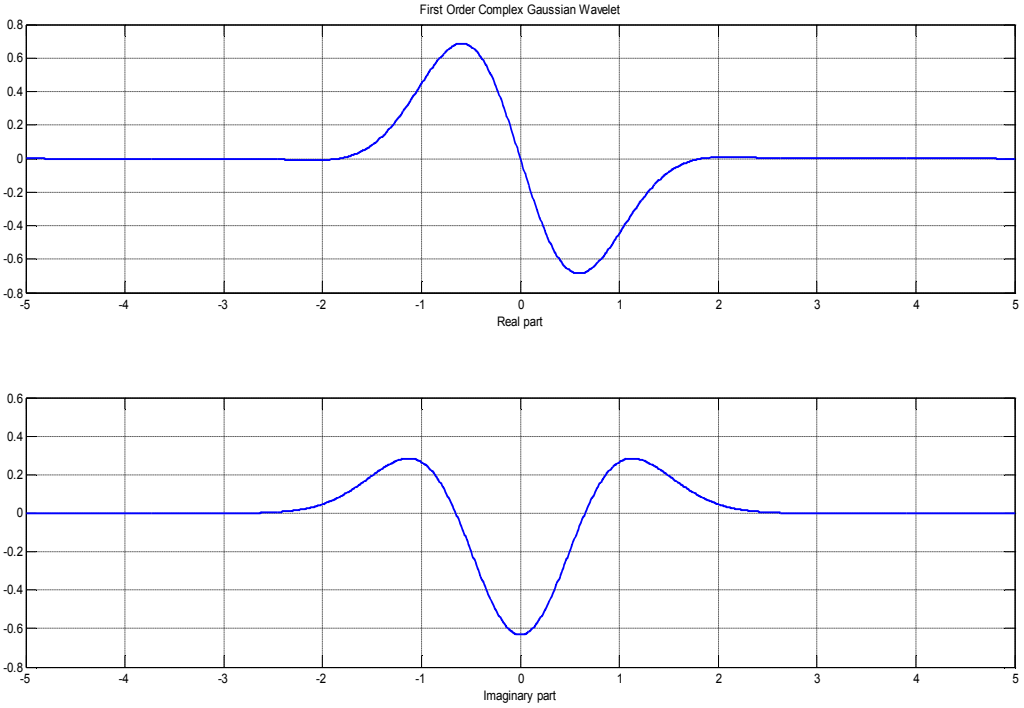

The first derivative Gaussian complex wavelet was used in the three studies that comprise this thesis. Panel 1 is the real component and panel 2 is the complex component of the wavelet.

It's really a very simple process. In fact, here are the five steps of an easy recipe for creating a CWT (Misiti, et al., 2008):

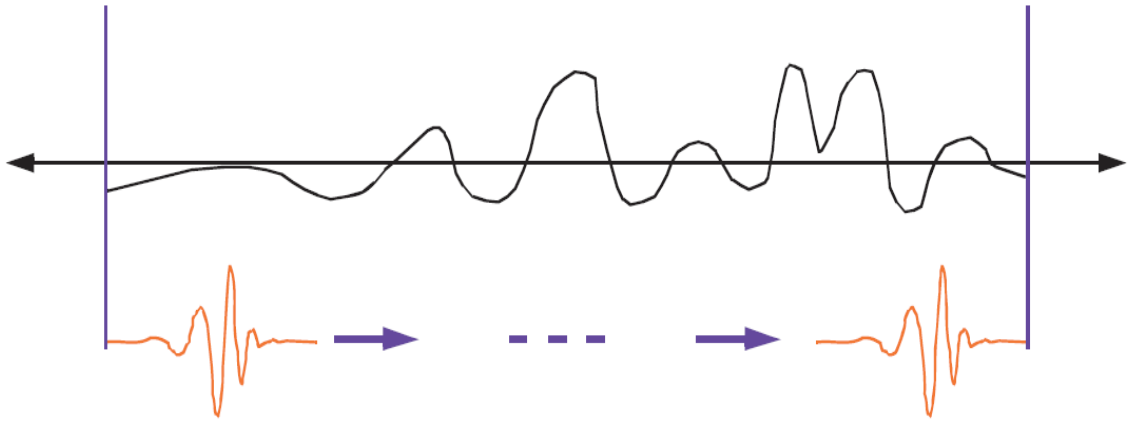

1) Take a wavelet and compare it to a section at the start of the original signal and keep on comparing to all data points (see figure above).

2) This simple comparison is really the calculation of a the term "C", that represents here how closely correlated the wavelet is with this section of the signal. The higher C is, the more the similarity. More precisely, if the signal energy and the wavelet energy are equal to one, C may be interpreted as a correlation coefficient. Note that the results will depend on the shape of the wavelet you choose. Therefore, this process creates a time series of C.

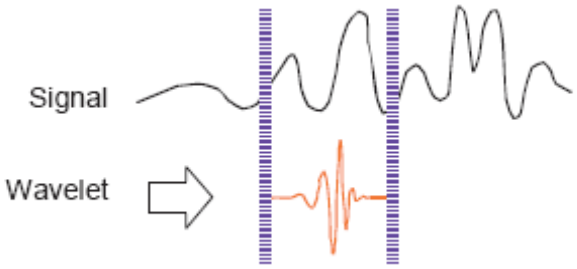

3) Shift the wavelet to the right and repeat steps 1 and 2 until you've covered the whole signal.

4) Scale (stretch) the wavelet and repeat steps 1 through 3.

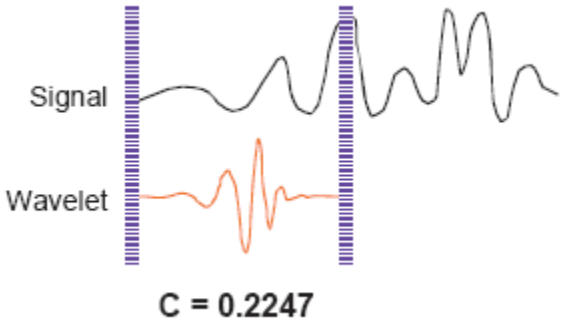

When you're done, you'll have a series of coefficients from different sections of the signal produced at different scales. The wavelet for one scale can be seen as a narrow bandpass filter, therefore a specific frequency of interest can be extracted, for example the corresponding wavelet scale is used. The left panel below shows the raw data, and the right panel shows the wavelet coefficients for the scale that can act as a 10 Hz narrow bandpass filter. Please note that the complex component of the coefficients has been removed and only the real component is plotted.

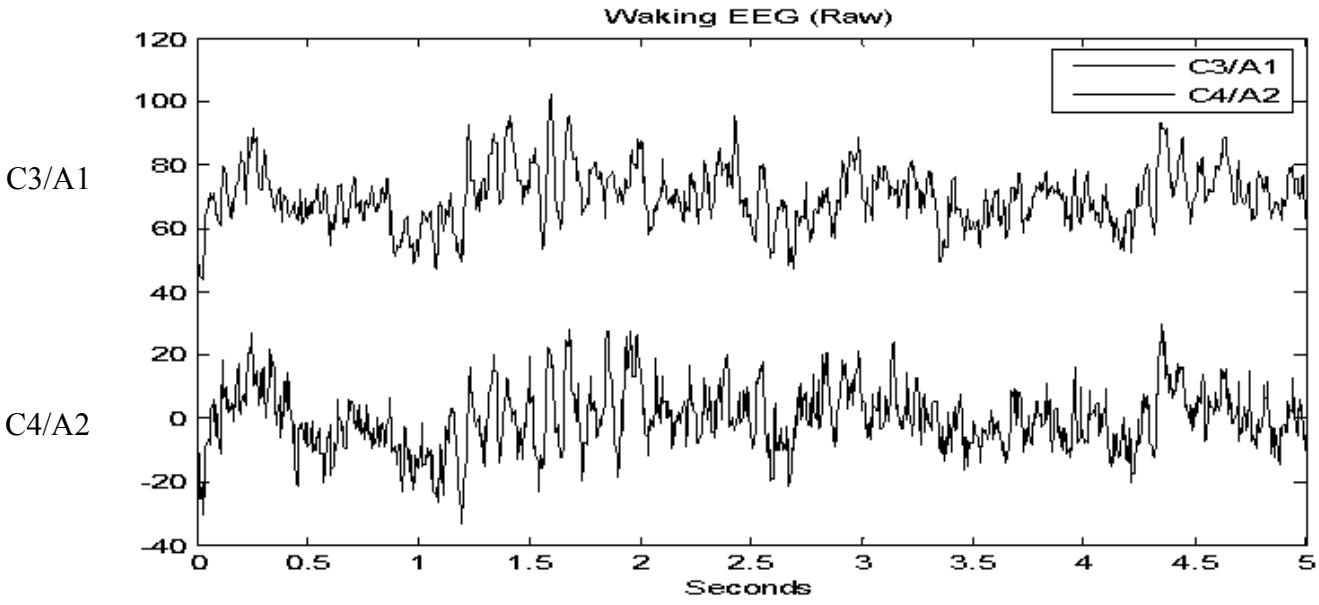

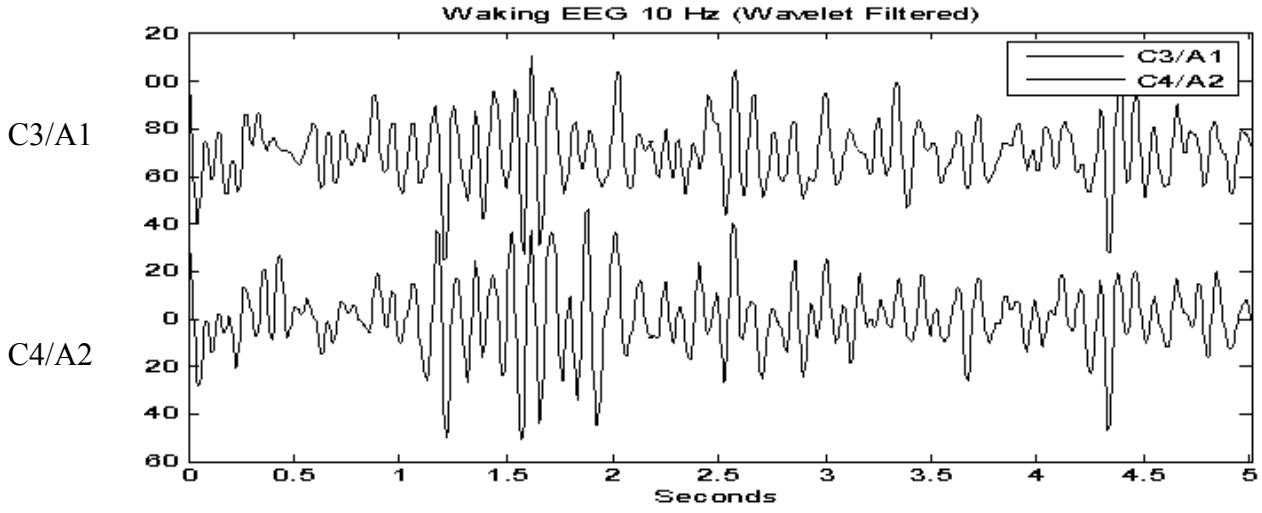

The complex component of C CWT results were transformed to an angular term and unwrapped, producing a phase time series for each EEG channel and allowing for the calculation of the phase differences between these channels. See below

C3/A1

C4/A2

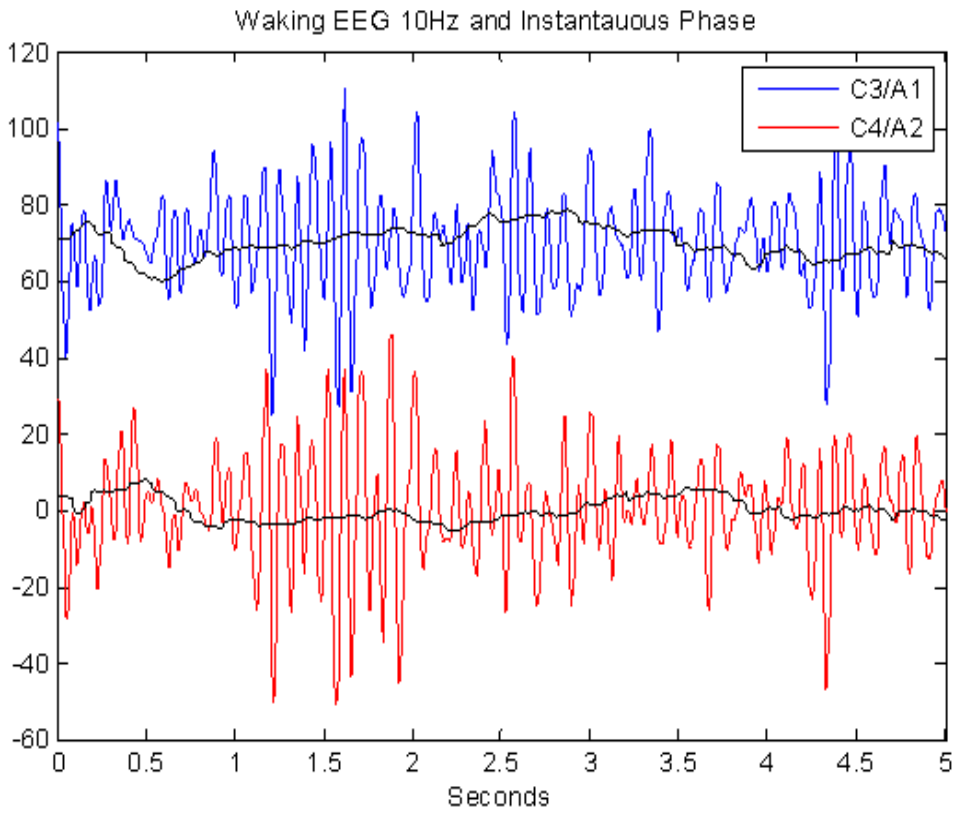

The transformed data were subjected to a series of synchrony analysis, as described below.

Phase Synchrony Method

All the phase synchrony methods used in these studies depend on difference between the two phase time series extracted from each signal (see figure below).

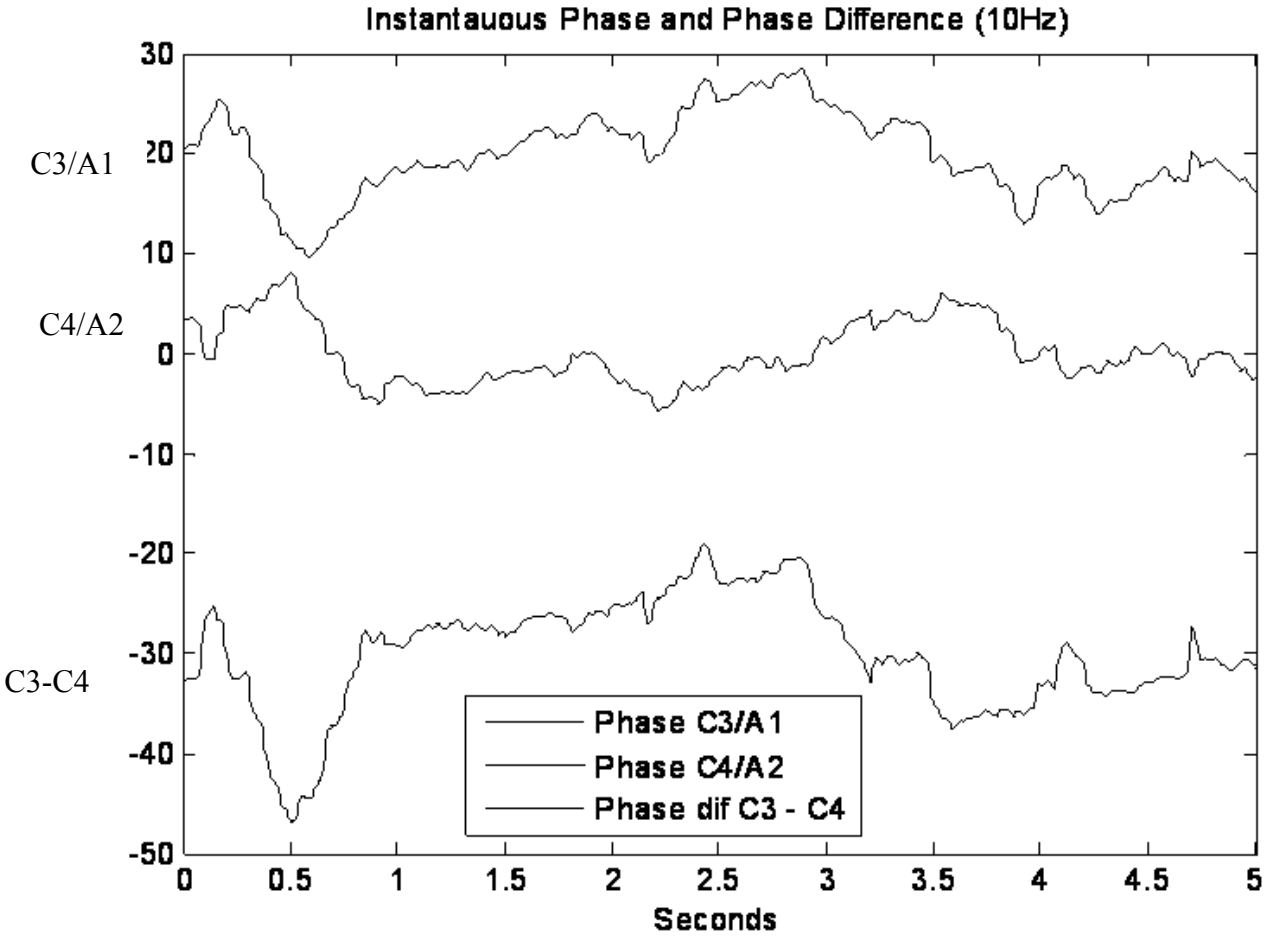

Synchrony Index (SI)

SI is the average normalized phase difference between two EEG channels, and measures the variability in the phase difference between two signals in time, such that if the difference between the phases of two signals is constant, the synchrony index has a value closer to 1; and when the phase difference changes erratically with time, then the synchrony index is closer to 0.

Synchrony Entropy Index (SEI)

How much information does the differences between the two phase time series contain Shannon's Entropy. The more information implies that the differences at specific times

for the two phase time series is not constant, if the phase differences was constant it would mean that the time series were time locked even though phase would change for both signals but the differences would be the same. A distribution of two very phase locked signals would be very narrow and contain very little information because the

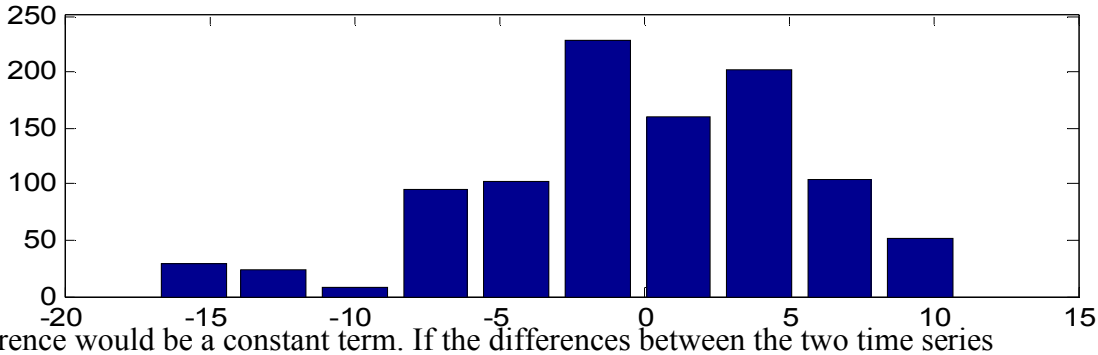

difference would be a constant term. If the differences between the two time series changed quite a bit it would contain very wide distribution implying that it contained quite a bit of information and was not phase locked. The SEI measure is an index that ranges from 0 to 1, at 0 is no synchrony and 1 means perfect synchrony. (Please see the methods section of papers 1 & 2 for a formal description of the methods)

Instantaneous Phase Synchrony Distribution (IPSD)

$$KU = \frac{E[(y-\mu)^4]}{\sigma^4}$$

This measure is a novel measure that I developed. This measure uses the statistic kurtosis as a way of measuring how much a distribution of phase differences differs from a normal (mesokurtic) distribution (see fig below). If a distribution is Leptokurtic it means that the scores are very close to the mean and it is a very narrow distribution with very little variability implying that the phase difference between the two channels is pretty constant and therefore there is phase locking or synchrony. If a platykurtic distribution is observed it means that there is a great deal of variability in the phase differences demonstrating that there is no or low synchrony. These platykurtotic distributions or fat-

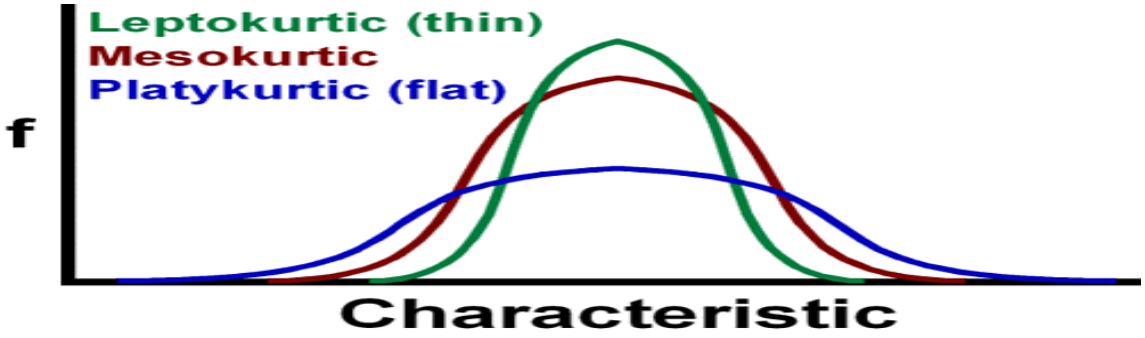

tailed distributions in econometrics in a variety of market measures imply volatility or instability. A random distribution looks is totally flat, the most similar to a platykurtic distribution, and if this was the case for the phase difference distribution it would imply that all values within the range of the distribution have equal opportunity of appearing and it would be very non-synchronous.

Amplitude Synchrony Measures

In order to perform amplitude synchrony analysis the demodulated amplitude of the real component of the complex wavelet coefficients was extracted using a Hilbert transform, which involves the convolution of the signal with $h(t)=1/\pi t$. In the figure below the dark blue and light blue are the instantaneous amplitude (amplitude envelopes) for the C3 and C4 channels. Two amplitude synchrony measures are used in this series of studies. The amplitude entropy index is the same approach used in the phase synchrony measure Synchrony Entropy index except that the differences between the amplitude envelopes for the two signals see panels below

C3/A1

C4/A2

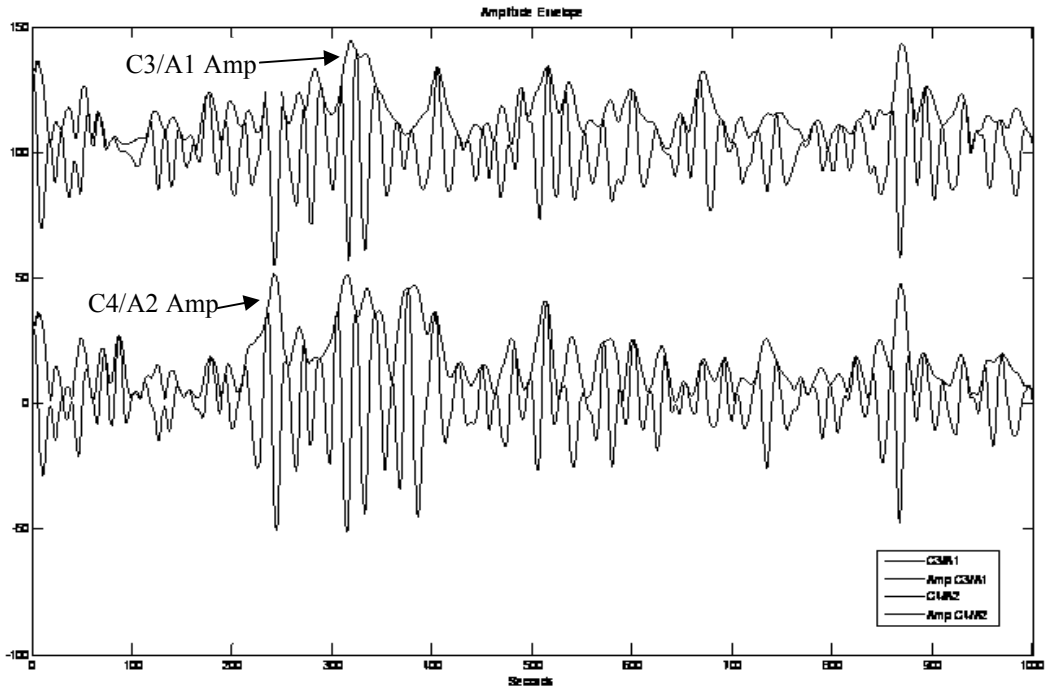

The amplitude synchrony (ASI) measure, takes another very different approach than the AEI which examines the information content of the difference between the two signals to assess synchrony. The ASI measures the correlation between the instantaneous amplitude between both channels to demonstrate how similar they are. Therefore, the higher the correlation coefficient the greater the amplitude synchrony between both channels. Below is the scatter plot, of these two channels and the correlation coefficient = .64.

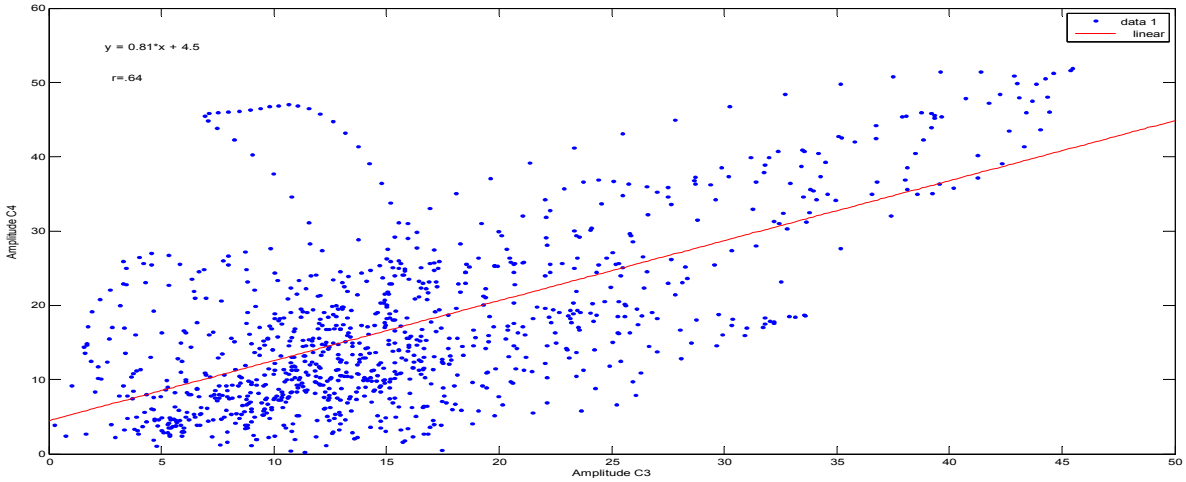

C4/A2

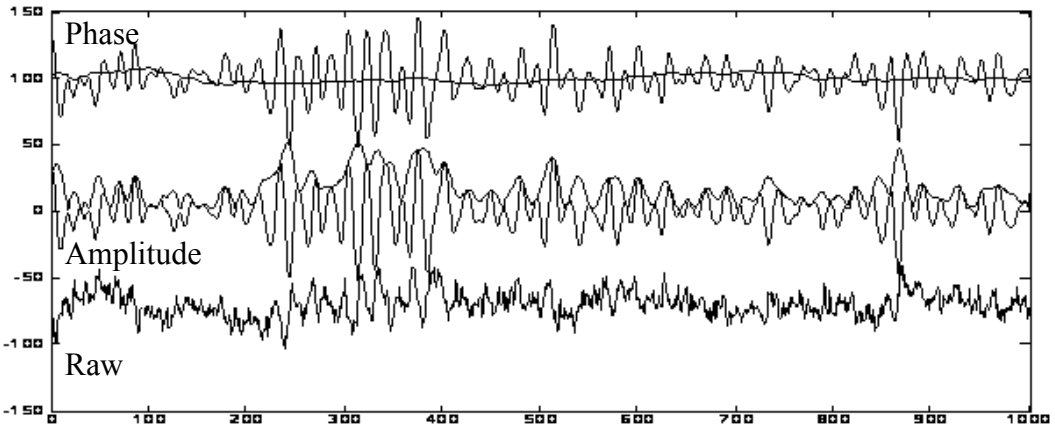

C3/A1

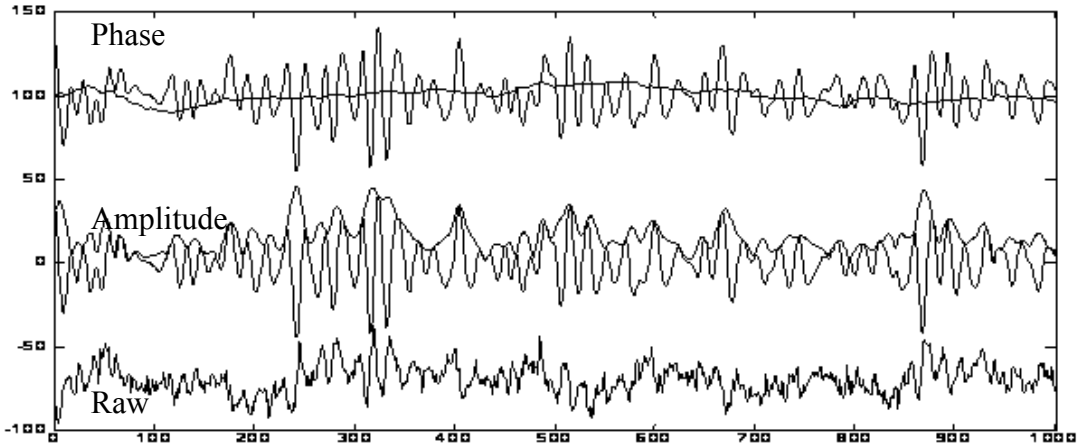

Overall it is possible to visually examine how similar are two signals when the demodulated amplitude and phase is extracted separately. The raw signal for both channels is difficult to examine the green signal in each panel represents a separate channel. However, if the phase time series is examined the blue lines in the first signal for both channels, it is quite obvious that they are significantly different. However, if the amplitude time series is examined, which is the blue lines in the second signal for both channels, it is quite obvious that they are similar.

A way to conceptualize this information in a straightforward mathematical model would be to conceptualize the filtered 10 Hz EEG signal using simple sinusoidal model where the 10 Hz signal is the carrier wave and the amplitude time series is the amplitude modulation as instantaneous amplitude and the phase modulation the phase time series as instantaneous phase.

The Rationale for the Use of Phase Synchrony Measures to Detect Epileptic Seizures: Empirical Assessment of the question

Phase synchrony or phase locking between EEG channels is a feature of epileptic seizures, where entrainment of complete neural populations by one or more foci takes place. Therefore, in order to detect changes in synchrony between EEG channels that can produce catastrophic events it is very important to have precise estimates of intra-channel synchrony.

Theoretical considerations

Conventionally, synchrony has been estimated in the time domain by the use of cross correlation and in the frequency domain by the use of coherence which is basically a cross correlation of FFT spectral values. These classical methods have been extensively used in neuroscience (see, e.g. Bullock and McClune, 1989; Bressler et al., 1993; Menon et al., 1996).

However, these linear approaches have two major limitations for the analysis of EEG signals: 1) The lack of stationarity that violates assumption of the analysis method that amplitude and phase are constant throughout the dataset making the results difficult to interpret 2) Ascertaining the source of the variance in the classical coherence measures again making the results difficult to interpret.

The first limitation is that time dependent cross correlation and coherence methods based on fourier analysis are highly dependent on the temporal stationarity of the measured

signals. Phase and amplitude that govern the non-linear behavior of EEG signals demonstrate a high level of time dependent variability that produces a signal with a low level of stationarity. However, this limitation to some extent can be dealt with a time dependent applications of these two methods.

The second limitation is the conflation of amplitude and phase coherence, because coherence methods are a measure of spectral covariance, and thus do not separate the effects of amplitude and phase in the interrelations between two signals, and the relative importance of amplitude and phase covariance in the coherence value is not clear. This is also the case with the cross correlation measure which is also sensitive to same limitations as coherence because the changes in the covariance values cannot be directly attributed either to amplitude or phase changes.

This is a critical issue because non-linear signals like EEG can have a high degree of phase locking and at the same time can differ greatly in regards to amplitude and thereby masking the high level of phase synchrony that could be a marker for the onset of an epileptic seizure.

Very effective analytical approaches such as the synchrony index have been developed to deal with these limitations associated with nonlinear signals (Tass 1998). One of these methods, for example the synchrony index estimates how the instantaneous phase of two signals covaries in time. However, the phase component of the signals must be extracted using some sort of demodulation method. An effective demodulation approach and the one used in the empirical section of the paper, the signal is convoluted with complex

gaussian wavelets at several scales using a continuous wavelet transform. The complex component of the coefficients generated by this analysis is transformed to angular terms and unwrapped to produce instantaneous phase of the signals for all the scales. Additionally, the instantaneous amplitude parameter can be extracted using the hilbert transform of the real component of the generated coefficients.

Applying this method the EEG signals can be modeled quite simply using a trigometric function with two independent parameters that are time variant. This is critical because the source of variance can be ascribed specifically to phase or amplitude covariance changes or both.

$$Y_t = \mathrm{Cos}(t \cdot 2\pi \cdot f_n + \varphi_t)\, a_t$$

$t = 1$ to N

- φ instantaneous phase
- **a** instantaneous amplitude
- **f** frequency estimated from each complex gaussian wavelet scale
- **t** time as a function of sampling frequency
- **n** total number of didactic wavelet scales
- **N** total number of time points
- **Y** EEG signal

Phase synchrony can be estimated using a variety of methods which is basically analyzing the difference between the demodulated phase parameters of both signals. The differences between phases if it produces a plateau for a large part of the time series implies a high level of synchrony. This can happen eventhough the signals demonstrate stochastic-like properties because the temporal divergence between the two signals phase components is minimal and the distance between them is almost constant. A variety of methods have been designed to quantify this sort of phenomena which is the degree of phase locking between two signals. The principal one is the syncrony index (SI) which

is basically the mean of the distances between the trigonometric transformed instatntaneous phases of both signals. This produces a statistic that ranges from 0 to 1, which is no synchrony to complete phase locking.

$$SI = \frac{\Sigma \left| Cos(S_1 \varphi t) - Sin(S_2 \varphi t) \right|}{N}$$

A similar synchrony statistic can be calculated using an entropy approach, where the information content of the phase difference of both signals is computed (ref). If the information content is high it implies that the phase distances between both signals is not constant and highly variable. A static to SI can be generated that is highly correlated to SI. With numerical simulations using bootstraping methods it is possible calculate 95% confidence intervals, and using resampling methods to formally test the null hypothesis that the two signals have 0.0 degree synchrony and with this approach produce the much desired p value.

A constant phase distance value is an indication of phase locking between both signals, basically they covary together and stationarity is not an issue in this approach because the assessment of the distance between the two phase parameters takes place at each time point instead of the total datasets at once.

Empirical Support for the Use of Synchrony Measures

It is possible to take an empirical approach to demonstrate that synchrony index measures are quite different than classical synchrony measures and that they provide a clearer picture of the degree of phase locking between two signals.

For the sake of brevity, the obvious limitation of stationarity will be computationally removed from the milieu for the classical synchrony measures. Therefore a windowing function will be applied to the dataset to deal with the stationarity issue, by limiting the analysis to a smaller subsets of the complete dataset, the EEG signals will locally exhibit a limited stationarity. In order to do this a moving window of 500 datapoints will be used to calculate all the synchrony statistics and this window will move by one datapoint at a time through the complete dataset.

If the limitation of stationarity is dealt with the problem of ascertaining the source of the covariance to amplitude or phase effects is the critical issue. We will empirically do this by analyzing a squirrel monkey EEG dataset (subject male monkey: Adonis. source: N

Figure1 Raw data: the lower signal is the hippocampal data and the baseline shifted higher signal is the cortical EEG data.

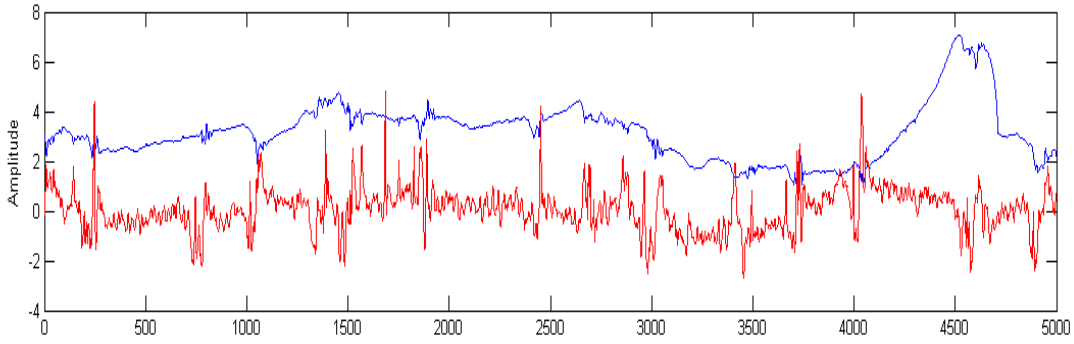

Ludvig) sampled at 1k from two ipsilateral locations (see figure 1): 1) the hippocampus (red signal) and 2) the temporal cortex (baseline shifted and blue)

In EEG seizure studies phase locking that takes place between two EEG locations. Obviously then it is important to localize the source of the covariance that reflects phase synchrony effects instead of amplitude similarities between two signals. Therefore we will empirically demonstrate that classical measures of synchrony such as cross correlation are highly sensitive to the covariance of instantaneous amplitude and the covariance of phase is not easily discernible in this measure.

Three analysis methods will be performed to substantiate this point using a moving window approach.

1) Cross correlation (CC) of the real part of the wavelet coefficients for both signals

2) Synchrony index (SI) using the demodulated phase values for each both signals

3) Ascertaining with a correlation measure the amplitude covariance using the demodulated amplitude values for each signal and computing the correlation between both channels which will refer to as the Amplitude Synchrony Index (SAI).

(Please note that the three analysis approaches will be performed on the wavelet coefficients from scale that is approximately 8 hertz, which is equivalent to passing the dataset through a narrow bandpass filter centered around 8 hertz).

Visually examining the time course of SI, SAI and CC it is apparent that some of these statistic are quite different and others are not (See figure 2 panels 1-3). This is quantified

by simply computing a correlation coefficient between these measures. SI and CC time series correlation is neglible (r= 0.07, ns), and the correlation between SI and SAI is also miniscule (r= 0.04 ns). However, the SAI and CC time series is moderate (r = 0.38, p =0.04).

The negligible correlation between SI and SAI is predicted from the earlier presented sinusoidal model were amplitude and phase are two independent terms. The moderate correlation between CC and SAI implies that amplitude covariance explains a part of the CC covariance, while the phase produced SI explains none of the CC covariance. There are two probable reasons for these results 1) Cross correlation cannot detect phase synchrony in or 2) In cross correlation, the phase covariance information is masked by the amplitude covariance and source of the covariance cannot be ascertained.

What is concluded from the theoretical and empirical assessments of classical synchrony and SI is that SI methods is more valid approach, and therefore the logical choice for measuring phase locking in non-linear signals such as EEG.

Hippocampal- Neocortical Phase and Amplitude Synchrony Changes Precedes Seizure Events in Freely Behaving Rats

Hans von Gizycki, Dissertation Part 1

Cognitive Neuroscience Program CCNY, CUNY

Dissertation Supervisor: Arthur J. Spielman

Scientific Computing Center, SUNY Downstate Medical Center, Brooklyn, NY, U.S.A.

Key words: Phase Synchrony, Amplitude Synchrony, NMDA, EEG activity, Focal seizures, Instantaneous Phase Synchrony Distribution.

Running title: Synchrony Changes Pre-seizure

Corresponding author: Hans von Gizycki, Scientific Computing Center, SUNY Downstate Medical Center, 450 Clarkson Avenue, Box 7, Brooklyn, New York, 11203, USA ; Tel.: (718) 270-7474; Fax: (718) 270-7461;

E-mail: vongizycki@downstate.edu

ABSTRACT

Introduction: This presentation focuses on the assessment and validation of phase and amplitude synchrony measures using a controlled experimental animal model, where EEG seizures are induced in the hippocampal—temporal cortical circuitry. The main advantage of using such a seizure model is the ability to know the etiology of the seizure and clearly identify the timing of pre-seizure EEG events, which is not available from clinical human seizure data.

Methods: EEG was recorded from 5 freely behaving rats that were implanted with bilateral hippocampal and parietal cortical electrodes. 500 microM NMDA was delivered into the hippocampus via a hippocampal microdialysis probe or minipump-connected microinjector , which caused EEG seizures. EEG data was assessed during the following treatment conditions: 1) baseline (pre-NMDA state), 2) pre-seizure (post-NMDA state prior to seizure) and, 3) seizure (post-NMDA state during seizure). Several types of synchrony measures were assessed, including: a) conventional methods, cross correlation (CC), coherence (Coh); b) phase synchrony measures, synchrony index (SI), synchrony entropy index (SEI), and instantaneous phase synchrony distribution (IPSD); and c) amplitude synchrony measures: synchrony amplitude index (SAI), and entropy amplitude index (EAI).

Results: Repeated measures factorial ANOVA and post hoc tests, with EEG frequency bands and NMDA treatment condition as factors, demonstrated that it was possible to differentiate between baseline and seizure conditions at all frequencies in many of the synchrony (phase and amplitude) and EEG power measures. However, the analysis of interest is the differentiation between baseline and pre-seizure, which appears to be more

of a difficult task because it was possible to do so with only three of the synchrony measures at specific frequencies: CC, IPSD at 8 Hz, and ASI at 60 Hz. Amplitude and phase synchrony measures are not significantly correlated and are both independent predictors of cross correlation, which is composed of both amplitude and phase synchrony. However, both methodological approaches allowed for the differentiation between baseline and pre-seizure EEG.

Conclusion: Phase and amplitude synchrony analyses provide information that is helpful in differentiating between the baseline and pre-seizure conditions. Additionally, our newly developed IPSD measure also seems to be a valuable tool for differentiating between normal baseline and pre-seizure EEG states. Therefore, in order to develop algorithms to predict seizure onset on a timely basis that allows for medical intervention, it is optimal to use a variety of measures based on both phase and amplitude synchrony analyses.

Introduction

Seizures are characterized as excessive hyper-synchronous discharges above the synchronous EEG activity that is typified by normal brain function. Because of the deleterious effect of untreated epileptic seizures, there has been an exploration of the viability of seizure prediction algorithms in assisting in the treatment of epilepsies that are both resistant to pharmacotherapy and unsuitable for surgical resections (i.e. electrical stimulation or drug delivery) (Ludvig, 2000; Fischell et al., 2000; Stein et al., 2000; Litt et al., 2001; Ludvig and Kovacs, 2002; Turner et al., 2005; Worrell et al., 2005; Iasemidis et al., 2005). Recently, there has been substantial effort to develop a reliable analytical approach to detect in advance the onset of a seizure by application of a variety analytical methods on clinical EEG data collected from epileptic patients (Elger and Lehnertz, 1998; Salant et al., 1998; Litt and Echauz, 2002; Drury et al., 2003; Ashenbrenner-Scheibe et al., 2003; Mormann et al., 2005; Chaovalitwongse et al., 2005). However, as Mormann et al. (2007) recently noted, "While most of the studies published in the 1990s and around the turn of the millennium yielded rather promising results, more recent evaluations could not reproduce these optimistic findings, thus raising the debate about the validity and reliability of previous investigations".

Taking into account the previous work in algorithm development and the reassessment of this work (Mormann et al. 2007), we propose two novel methodological approaches in this study that can provide a model for seizure prediction algorithm research: 1) control the variability of the seizure dynamics by the experimental manipulation of seizure

parameters in an animal model that we previously developed; and 2) the application and assessment of novel and known synchrony methods. In this controlled experimental environment, a more accurate assessment of synchrony measures can be performed.

An experimental animal model of seizures and epilepsy can provide new opportunities for approaching the problem of seizure prediction. The advantage of using an animal model is that seizures can be elicited under experimentally controlled conditions, making it possible to clearly identify the time when the abnormal, pre-seizure neural events start. This, in turn, allows the monitoring of the entire course of events that ultimately lead to paroxysmal activity. In addition, this helps the separation of significant pre-seizure indicators from irrelevant signs, and offers the testing of emerging hypotheses in well-controlled conditions. The seizure etiology is well defined in this study because we used an animal seizure model (Ludvig et al., 1992; Ludvig and Tang, 2000), which we have previously developed. This approach is very different from that which is taken with human EEG data, where the etiology is extremely varied and not well understood. Additionally, in humans, the exact location of the source of the seizure is not always apparent and usually varies across subjects in a sample to be studied. Furthermore, the intensity of the seizure varies greatly in humans, unlike the animal model where the seizure producing agent (NMDA) is administered at the same location across all animals at the same dosage. Therefore, because of the above mentioned considerations, it is not unexpected that issues of validity and reliability have been brought forward, stemming from the fact that it is very challenging to carry out well-controlled experiments with human data.

Well controlled experimental data is particularly suited to validate and assess the ability of synchrony measures to differentiate between normal-baseline EEG and pre-seizure EEG (propensity to seizure with no obvious sign). We propose to validate established measures as well as our newly developed phase synchrony measure, the instantaneous phase synchrony distribution (IPSD), using this experimental paradigm. Among the measures that were considered here are phase synchrony (i.e. synchrony index, Tass et al., 1988) and amplitude synchrony (Nikouline et al., 2001, Burns et al., 2000), which we hypothesize to be independent of each other, suggesting they carry dissimilar types of information that can contribute to the discrimination between baseline EEG and pre-seizure. We will also utilize more conventional measures that combine both amplitude and phase synchrony (i.e. coherence and crosscorrelation).

In order to develop a reliable paradigm that could be useful for seizure prediction we carried out a study where we manipulated the seizure parameters such as etiology, timing, and intensity of a seizure. Furthermore, as a validation of the previously mentioned synchrony measures, we examined their ability to assess the changes in synchrony that were experimentally produced by manipulating the degree of hyper-synchrony by using the epileptogenic drug NMDA.

Methods

Animals

Male Long-Evans rats (n = 5), weighing 300-400 g, were used. They were subjected to an experimental protocol that was approved by the Institutional Animal Care and Use Committees at NYU School of Medicine (# 060102-01) and SUNY Downstate Medical Center (#07-237-06).

Surgical procedures

Each rat was anesthetized with 50 mg/kg pentobarbital, i.p. Additional injections of 0.1 mg/kg atropine, s.c, and 30,000 units/100g Penicillin G Benzathine/Penicillin G Procaine, s.c., served to reduce secretion in the respiratory system and prevent infection, respectively. The rat was placed in a stereotaxic apparatus and the skull exposed. A 2.5 mm diameter craniotomy was drilled above the right hippocampus, and 1.5 mm diameter craniotomy was drilled above the right visual cortex, according to the atlas of Paxinos and Watson (1988). Next, a visual cortical – hippocampal EEG electrode assembly coupled with a dual microdialysis/microinjection guide cannula for intrahippocampal NMDA delivery (see Fig. 1) was stereotaxically implanted.

The tip of the visual cortical bipolar electrode was positioned 1.5 mm below the cortical surface, while the tip of the hippocampal bipolar electrode was positioned 1 mm below the CA1 stratum oriens. Each tube of the dual microdialysis/microinjection guide cannula was protected with an inserted stylet. The surgical procedures were completed

by anchoring the entire assembly to the skull with dental acrylic and approximating the skin, treated with Animax antibiotic ointment, with a suture. The EEG recording/behavioral monitoring/epidural drug delivery sessions (see below) started on the second or third postoperative day. After surgery, Penicillin G Benzathine/Penicillin G Procaine was repeatedly administered to the rats, twice a week, throughout the course of the study.

EEG recording

Throughout EEG recording, the rat was behaving freely in a 30 cm wide, 30 cm long and 35 cm high wooden test chamber equipped with a water bottle. Since no experimental session lasted longer than 45-60-min, food was not available for the rat during these sessions. This eliminated the effects of eating behavior on EEG activity. A Faraday cage was built around the test chamber to prevent 60-Hz mains power interference and. As in our previous EEG/seizure studies (Ludvig and Tang, 2000; Ludvig et al., 2006), movement artifacts were eliminated from the recordings by using a recording cable with a built-in operational amplifier. The EEG signals were amplified (10,000 x) and filtered (using a band-pass of 1.0 – 100.0 Hz). The analog data were digitized at 1000 Hz with a National Instruments PCI-MIO-16E-4 (12-bit) A/D board and stored in a binary data structure using proprietary software on a PC. During data collection the EEG was displayed both on the PV and on an oscilloscope, with a camcorder.

Behavioral monitoring

The behavior of the animal in the test chamber was continuously monitored with a second camcorder. With use of a Videonics (Campbell, CA) MXProDV device, the video signals from this camcorder were mixed with the other camcorder facing the oscilloscope, allowing us to monitor the animal's behavior and the EEG activity simultaneously on the same screen. Notes were made on the rat's behavior before, during and after drug applications.

NMDA-delivery protocol

Each recording/NMDA delivery session started with a 5-min collection of baseline cortical and hippocampal EEG data. Baseline data collection was performed only when the rat was quietly resting in the test chamber. This assured constant behavior prior to seizure-induction. In each recording session, a seizure episode was induced by either of two NMDA delivery methods. Thus, NMDA was delivered either via microdialysis (in 3 rats) or microinjection (in two rats). When microdialysis was used, 500 μM NMDA was perfused for 5 minutes at a flow rate of 10 μl/min, as in our previous study (Ludvig and Tang, 2000). When microinjection was used, 2 μl of a 500 μM NMDA solution was delivered over a 1-min period, with the use of our custom-made minipump (Ludvig et al., 2005) secured to the recording cable.

Data Selection

The EEG data files collected from the 5 seizure-exposed rats were analyzed with proprietary software. Each data file was divided into 3 phases.: the 1st phase represented

the background cortical and hippocampal EEG activity prior to NMDA delivery, the 2nd phase represented the cortical and hippocampal EEG activity that occurred in between the start of the NMDA delivery and the onset of the EEG seizure, and the 3rd phase represented period of the EEG seizure. Fig. 2 demonstrates the characteristic EEG waves during the course of these experimental phases. Next, three representative segments, 3 seconds each, were selected from each recording phase. This yielded the 45 recording segments that were processed for the main analysis of this study, as detailed below.

Histology

After the end of the experiments, the rats were sacrificed for histological verification of the implanted electrodes. In all rats, the electrodes found to be correctly localized in the visual cortex and the hippocampus.

Data Acquisition

During recordings, the rat behaved freely in a chamber surrounded by a Faraday cage, which eliminated 60-Hz mains power interference. Movement artifacts were eliminated with operational amplifiers built in the recording cable. The EEG signals were amplified (10,000 x), filtered (using a band-pass of 1.0 – 100.0 Hz), and digitized at 1000 Hz. Each recording/NMDA delivery session started with a 5-min collection of baseline cortical and hippocampal EEG data. Then a seizure episode was induced by either the intrahippocampal microdialysis of 500 μM NMDA, as described (Ludvig and Tang,

2000), or the intrahippocampal microinjection of the same concentration of NMDA, using our custom-made minipump (Ludvig et al., 2005).

Data Analysis

Each data file was divided into 3 phases as follows: 1) Background cortical and hippocampal EEG activity prior to NMDA delivery, 2) the cortical and hippocampal EEG activity that occurred in between the start of the NMDA delivery and the onset of the EEG seizure, and 3) the period following the onset of the EEG seizure. Three 10 second artifact free EEG samples were selected randomly from each condition. Fig.2 demonstrates the characteristic EEG waves during the course of these experimental phases.

Preliminary data transformation prior to synchrony analysis was performed as follows: First, EEG signals at 8, 14, 20, 40 and 60 Hz were extracted from the EEG data using a continuous wavelet transform (CWT), applying a first order complex Gaussian wavelet (Matlab Wavelets Toolbox, Mathworks, inc). The CWT is useful for examining the time varying behavior of the frequency spectrum of a finite signal segment, and is mathematically defined as:

$$CWT_x^{\psi}(\tau, s) = \frac{1}{\sqrt{s}} \int x(t)\psi\left(\frac{t-\tau}{s}\right) dt$$

where *x(t)* is the signal segment, *s* is the scale that adjusts the wavelet to a particular frequency (higher scale corresponds to "stretched" lower frequency versions of the wavelet), τ is the window size for the wavelet, and *ψ(t)* is the Gaussian wavelet defined as the first derivative of the Gaussian function normalized to have an area of 1:

$$\psi(t) = \frac{-t}{\sqrt{2\pi\sigma^3}} e^{\frac{-t^2}{2\sigma^2}}$$

The CWT is analogous to the Fourier Transform (FT), which identifies the frequencies present in a signal (i.e. spectrum), but resolved in the time domain such that with a CWT, one can identify the time course of the appearance and disappearance of particular frequencies present in a signal. Likewise, the real and imaginary components of a CWT are also comparable to the FFT amplitude and phase.

The imaginary components of the CWT results for both channels were transformed to an angular term and unwrapped, producing a phase time series for each EEG channel and allowing for the calculation of the phase differences between these channels. Additionally, the demodulated amplitude of the real component of the complex wavelet coefficients was extracted using a Hilbert transform, which involves the convolution of the signal with $h(t)=1/\pi t$. The transformed data were subjected to a series of synchrony analysis, as described below.

First we examined cross correlation and coherence between the hippocampal and cortical recordings.

Crosscorrelation

Crosscorrelation is an estimate of how similar two time series measurements are in the time domain while coherence is an estimate of how similar two time series measurements are in the frequency domain, taking the contribution of autocorrelations of each of the signals into account. Thus, coherence detects the frequency components that are common to a set of signals, much like cross-correlation detects temporal associations between two time-series measurements. (Farmer et al.,1993). The cross-correlation approach used was an ordinary normalized covariance function, *R*, as given by

$$R(i,j) = \frac{C(i,j)}{\sqrt{C(i,i)C(j,j)}}$$

where *C* represents values in the covariance matrix as given by:

$$C_{(x_1,x_2)} = E[(x_1-\mu_1)(x_2-\mu_2)]$$

where E represents the mathematical expectation and $\mu_i=Ex_i$. These computations were performed using built-in functions in Matlab, however the innovation here is in the application of these techniques to determining the correlation between the real component of the complex wavelet coefficients from the two EEG channels at all previously extracted frequencies or scales.

Coherence

The coherence analysis employed here involves an approach analogous to the one used for cross correlation, where we examine the synchrony of the two EEG channels after using data processed with the CWT for all the frequencies of interest. Coherence is a FFT-based synchrony measure that estimates the magnitude squared coherence using power spectra as:

$$C_{xy}(f) = \frac{\left|P_{xy}(f)\right|^2}{P_{xx}(f)P_{yy}(f)}$$

where *Pxy* represents the cross power spectrum density between two inputs *x* and *y*, and *Pxx* and *Pyy* are the power spectral densities of signals *x* and *y*, respectively. This measure is bounded between 0 and 1, where 0 indicates that x and y have no linear relationship, and 1 indicates that x can perfectly predict y in a linear fashion.

In practice, cross-correlation and coherence are affected by both the amplitude and phase structure of each signal. Cross-correlation has a value between –1 and 1, such that there is no temporal association between the two signals when the cross-correlation is zero, and a high degree of negative or positive temporal association between the two signals when the value is –1 or 1, respectively. Coherence has a value closer to 1 when the phase difference between two signals is constant and/or when the frequency domain amplitudes of the two signals are correlated with each other. To elicit the contribution of the amplitude to the cross-correlation, both the cross-correlation and cross-correlation amplitude were considered as metrics. The coherence metric used in these studies was

derived from the real component of the complex wavelet coefficients between the two channels at the previously chosen extracted frequencies.

Synchrony Index

The Synchrony Index (SI) used here was developed based on the method of Quiroga et al. (2002). SI is the average normalized phase difference between two EEG channels, and measures the variability in the phase difference between two signals in time, such that if the difference between the phases of two signals is constant, the synchrony index has a value closer to 1; and when the phase difference changes erratically with time, then the synchrony index is closer to 0. In essence, SI represents the phase contribution in the coherence calculation. The formula to compute the instantaneous non-linear SI is given as:

$$\gamma_{SI} = \text{sqrt}(\text{mean}[\cos(\phi_{xy})]^2 + \text{mean}[\sin(\phi_{xy})]^2)$$

where $\phi_{xy}=n*\phi_x(t) - m*\phi_y(t)$, *n* and *m* are integers, and ϕ_x and ϕ_y are the phases as obtained using the CWT described above. The key feature of γ_{SI} is that it is only sensitive to phase, and is consequently independent of signal amplitude. The SI metric was developed using custom-made software written in Matlab, with γ_{SI}, $n=m=1$.

Synchrony Entropy Index

Synchrony Entropy Index (SEI) measures the deviation of phase differences from the uniform distribution. The SEI metric was quantified using an index based on Shannon's

entropy (Tass et al. 1998).First, a histogram of the phase differences ϕ_{xy} is created for all the time points in the window, and divided into bins uniformly distributed around the unit circle. The entropy h_N is then defined as:

$$h_N = -\sum_{j=1}^{L} p_j \log p_j$$

where p_j is the probability corresponding to the jth bin, and L is the number of bins. This value can then be normalized to the maximum entropy, which is achieved with a uniform distribution where $p_j = 1/L$ for all bins j, and $h_N^{max}=\log(L)$. This normalized entropy is the SEI, calculated as:

$$SEI = \frac{h_N^{\max} - h_N}{h_N^{\max}}$$

SEI has values between 0 and 1, and is a measurement that reflects the degree of clustering of the distribution of the phase differences. Thus, if there is are similarities between the phase difference values in particular segments of the time series (i.e. phase difference is more constant), SEI has a value closer to 1, and if the phase differences are more erratically distributed, then SEI has a value closer to 0. A similar method was used to calculate Entropy Amplitude Index (EAI), which measures the degree of clustering in the distribution of amplitude differences. The SEI metric was developed using custom-made software written in Matlab.

Instantaneous Phase Synchrony Distribution

Instantaneous Phase Synchrony Distribution (IPSD), our own innovative method examined the kurtosis (fourth moment) of the distribution of phase differences between both channels, and is given by (Press et al., 1988).

$$k = \frac{E(x-\mu)^4}{\sigma^4}$$

where μ is the mean of x, σ is the standard deviation of x, and $E(t)$ is the expected value of quantity t based on a Gaussian probability density function.

Kurtosis is a measurement that reflects the shape of the distribution about the mean, compared to the normal distribution. Thus, if a distribution is sharp, with few outliers and most values centered about the mean, then it is called "leptokurtic" and has a lower kurtosis value, whereas if the distribution is flat, with more outliers and a broad distribution about the mean, then it is called "platykurtic" and has a higher kurtosis value. Examining the shape of the distribution of the phase differences may provide unique insight into the limits of synchronization between two parts of the brain and how they change during a seizure when compared with baseline conditions.

Finally, we implemented two amplitude synchrony measures.

The Amplitude Synchrony Index (ASI) of two EEG time series for each frequency was estimated by computing the correlation between the demodulated amplitude parameter (Nikouline et al., 2001, Burns et al., 2000).

Entropy Amplitude Index

We applied the same entropy measure (SEI) that was used for phase to the demodulated amplitude to create the Entropy Amplitude Index (EAI).

Statistical Analysis

To assess all synchrony measures, repeated Measures Factorial ANOVA (GLM) with two factors was used: a) EEG frequency with 5 levels (8, 14, 20, 40 and 60 Hz), and b) seizure condition with 3 levels (baseline, pre- seizure, and seizure). Post-hoc tests (Tukey's HSD) were assessed to localize the source of the variance. General linear mixed models repeated measures regression was used to test the statistical independence of amplitude and phase synchrony measures. General linear mixed model approach will be taken to perform repeated measures regression to predict phase synchrony measures using amplitude synchrony measures as a test of independence

Results

Hippocampal and Cortical Power

The analysis of hippocampal EEG power revealed significant main effects for frequency ($F_{4, 206} = 63.30$, $p < 0.001$) and seizure condition ($F_{2,206} = 44.60$, $p < 0.001$) and also a significant interaction between these two factors($F_{8,206} = 4.85$, $p < .001$). Post hoc tests demonstrated significant drops in EEG power between baseline and pre-seizure at the 8, 14, 20 and 40 frequencies ($p < .028$, for all frequencies).

The analysis of cortical power demonstrated similar effects; significant main effects for frequency ($F_{4, 206} = 12.94$, $p < 0.001$) and seizure condition ($F_{2,206} = 15.1$, $p < 0.001$) but no significant interaction between these two factors($F_{8,206} = 1.144$, $p = .335$). Post hoc tests demonstrated significant drops in EEG power between baseline and pre-seizure at the 8, 14 and 20 frequencies ($p < .035$, for all frequencies).

Phase Synchrony

IPSD

Figure 3 shows the results for the IPSD metric comparison between hippocampal and neocortical EEG channels. ANOVA results demonstrate no main effect differences, however, a significant interaction between frequency and pre-seizure condition ($F_{8,206} = 2.16$, $p = 0.033$) is observed implying that synchrony differences are condition and frequency dependent. Post-hoc tests supported this finding because only at 8 hz frequency there is a significant difference between the baseline (mean = -1.208) and pre-seizure (mean= -1.048) conditions. This implies that the probability density function of the baseline condition is more leptokurtic than pre-seizure condition because the kurtosis value is lower. Therefore, the baseline condition has a sharper distribution when compared with the pre-seizure condition at 8Hz (see figure 3).

Synchrony index

The analysis SI demonstrated significant main effects for frequency ($F_{4, 206} = 16.90$, $p < 0.001$) and a trend in seizure condition ($F_{2,206} = 2.30$, $p = 0.102$) but no significant

interaction between these two factors. Post hoc test could differentiate between the baseline and pre-seizure condition at any frequency, but at 14 Hz it could differentiate between baseline and seizure ($p = .001$) and pre-seizure and seizure ($p = .016$).

SEI

Similar to SI the analysis of SEI demonstrated significant main effect for frequency ($F_{4, 206} = 25.85$, $p < 0.001$), however, this was not the case for seizure condition or the interaction between these two factors. Post hoc test could not differentiate between the baseline and pre-seizure condition at any frequency, but at 14 Hz it could differentiate between baseline and seizure ($p = .001$) and pre-seizure and seizure ($p = .013$).

Amplitude Synchrony

The ASI demonstrated significant main effects for frequency ($F_{4, 206} = 2.45$, $p = 0.044$) and seizure condition ($F_{2,206} = 27.13$, $p < 0.00001$) but no significant interaction between these two factors. Post-hoc tests demonstrated that at 60 Hz frequency could baseline and pre seizure conditions could be differentiated ($p = .041$).

Similar findings EAI were observed with significant main effects for frequency ($F_{4, 206} = 63.58$, $p = 0.01$) and seizure condition ($F_{2,206} = 5.95$, $p = 0.003$) but no significant interaction between these two factors, however post hoc test could not differentiate between the baseline and pre-seizure condition at any frequency (see figure 4).

Joint Amplitude and Phase Synchrony Measures

Cross-Correlation (CC)

The CC synchrony measure demonstrated no significant main effect for frequency but there was for seizure condition ($F_{4, 206} = 17.51$, $p < 0.001$) and not for the interaction between these two factors. Post hoc tests could only differentiate between the baseline and pre-seizure condition at 8 Hz ($p = .03$).

Coherence (Coh)

Similar to the CC measure the analysis of Coh demonstrated that there were no significant main effect for frequency but there was for seizure condition ($F_{4, 206} = 19.46$, $p < 0.001$) and not for the interaction between these two factors. Post hoc test could not differentiate between the baseline and pre-seizure condition at any frequency

Regression and Correlation

A general mixed model was used to perform repeated measures regressions in order to predict CC values for the cortical and hippocampal channels from amplitude and phase synchrony measures while taking into account the main and interaction effects for frequency and seizure condition factors. It was discovered that the amplitude synchrony measure (ASI, $p < .001$) and the phase synchrony measure (SI, $p= .034$) were significant predictors and this regression model explained 29% of the variance (estimated R^2). Additionally, the same analytical approach was used to predict Coh using amplitude

synchrony (ASI, p = .032) and the phase synchrony measure (SI, p= .026), which turned out to be significant predictors, and this regression model explained 25% of the variance (estimated R^2).

IPSD was significantly correlated to the other phase synchrony measures, SI (r = -.683), and SEI (r= -.737) only at 8 Hz and not at any other frequencies implying that IPSD is also a valid measure of synchrony. These results were substantiated with a repeated measures regression model that was used to predict IPSD, from SI and SEI while adjusting for condition, frequency, and their interaction. SI ($p < .001$) and SEI ($p = .003$) were significant predictors, CC approached significance (p =.099), and as expected SAI was not a significant predictor. This model explained 16% of the variance. Additionally, in another similar model we found that the interaction between frequency, condition, and SI was highly significant ($p < .001$) implying that the linear relationship between IPSD and SI is frequency and condition dependent, supporting the findings that correlation between IPSD and the other phase synchrony measures can be found only at 8 Hz. Additionally, this regression model explained 34% of the variance (estimated R^2).

Repeated measures regression was used to predict ASI values from amplitude and phase synchrony measures while taking into account the main and interaction effects for frequency and seizure condition factors. It was discovered that the amplitude synchrony measure (EAI, $p < .001$) was a significant predictor and the phase synchrony measures SI, SEI and IPSD were not. However, the joint synchrony measure CC was also a significant predictor ($p < .001$);,and this regression model explained 57% of the variance. The same repeated measures regression approach was used to predict ASI from

hippocampal and cortical power, but these measures were not significant predictors. Interestingly, these same measures were found to be significant predictors of the other amplitude synchrony measure EAI (hippocampal, $p < .001$, and cortical, $p = .008$), and in this model, 12.5% of the variance was explained. These results are reflected by the significant correlation of $r = .609$ between ASI and EAI at all frequencies and similar significant values at the five individual frequencies that range from $r = .55$ to $r = .68$ and a mean of $r = .60$.

Discussion

In this investigation we validated our novel phase synchrony method, IPSD, and assessed the capabilities of widely used synchrony methods, by the application of these methods to the task of detecting subtle changes in the EEG synchrony that precede a seizure. This validation and assessment were made possible because of the highly controlled environment of an experimental seizure model where the etiology, intensity, and the exact timing of the pre-seizure condition were known. When timing is known it is possible to clearly identify a pure baseline condition, where the EEG has no propensity to seizure, and it also makes it easier to identify the pre-seizure and seizure condition. In this experimental paradigm the effect size is maximized because the experimental manipulation is considerable and the non-experimental variability between and within animals is minimal, therefore, it is possible to detect subtle differences in synchrony between baseline and pre-seizure. Therefore, we propose that in order to assess any new

synchrony method, a similar experimental protocol to the one we have applied should be considered.

It was possible to differentiate between baseline and seizure conditions at all frequencies in many of the synchrony and power measures, which was not unexpected because a seizure elicited this way produces large and global brain dynamical changes (See Table 1). However, the analysis of interest is the differentiation of baseline and pre-seizure, which appears to be more of a difficult task because it was possible to do so with only three synchrony measures at a specific frequencies: CC, IPSD at 8 Hz, and ASI at 60 Hz. Hippocampal and cortical power could both differentiate between baseline and pre-seizure conditions at 8, 14, and 20 Hz, while at 40 Hz, only the hippocampal channel could. Even though there are power differences between the baseline and pre-seizure conditions, this is not a reliable indicator that there is a propensity to seizure because there are many other factors that can modulate EEG amplitude (e.g., changes in arousal, eyes opening or closing, etc.). In the amplitude synchrony modality, ASI and EAI are highly correlated to each other but only EAI is correlated to hippocampal and cortical power. ASI differentiates between baseline and pre-seizure at the gamma range (60Hz) while the hippocampal and cortical power do not. Therefore, we propose that the capacity of ASI to differentiate between baseline and pre-seizure is independent of the EEG power measures because there is no correlation between them. Furthermore, phase synchrony measures are not predictors of ASI, and we also propose that amplitude synchrony measures are independent of phase synchrony and provide a totally different piece of information, and therefore should also be considered when synchrony is

assessed. Chavez et al., (2003) reported phase and amplitude synchrony measures depicted similar results, however, this effect can be ascribed to the fact that the dataset was limited (two subjects) and instead of an experimental animal model, a human model was used.

Furthermore, the regression models for joint measures of synchrony, cross-correlation and coherence, demonstrate that amplitude and synchrony measures contribute different and apparently independent sources of the total synchrony between two channels. Additional support for these results is that in other regression models, amplitude synchrony measures are not predictors of phase synchrony measures, and vise versa.

The similarities and differences between measures have revealed that even though many of these measures are based on phase synchrony, they may be describing similar or different aspects of this phenomenon. As exemplified by the correlation and a regression model, the linear relationship between IPSD and SI is frequency dependent.

The regression models for the joint amplitude and synchrony measures CC and Coh show that amplitude and phase synchrony measures only explain a small to moderate amount of the total variance leaving a large amount of variance unexplained. Therefore, it is still worthwhile to use CC and Coh in examining EEG seizure data because the unexplained variance might be sensitive to synchronous EEG changes not detected by phase and amplitude synchrony measures.

Unlike many of the techniques used to generate the metrics used to predict onset of seizure, the IPSD technique may not be as susceptible to the non-linear and time-variant nature of EEG, mainly because it probes a distribution of phase differences, rather than using instantaneous differences. IPSD may also provide evidence for key physiological consequences of seizures. Hippocampal interneurons contribute an ~8Hz theta rhythm to the overall EEG signal, which is generally present whenever the hippocampus is active. Recent data has shown that the hippocampal theta rhythm is dramatically affected by seizures, such that shortly after a seizure, the hippocampal theta rhythm shifts from ~8Hz to ~6Hz, and gradually comes back to normal well after a seizure has stopped. (Huxter, 2007) Thus, a large proportion of cells that normally fire at ~8Hz may shift their firing properties towards a lower average frequency set point following a seizure, resulting in more outliers and a lower peak about the 8Hz mean, potentially yielding a broader "platykurtic" distribution with respect to 8Hz. Our data support this theory, since the IPSD mean value does become significantly higher about 8Hz in the pre-seizure (mean = -1.048) when compared with the baseline (mean= -1.208) conditions ($p<.01$), demonstrating that the distribution of cell firing is more "platykurtic", and suggesting that the shift in the theta rhythm observed following a seizure may occur to a smaller extent immediately preceding seizure onset. There is also evidence that the delta rhythm may be affected in a similar fashion by seizures, and the application of IPSD about a frequency value in this range may be useful in further increasing the accuracy of a seizure prediction algorithm.

As useful as these measurements are, there are a number of limitations to these techniques that must be addressed. EEG recordings have a complex time- and frequency-domain structure that tends to be non-linear and time-variant, and were processed with the CWT for the purposes of generating many of the metrics described in this paper. The CWT is calculated using a process that is analogous to the Fourier Transform (FT), which is a linear operator that was originally defined for use with linear time-invariant signals. Since EEG signals tend to be non-linear and time-variant over a physiologically relevant time scale, seizure prediction algorithms that are based strictly on the FT, and the CWT, may not be reproducibly precise. Since SI is a non-linear measurement based on the CWT, it can also be susceptible to the breakdown in accuracy due to the non-linear and time-variant nature of EEG signals.

The coherence calculation is also based on the same assumptions as were used to generate the CWT, namely that the two constituent signals are linear and time-invariant. Based on these assumptions, the coherence is bounded between 0 and 1 due to the "cross-spectrum inequality", which states that the cross-spectrum squared will always be less than or equal to the product of the autocorrelations of the constituent signals. (Bendat and Piersol, 1993) These assumptions break down when non-linear time-variant EEG signals are used, leading to a potential loss in accuracy in seizure prediction when coherence is used alone.

Conclusions

In summary there are several finding of import in this study. First of all, it was possible to differentiate between baseline and pre-seizure EEG with several methods at different frequencies. In addition, our newly developed IPSD analysis also appears to be a valid tool for differentiating between baseline and pre-seizure EEG states and with further development it could be an important measure of synchrony in epilepsy research. Si milarly, amplitude synchrony measures were found to be independent from phase measures and we speculate that they are measuring two very different neural synchrony mechanisms. The experimental animal model used in this study provided the controlled experimental platform from which to carry out the assessment of the synchrony measures. Therefore, in order develop algorithms to predict seizure onset on a timely basis to allow for intervention, we propose that it is optimal to use a variety of measures based on both phase and amplitude synchrony analyses. Moreover, this experimental approach and analysis methods, if coupled with a careful comparison with human pre-seizure/seizure EEG recordings, should be invaluable for the development of a useful seizure prediction algorithm.

Table 1. shows the post-hoc test p-value results for the comparison of all the metrics across the 6 frequencies, separated by the 3 EEG conditions. When considering only one frequency at a time, the ability of cross-correlation, coherence, entropy, and wavelet methods to distinguish between baseline and pre-seizure EEG states broke down. For example, the cross-correlation metric was only able to distinguish between the two states of interest at 8Hz only ($p<.05$). The wavelet and IPSD methods were the only ones to reliably distinguish baseline and pre-seizure EEG states, particularly at 8Hz.

Table 1: p-values associated with comparison of metrics across frequencies separated by EEG states

Post-Hoc Tests (LSD)										
Freq	Conditions	CC	Coh	SI	SEI	ASI	IPSD	EAI	WaveP1	WaveP2
8Hz	**1 vs 2**	0.03	ns	ns	ns	ns	0.008	ns	< 0.001	< 0.001
	1 vs 3	0.002	0.001	ns	ns	0.038	ns	ns	ns	< 0.001
	2 vs 3	ns	ns	ns	ns	ns	ns	ns	< 0.001	ns
14Hz	**1 vs 2**	ns	ns	ns	ns	ns	ns	ns	< 0.001	0.005
	1 vs 3	0.013	< 0.001	0.001	0.001	0.005	0.03	ns	ns	0.006
	2 vs 3	ns	ns	0.016	0.013	ns	0.002	ns	< 0.001	ns
20Hz	**1 vs 2**	ns	ns	ns	ns	ns	ns	ns	< 0.001	0.034
	1 vs 3	0.025	0.004	ns	ns	0.001	ns	ns	ns	0.024
	2 vs 3	ns	ns	ns	ns	0.027	ns	ns	0.004	ns
40Hz	**1 vs 2**	ns	ns	ns	ns	ns	ns	ns	0.027	ns
	1 vs 3	0.01	ns	ns	ns	< 0.001	ns	0.015	ns	ns
	2 vs 3	ns	ns	ns	ns	0.009	ns	ns	ns	ns
60Hz	**1 vs 2**	ns	ns	ns	ns	0.041	ns	ns	ns	ns
	1 vs 3	0.008	0.041	ns	ns	< 0.001	ns	0.023	ns	ns
	2 vs 3	0.048	ns	ns	ns	0.032	ns	ns	ns	ns

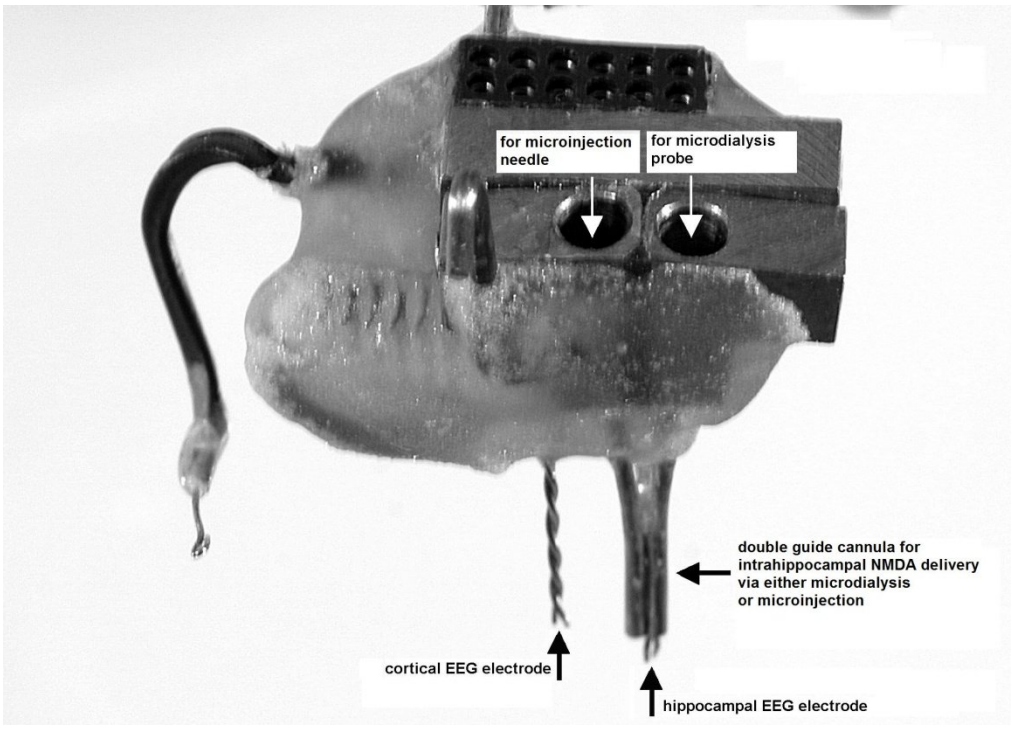

Fig. 1. Electrode and microdialysis setup

Fig 2

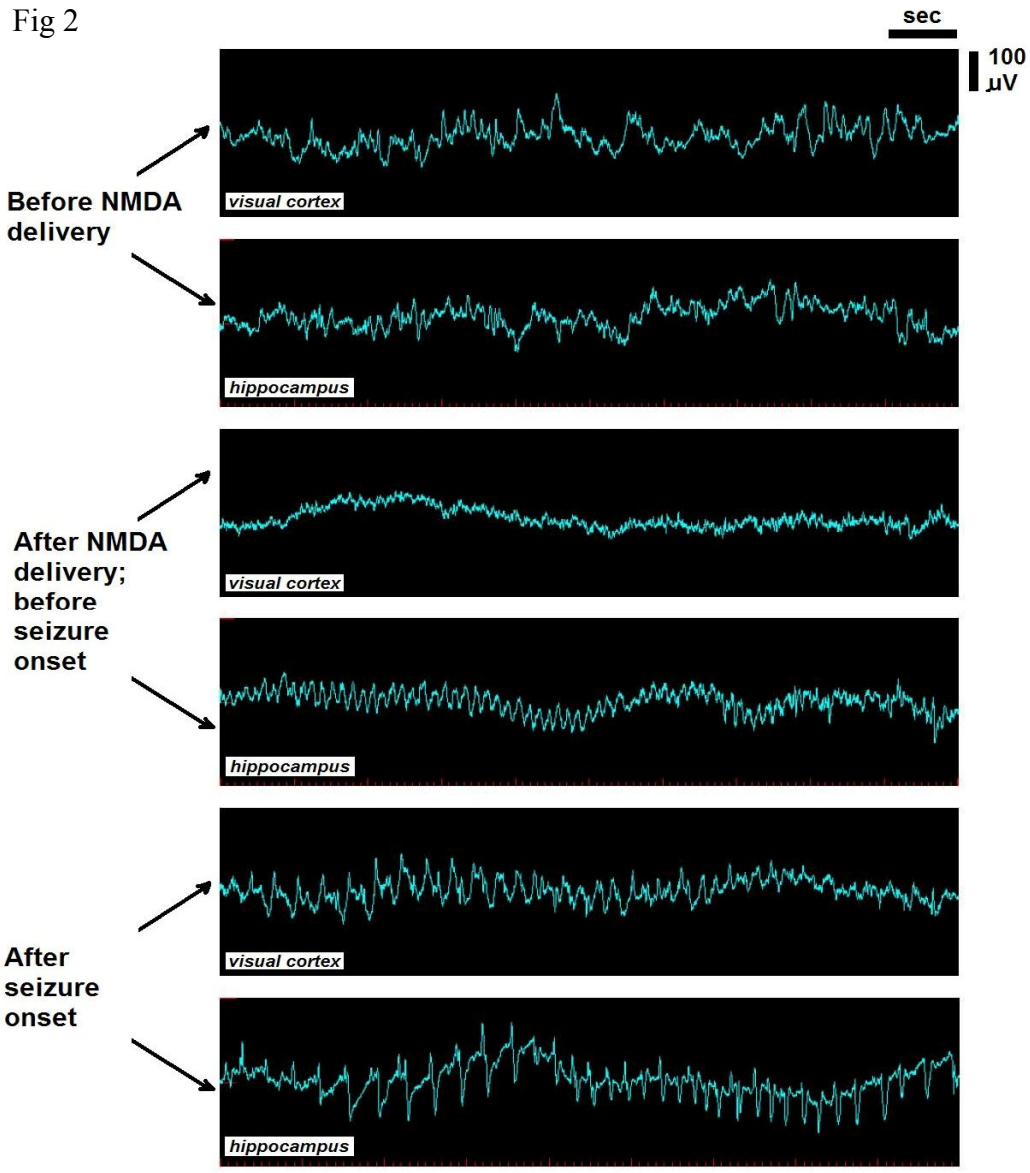

Fig. 2
EEG hippocampal and neocortical data from the three experimental phases: Baseline (before NMDA) , pre seizure (after NMDA), and seizure.

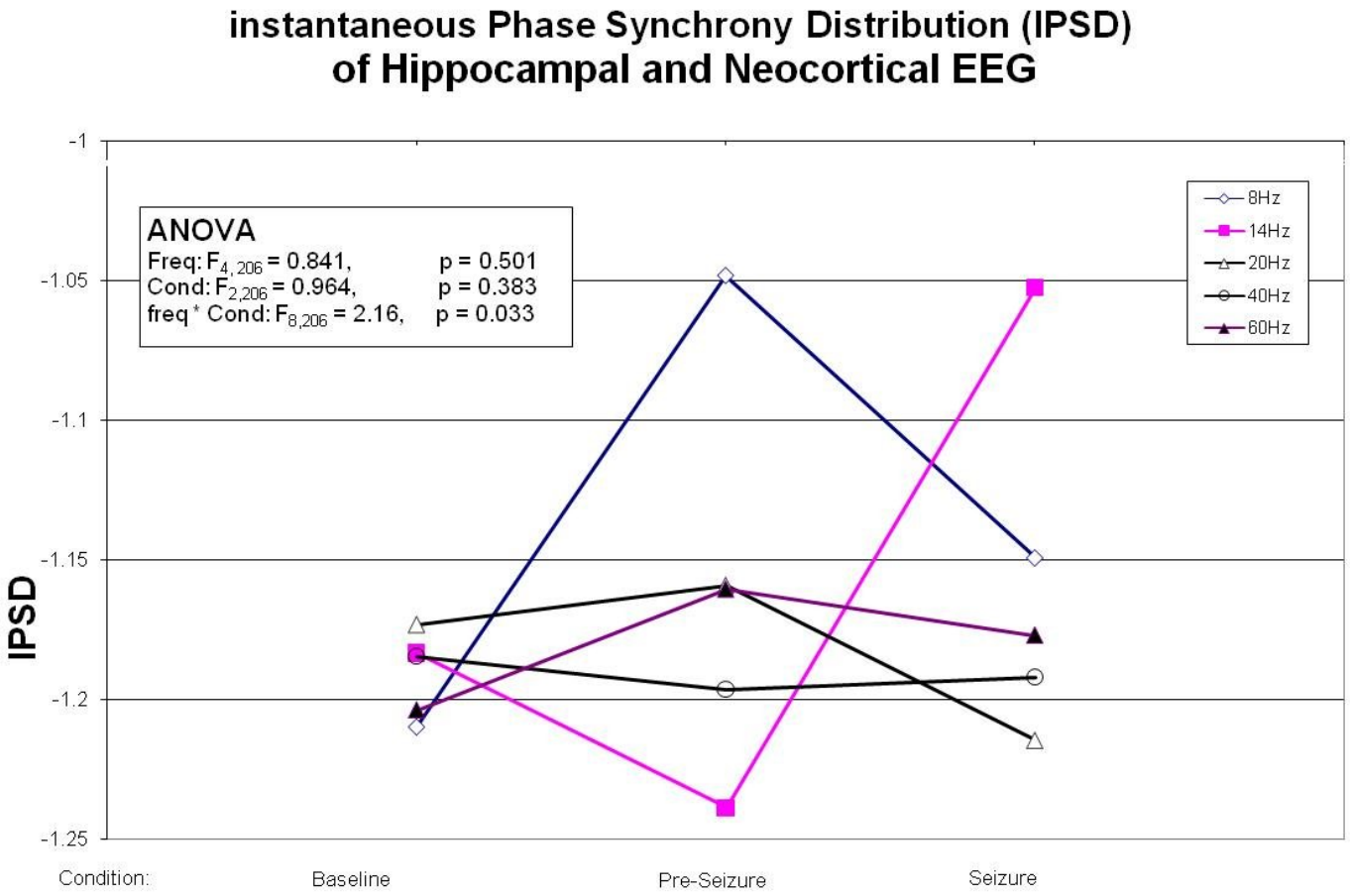
instantaneous Phase Synchrony Distribution (IPSD)
of Hippocampal and Neocortical EEG
ANOVA
Freq: $F_{4, 206}$ = 0.841, p = 0.501
Cond: $F_{2,206}$ = 0.964, p = 0.383
freq * Cond: $F_{8,206}$ = 2.16, p = 0.033
8Hz
14Hz
20Hz
40Hz
60Hz
IPSD
-1
-1.05
-1.1
-1.15
-1.2
-1.25
Condition:
Baseline
Pre-Seizure
Seizure

Fig. 3

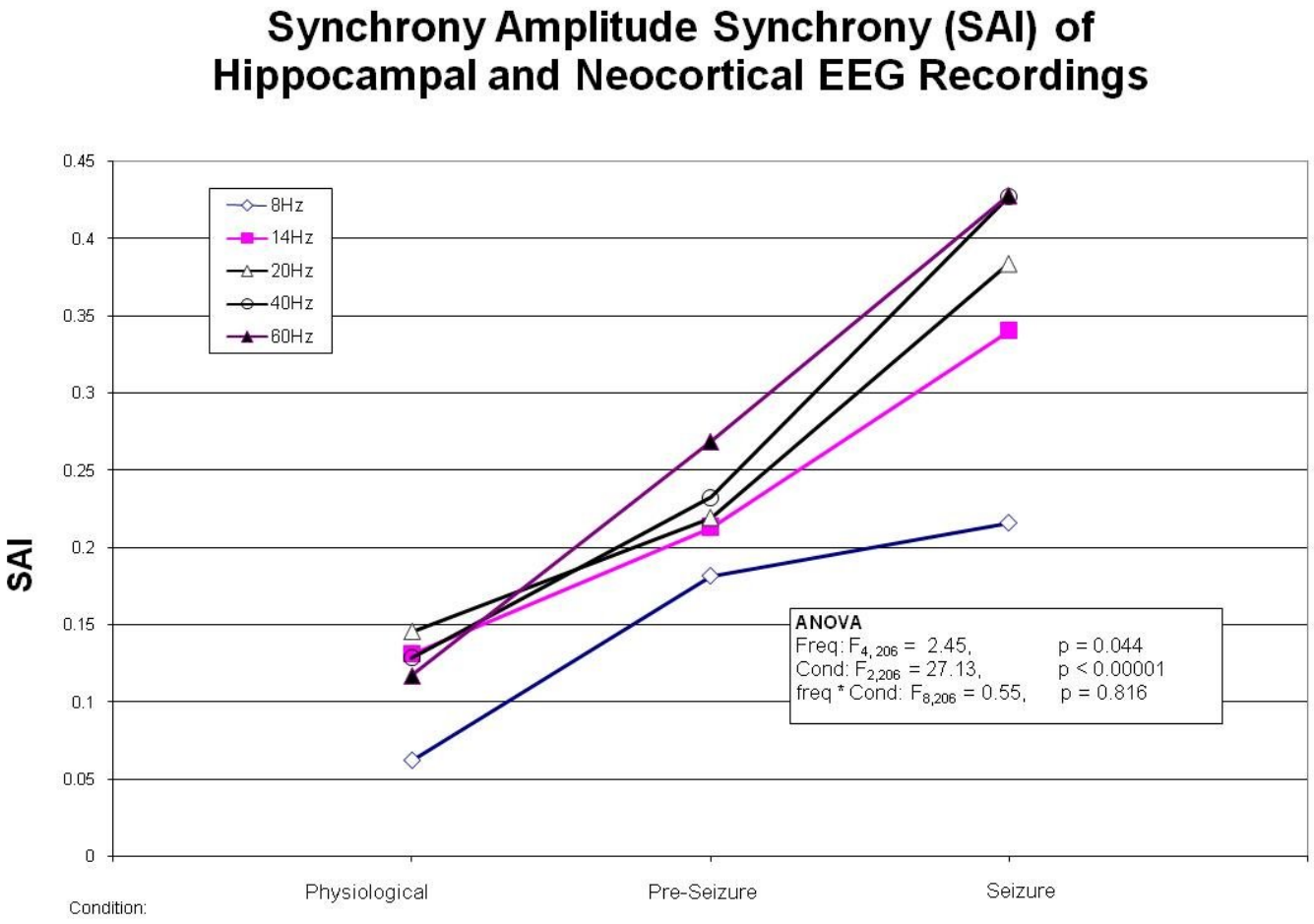
Synchrony Amplitude Synchrony (SAI) of Hippocampal and Neocortical EEG Recordings
SAI
0.45
0.4
0.35
0.3
0.25
0.2
0.15
0.1
0.05
0
8Hz
14Hz
20Hz
40Hz
60Hz
ANOVA
Freq: F4, 206 = 2.45, p = 0.044
Cond: F2,206 = 27.13, p < 0.00001
freq * Cond: F8,206 = 0.55, p = 0.816
Physiological
Pre-Seizure
Seizure
Condition:

Fig. 4

Gradual and time-locked changes in amplitude and phase synchrony observed in EEG during sleep onset

Hans von Gizycki, Dissertation Part2, Cognitive Neuroscience, CCNY, CUNY

Dr. Arthur J. Spielman, Dissertation Supervisor

Scientific Computing Center, SUNY Downstate Medical Center, Brooklyn, NY, U.S.A.

Key words: Phase Synchrony, Amplitude Synchrony, sleep onset, EEG activity, Instantaneous Phase Synchrony Distribution.

Running title: Sleep Onset Synchrony Changes

Corresponding author: Hans von Gizycki, Scientific Computing Center, SUNY Downstate Medical Center, 450 Clarkson Avenue, Box 7, Brooklyn, New York, 11203, USA ; Tel.: (718) 270-7474; Fax: (718) 270-7461;

E-mail: vongizycki@downstate.edu

Abstract

Introduction: Spectral power, crosscorrelation, and coherence are among the most common mathematical measures used to analyze EEG sleep data. This presentation aims to analyze the evolution of EEG through the sleep onset process with Continuous Wavelet Transform (CWT) based measures of phase and amplitude synchronization, which have already been successfully used to analyze the EEG changes associated with seizures.

Methods: EEG was recorded from patients undergoing multiple sleep latency tests (MSLT) with full-night diagnostic polysomnogram. Resultant data were first visually examined in 10-15 second epochs and scored based on the attenuation of occipital alpha to create 11 second epochs of EEG data comprised of 5 seconds prior to sleep onset, 1 second of the actual sleep onset transition and 5 seconds post sleep onset. Data was then split into montages designed to assess inter- and intra-hemispheric changes in the measures considered, which included: a) conventional methods: cross correlation (CC) and coherence (Coh); b) phase synchrony measures: synchrony index (SI), synchrony entropy index (SEI), and instantaneous phase synchrony distribution (IPSD); and c) amplitude synchrony measures: synchrony amplitude index (SAI), and entropy amplitude index (EAI).

Results: Repeated measures factorial ANOVA and post hoc tests, with EEG frequency bands, montage, and wake/sleep transition as factors, demonstrated that it was possible to differentiate between wake and sleep in the EEG power measures, as well as in many of the amplitude and phase synchrony/entropy measures. Multiple regression analysis of the synchrony and entropy measures confirmed that the time course of the sleep onset

process is composed of both gradual and abrupt changes in the EEG time course, lending further evidence for the role of thalamocortical cells in regulating sleep onset. Furthermore, results demonstrate that amplitude and phase synchrony measures are not significantly correlated and are both independent predictors of cross correlation, which is composed of both amplitude and phase synchrony. Nevertheless, both methodological approaches allowed for the differentiation between wake and sleep. Furthermore, synchrony and entropy measures were shown to be independent of each other, suggesting they may both be useful in the analysis of the sleep cycle.

Conclusion: Phase and amplitude synchrony analyses provided quantitative results helpful in differentiating between wake and sleep conditions, as well as examining the EEG changes that occur throughout sleep onset. Results demonstrated that synchrony and entropy measures were able to detect the gradual and abrupt EEG changes in sleep onset, providing supporting evidence for the theory that thalamocortical networks are responsible for controlling the sleep cycle. Furthermore, the results showed that the amplitude and phase synchrony measures are independent of each other, and yet are both predictors of the crosscorrelation, demonstrating that crosscorrelation is a mix of amplitude and phase synchronization patterns. Taken together, amplitude and phase synchrony and entropy measures were invaluable in the study of sleep onset, and the sleep cycle in general. Use of these measures may be critical in developing algorithms for detecting sleep onset, sleep phase transitions, and sleep pathologies.

Introduction

Sleep onset in humans is closely linked to characteristic changes in behavior, mental activity, physiological state, and the temporal dynamics of EEG signals. (Ogilvie 2001). Some of the more commonly recognized sleep related events observed in EEG during sleep onset include the appearance of sleep spindles and K-complexes, as well as a gradual decrease in power in the beta (15-30Hz) spectral band occurring simultaneously with an increase in power in the delta (1-4Hz), theta (4-8Hz), and sigma (12-15Hz) spectral bands. Power in the alpha (8-11Hz) band displays strikingly different temporal changes, declining gradually across the sleep onset period with high-frequency EEG components, reaching a minimum at sleep onset, and gradually rising with the lower-frequency components of the EEG (Ogilvie, 2001).

The onset of sleep has been described in detail as a sequelae of events by Hori et al., (1994) who divided the sleep onset process into 9 distinct stages defined as first a gradual decrease in the alpha activity (stages 1-4), followed by the appearance of vertex sharp waves (K-complexes) and eventually spindles. This classification system demonstrates that sleep onset as monitored by EEG is concurrently a gradual and abrupt process: gradual onset of specific long-term changes, such as a gradual decrease in the alpha activity, followed by abrupt changes detected as spindles and K-complexes, which may correspond to "on/off" transitions that occur as certain regions in the brain enter a new sleep state (Hori 1994; Ogilvie, 2001). Based on these criteria, the onset of sleep was based on the changes in alpha waves as well as presence of spindles.

Spectral power methods have proven useful in the quantification of the types of changes that occur in EEG signals recorded during the sleep onset period, allowing for valuable comparisons to other quantitative physiological measures. The decrease in power of the high frequency component of the EEG, for example, has been shown to occur simultaneously with a decline in the firing rate of cholinergic brainstem-thalamic wake-promoting neurons, which are responsible for inhibiting GABAergic sleep-promoting neurons localized to the ventrolateral preoptic (VLPO) area of the hypothalamus (Merica 2004). Furthermore, it has been hypothesized that synchronization of low (i.e. delta) and high frequency (i.e. spindles) components of thalamic activity, which may arise from an intracortical neuronal network that generates synchronous slow oscillations, may be responsible for the complex time-varying signals observed by EEG at the cortex (Steriade et al., 1991; Timofeev and Steriade, 1996). Such synchronous low frequency oscillations are a typical feature of normal physiological sleep in the cat (Steriade et al., 2001; Destexhe et al., 1999) and in humans (Achermann and Borbely, 1997; Steriade and Amzica, 1998). Increases in delta and theta power have also been closely associated with an increase in interhemispheric coherence (Achermann and Borbely, 1998). There is substantial evidence supporting the theory that changes in interhemispheric coherence and crosscorrelation in the delta and spindle frequencies associated with sleep are mediated by the corpus callosum (Corsi-Cabrera et al., 1996; Achermann and Borbely, 1998). Coherence has also been shown to have a topographic pattern, such that the anterior regions of the brain are more coherent during sleep-promoting stages of EEG, whereas posterior regions are more coherent during wake-promoting stages of EEG (Hori 1998). The methods used by previous studies to assess hemispheric synchrony changes

during sleep onset are coherence and crosscorrelation, which are both joint measures of phase and amplitude synchrony. (Corsi-Cabrera et al., 1996; Achermann and Borbely, 1998).

One major outcome of the study of time-courses of power, crosscorrelation, and coherence in the different frequency bands of EEG recorded during sleep is the experimental confirmation of the Neuronal Transition Probability (NTP) model (Merica 2004). The NTP model hypothesizes that the changes observed between the beta, sigma, and delta EEG bands throughout sleep onset are the result of stochastic transitions of the firing-rate frequencies of the brainstem-thalamic "wake"-promoting cholinergic neurons: first a cascade of transitions that decrease the mean firing rate and firing-rate frequency towards sleep onset, followed by a cascade of transitions that increase the firing rate and frequency away from deep sleep. The time-courses of firing rate patterns corresponding to each sleep state form an overall template that modulates thalamic and cortical output. The stochastic firing rate changes generated in the brainstem/thalamus form the complex waveforms detected by EEG at the cortex, and the EEG power spectrum changes are related to the proportion of the entire brain-stem population that transitioned to a particular sleep-state related firing pattern – a process that can be gradual or abrupt depending on sleep state (Merica 2003; Merica 2004; Hori 1994).

Fourier- and correlation-based methods, including the power spectrum and coherence, have been useful in identifying the types of EEG changes observed with sleep onset, however, these methods are severely limited when compared with newly developed synchrony methods (Tass et al., 1998). We propose to apply novel and known synchrony

methods to examine the time course of sleep onset EEG from humans that underwent a Multiple Sleep Latency Test (MSLT) protocol. Previous work with EEG signals obtained from a well-controlled experimental animal model of seizures has demonstrated that such measures are reliably sensitive to subtle changes in synchrony of the signals that occur prior to and after onset of seizure (von Gizycki 2008). These measurements may be useful in analyzing synchronization/desynchronization transitions that occur throughout the time course of sleep onset, and may be invaluable to examining the gradual and abrupt EEG changes expected based on the Hori sleep stage classification system. The measures considered as part of this study included: phase & amplitude synchrony (Tass et al., 1998; Nikouline et al., 2001; Bruns et al., 2000), which we hypothesize to involve different types of information, and suggesting that they are independent of each other; synchrony entropy index (SEI) and instantaneous phase synchrony distribution (IPSD), which examine the shape characteristics of the phase synchrony distribution; and entropy amplitude index (EAI) which examines the shape of the amplitude synchrony distribution. Using the above synchrony and distribution-based measures at a high temporal resolution in the analysis of EEG patterns will allow for a quantitative examination of the observations that have been described qualitatively by others: that sleep onset may lead to a combination of gradual and abrupt changes in the synchronization patterns of EEG across hemispheres (Ogilvie 2001, Merica 2004). We will also utilize more conventional measures of cross-correlation and coherence, which reflect the similarity of both the amplitude and phase synchrony information simultaneously.

Methods

Subjects: Patient data for this study were selected from among all the patients evaluated by the New York Methodist Hospital Sleep Center during a 2007 year (N=17). Use of the clinical data for research purposes was approved by the Institutional Review Board of New York Methodist Hospital. Data will be obtained from previously collected clinical data from multiple sleep latency tests (MSLT) and it will be utilized to test the hypothesis for this study. Patients underwent a full-night diagnostic polysomnogram (NPSG) and for evaluation of hyper-somnolence prior to their MSLT. Each subject will provide data from five MSLT naps where they had an opportunity to fall asleep in an environment conducive for sleep. The MSLT naps where conducted starting at 9 am at 2-hour intervals with each nap lasting 20 minutes (Arand et. al, 2005). Therefore, within this nap context it is possible to record one or more episodes of sleep onset.

The patients were evaluated in an accredited sleep laboratory in sound attenuated rooms, monitored by an infrared camera. A 10-channel montage was utilized for MSLT recordings comprised of EEG, EOG, EKG, and chin EMG. Telefactor/EEG32 hardware and software were utilized for polysomnographic recordings. Standard sleep recording montage was used (C3, C4, O1, 02, referenced to contra-lateral mastoid. EEG was sampled at 200 Hz, with 12 bit precision. Amplifier settings for the EEG channels were set as follows: sensitivity = 200 μV, high pass filter = .3Hz, low pass = 70Hz, and 60Hz a notch filter.

Montages

Synchrony was measured across two channel derivations in a several montages to assess different types of brain inter-connectivity: 1) Inter-hemispheric synchrony measured across a) ipsilateral posterior derivations (O2/A2/-O1/A1), and b) across ipsilateral central derivations (C4/A2-C3/A1). 2) Intra-hemispheric synchrony a) across ipsilateral posterior to central derivations (O2/A2-C4/A2), and b) across (differential) central-posterior derivations (C3/C4-O1/ O2).

Data Selection and Visual Scoring

The EEG data was selected using Grass Telefactor PSG TWin 2.6 from the overall data set for each MSLT nap. Each nap was delimited and selected from the formal beginning of the nap "lights out" to the formal end "lights on". Transitions from wake to sleep are very labile during the early sleep onset period. Therefore, we examined relatively short epochs of stable sleep onset events that usually lasted under 15 seconds (Figure 1). EEG was first scored in 10-15 second epochs and then each epoch was rescored in five second epochs.

In order to localize the sleep onset transition wake/sleep scoring was performed at five second intervals and defined as the attenuation of occipital alpha (Hori 1994, Rechtschaffen & Kales, 1968). Additionally, the exact moment of sleep onset was visually defined, because it was precisely with proprietary software where the investigator put a cursor right at the estimated moment of sleep onset (Figure 1). This

scoring approach was used to create 11 second epochs of EEG data comprised of 5 seconds prior to sleep onset, 1 second of the actual sleep onset transition and 5 seconds post sleep onset.

Data Analysis

Continuous Wavelet Transform

Wavelets were used to extract phase and amplitude information because wavelets allow synchrony measures to have a higher temporal resolution than FFT based measures, such as coherence. Preliminary data transformation prior to synchrony analysis was performed as follows: First, EEG signals at 8 and 12 Hz were extracted from the EEG data using a continuous wavelet transform (CWT), applying a first order complex Gaussian wavelet (Matlab Wavelets Toolbox, Mathworks, inc). The CWT is useful for examining the time varying behavior of the frequency spectrum of a finite signal segment, and is mathematically defined as:

$$CWT_x^{\psi}(\tau, s) = \frac{1}{\sqrt{s}} \int x(t)\psi\left(\frac{t-\tau}{s}\right) dt$$

where *x(t)* is the signal segment, *s* is the scale that adjusts the wavelet to a particular frequency (higher scale corresponds to "stretched" lower frequency versions of the wavelet), τ is the window size for the wavelet, and $\psi(t)$ is the Gaussian wavelet defined as the first derivative of the Gaussian function normalized to have an area of 1:

$$\psi(t) = \frac{-t}{\sqrt{2\pi\sigma^3}} e^{\frac{-t^2}{2\sigma^2}}$$

The CWT is analogous to the Fourier Transform (FT), which identifies the frequencies present in a signal (i.e. spectrum), but resolved in the time domain such that with a CWT, one can identify the time course of the appearance and disappearance of particular frequencies present in a signal. Likewise, the real and imaginary components of a CWT are also comparable to the FT amplitude and phase. The imaginary components of the CWT results for both channels were transformed to an angular term and unwrapped, producing a phase time series for each EEG channel and allowing for the calculation of the phase differences between these channels. Additionally, the demodulated amplitude of the real component of the complex wavelet coefficients was extracted using a Hilbert transform, which involves the convolution of the signal with $h(t)=1/\pi t$. The transformed data were subjected to a series of synchrony analysis, as described below.

First we examined cross correlation and coherence between the hippocampal and cortical recordings. All measures considered here were computed in 1-second analysis bins.

Crosscorrelation

Crosscorrelation is an estimate of how similar two time series measurements are in the time domain while coherence is an estimate of how similar two time series measurements are in the frequency domain, taking the contribution of autocorrelations of each of the signals into account. Thus, cross-correlation detects temporal associations between two

time-series measurements, much like coherence detects the frequency components that are common to a set of signal. (Farmer et al.,1993). The cross-correlation approach used was an ordinary normalized covariance function, *R*, as given by

$$R(i,j) = \frac{C(i,j)}{\sqrt{C(i,i)C(j,j)}}$$

where *C* represents values in the covariance matrix as given by:

$$C_{(x_1,x_2)} = E[(x_1-\mu_1)(x_2-\mu_2)]$$

where *E* represents the mathematical expectation and $\mu_i=Ex_i$. These computations were performed using built-in functions in Matlab, however the innovation here is in the application of these techniques to determining the correlation between the real component of the complex wavelet coefficients from the two EEG channels at all previously extracted frequencies or scales.

Coherence

The coherence analysis employed here involves an approach analogous to the one used for cross correlation, where we examine the synchrony of the two EEG channels after using data processed with the CWT for all the frequencies of interest. Coherence is a FFT-based synchrony measure that estimates the magnitude squared coherence using power spectra as:

$$C_{xy}(f) = \frac{|P_{xy}(f)|^2}{P_{xx}(f)P_{yy}(f)}$$

where *Pxy* represents the cross power spectrum density between two inputs *x* and *y*, and *Pxx* and *Pyy* are the power spectral densities of signals *x* and *y*, respectively. This measure is bounded between 0 and 1, where 0 indicates that x and y have no linear relationship, and 1 indicates that x can perfectly predict y in a linear fashion.

In practice, cross-correlation and coherence are affected by both the amplitude and phase structure of each signal. Cross-correlation has a value between –1 and 1, such that there is no temporal association between the two signals when the cross-correlation is zero, and a high degree of negative or positive temporal association between the two signals when the value is –1 or 1, respectively. Coherence has a value closer to 1 when the phase difference between two signals is constant and/or when the frequency domain amplitudes of the two signals are correlated with each other. To elicit the contribution of the amplitude to the cross-correlation, both the cross-correlation and cross-correlation amplitude were considered as metrics. The coherence metric used in these studies was derived from the real component of the complex wavelet coefficients between the two channels at the previously chosen extracted frequencies.

Synchrony Index

The Synchrony Index (SI) used here was developed based on the method of Quiroga et al. (2002). SI is the average normalized phase difference between two EEG channels, and measures the variability in the phase difference between two signals in time, such that if the difference between the phases of two signals is constant, the synchrony index has a value closer to 1; and when the phase difference changes

erratically with time, then the synchrony index is closer to 0. In essence, SI represents the phase contribution in the coherence calculation. The formula to compute the instantaneous non-linear SI is given as:

$$\gamma_{SI} = \text{sqrt}(\text{mean}[\cos(\phi_{xy})]^2 - \text{mean}[\sin(\phi_{xy})]^2)$$

where $\phi_{xy}=n*\phi_x(t) - m*\phi_y(t)$, n and m are integers, and ϕ_x and ϕ_y are the phases as obtained using the CWT described above. The key feature of γ_{SI} is that it is only sensitive to phase, and is consequently independent of signal amplitude. The SI metric was developed using custom-made software written in Matlab, with γ_{SI}, n=m=1.

Synchrony Entropy Index

Synchrony Entropy Index (SEI) measures the deviation of phase differences from the uniform distribution. The SEI metric was quantified using an index based on Shannon's entropy (Tass et al. 1998). First, a histogram of the phase differences ϕ_{xy} is created for all the time points in the window, and divided into bins uniformly distributed around the unit circle. The entropy h_N is then defined as:

$$h_N = -\sum_{j=1}^{L} p_j \log p_j$$

where p_j is the probability corresponding to the jth bin, and L is the number of bins. This value can then be normalized to the maximum entropy, which is achieved with a uniform

distribution where p_j = 1/L for all bins j, and h_N^{max}=log(L). This normalized entropy is the SEI, calculated as:

$$SEI = \frac{h_N^{\max} - h_N}{h_N^{\max}}$$

SEI has values between 0 and 1, and is a measurement that reflects the degree of clustering of the distribution of the phase differences. Thus, if there is are similarities between the phase difference values in particular segments of the time series (i.e. phase difference is more constant), SEI has a value closer to 1, and if the phase differences are more erratically distributed, then SEI has a value closer to 0. A similar method was used to calculate Entropy Amplitude Index (EAI), which measures the degree of clustering in the distribution of amplitude differences. The SEI metric was developed using custom-made software written in Matlab.

Instantaneous Phase Synchrony Distribution

Instantaneous Phase Synchrony Distribution (IPSD), our own innovative method examined the kurtosis (fourth moment) of the distribution of phase differences between both channels, and is given by (Press et al., 1988).

$$k = \frac{E(x-\mu)^4}{\sigma^4}$$

where μ is the mean of x, σ is the standard deviation of x, and $E(t)$ is the expected value of quantity t based on a Gaussian probability density function.

Kurtosis is a measurement that reflects the shape of the distribution about the mean, compared to the normal distribution. Thus, if a distribution is sharp, with few outliers and most values clustered about the mean, then it is called "leptokurtic" and has a lower kurtosis value, whereas if the distribution is flat, with more outliers and a broad distribution about the mean, then it is called "platykurtic" and has a higher kurtosis value. Examining the shape of the distribution of the phase differences may provide unique insight into the limits of synchronization between two parts of the brain and how they change during sleep onset.

Finally, we implemented two amplitude synchrony measures.

The Amplitude Synchrony Index (ASI) of two EEG time series for each frequency was estimated by computing the correlation between the demodulated amplitude parameters (Nikouline et al., 2001, Bruns et al., 2000).

Entropy Amplitude Index

We applied the same entropy measure (SEI) that was used for phase to the demodulated amplitude to create the Entropy Amplitude Index (EAI).

Statistical Analysis

All synchrony measures were assessed across factors using repeated measures ANOVA. Sleep wake analysis initially consisted of using a General Linear Mixed Model (GLMMixed) to perform a factorial ANOVA with three factors: a) EEG frequency (8 and

12 Hz), b) synchrony montage with 4 levels: O2/A2-O1/A1, C4/A2-C3/A1, O2/A2-C4/A2, C3/C4-O1/O2) and, wake/sleep with two levels (wake and sleep, which consists of the average synchrony for 6 seconds for wake and sleep). After the initial wake/sleep analysis was performed on our outcome measures, further more detailed analysis with a higher temporal resolution beyond the simple categories of wake and sleep was performed at central derivation (C4/A2-C3/A1). This was done by analyzing the effect of the time course of the wake to sleep transition, which is the time course of sleep onset. Repeated measures ANOVA (GLMMixed) was used to assess the time course of the sleep onset process that was examined with a much higher resolution beyond just wake and sleep, (with 5 seconds before and after sleep onset event, with 11 levels (-5, -4, -3, -2, -1, 0, 1, 2, 3, 4, 5). Time – 5, the subject is awake and at time 0 the subject falls asleep and continues in this state until time 5. The time course of the sleep onset process was examined for all EEG synchrony and clustering variables. Additionally, post-hoc tests (Least Significant Difference) were applied to localize the source of the variance for both the averaged wake sleep and time course of sleep onset.

To further assess the time course of sleep onset, a GLMMixed model repeated measures regression was used to assess how well the synchrony and clustering measures demonstrate relatively long-term gradual linear change in the time course of sleep onset. Furthermore, using ANOVA on the means of the residuals of the regression model we were able to locate abrupt changes along the time course that are not explained by a linear term, but are temporally associated with sleep onset.

Additionally, repeated measures regression methods were used to test the statistical independence of amplitude and phase synchrony measures. The effect of time of day was previously assessed for the outcome and it was found to have minimal effect, and was therefore excluded from the analysis.

Results

EEG Power

Figure 2 demonstrates the changes in delta, theta, alpha, and beta power that occur in the wake-to-sleep transition. Delta power did not demonstrate significant main effects for wake/sleep ($F_{1,437}$ =.601, p=.439), but the interaction for montage ($F_{3,1409}$ =14.974, p< .001), and between wake/sleep and montage ($F_{3,1418}$ =3.577, p= .013), was significant. Post-hoc tests showed that only the C3/C4 derivation was significant, and that delta power increased after sleep onset. Repeated measures regression demonstrated that delta power at the C3/C4 derivation was found to be linearly associated with the time course of sleep onset ($F_{1,446}$ =9.545, p= .002) and also demonstrated that delta power had a positive slope and increased as a function of time through the sleep onset process (b=.0397, p =.002).

Theta power demonstrated significant main effects for wake/sleep ($F_{1,433}$ =9.59, p= .002), and montage ($F_{3,1430}$ =196.05, p< .001), and the interaction been wake/sleep and montage ($F_{3,1437}$ =4.536, p= .004) was also significant. Post-hoc tests showed that only the C3/C4 derivation was not significant and that theta power significantly decreased after sleep onset for all the other derivations (all, p<.007).

Alpha power demonstrated significant main effects for wake/sleep ($F_{1,462}$ =64.68, p< .001), and montage ($F_{3,1406}$ =136.05, p< .001), and the interaction been wake/sleep and montage ($F_{3,1416}$ =3.156, p= .024) was also significant. Post-hoc tests showed that alpha power significantly decreased after sleep onset for all derivations (all, p<.001).

Beta power demonstrated significant main effects for wake/sleep ($F_{1,588}$ =33.339, p< .001), and montage ($F_{3,1404}$ =22.103, p< .001), while the interaction been wake/sleep and montage ($F_{3,1419}$ =2.127, p= .095) was not significant. Post-hoc tests showed that alpha power significantly decreased after sleep onset for all derivations (all, p<.001). Repeated measures regression demonstrated that beta power at the C3/C4 derivation was found to be linearly associated with the time course of sleep onset ($F_{1,449}$ =29.648, p< .001) and also demonstrated that beta power had a negative slope (b=-.0397, p =.002), therefore, it decreased as a function of time through the sleep onset process.

Time of day (TOD) effects was assessed for all frequency band in both wake and sleep conditions. Only theta band showed significance main effects for TOD ($F_{4,896}$=3.023, p=.017). It also showed significant differences between wake and sleep ($F_{1,1231}$=4.190, p=.041) and no interaction effects between wake/sleep and TOD. During wakefulness post hoc tests showed that theta power was higher during naps, 3, 4, and 5 when compared to nap 1 (all, p <.09). During sleep post hoc tests demonstrated that theta power was greater during nap, 4 when compared to nap 1 (p <.028).

Synchrony Index (SI)

TOD effect was examined in regards to SI in conjunction with the factor wake/sleep. TOD has 5 levels because the nap studies were repeated five times a day in two hour intervals. As expected from previous analysis there was a significant main effect for wake/sleep effect ($F_{7,1104}$ =17.289, p< .001), but this was not the case the case with the main effect for time of day because it was not significant. Furthermore the interaction

between TOD and wake/sleep was also not significant. Furthermore, the TOD factor was not significant for any of the synchrony measures, therefore, the time of day factor was excluded from further analysis.

The first order of consideration was to observe a difference in SI between wake and sleep, and to examine how this difference depended on montage and frequency of analysis (Figure 3). The analysis of SI demonstrated significant main effects for both frequency ($F_{7,1104}$=17.29, p <.001) and montage ($F_{3,16312}$=88.671, p <.001) but not for wake/sleep. Second order interactions were not found to be significant, such as frequency by montage and frequency by wake/sleep, however, montage by wake/sleep was significant ($F_{3,16219}$=3.432, p= .016). Additionally, the three-way interaction frequency by montage by wake/sleep was not significant. Post hoc tests, shown in Figure 3, demonstrated an increase in SI at 8Hz between wake and sleep inter-hemispherically, in the occipital (O2/A2-O1/A1, p=.019) and central derivations (C4/A2-C3A1, p=.036)

To enhance the temporal resolution of the wake/sleep changes, SI associated with the time course of sleep onset was assessed and significant main effects for freq ($F_{7,3486}$ =127.64, p < .001) were observed, but not by time course; however, there was significant interaction between these two factors ($F_{70,3264}$ =1.312, p = .043). Post-Hoc tests further demonstrated the time course effect on SI values: at 8 Hz, sleep onset differed from 1 and 2 seconds after sleep onset (all, p < .02) but this was not the case at 12 Hz, because there were no significant differences in the vicinity of sleep onset. Repeated measures regression demonstrated a linear relationship between SI and time from sleep onset for

several frequencies, 8 Hz (b=-.0119, p<.001), and 12 Hz (b= -.0113, p<.001). The analysis of the repeated measures residual did not demonstrate any significant differences for effects of frequency, time course or time course by frequency interaction.

Synchrony Entropy Index (SEI)

The SEI demonstrated significant main effects for frequency ($F_{7,5714}$= 1005.53, p < .001), montage ($F_{3,13591}$= 141.95, p < .001), and wake/sleep ($F_{1,6131}$= 70.92, p < .001). Second order interactions demonstrated that, frequency by montage ($F_{21,13593}$= 11.34, p < .001), montage by wake/sleep ($F_{1,6131}$= 70.92, p < .001), and frequency by wake/sleep ($F_{7,6126}$= 23.177, p < .001) were significant.

The three-way interaction of frequency by montage by wake/sleep was not significant. Post-hoc tests, shown in Figure 4, demonstrated that SEI at 8 and 12 Hz decreased inter-hemisphericaly, principally in the central (C3/A1-C4/A2) and occipital montages (p<.001). Additionally, intra-hemispherical (O2/A2-C4/O2) and central-posterior SEI differences at 12 Hz were also significant (p<.02).

The frequency dependent analysis of the time course of sleep onset for SEI demonstrated a significant effect for the time course ($F_{10,1259}$ = 5.170, p<.001) and for frequency ($F_{7,2460}$ = 271.7, p<.001). Additionally, the frequency by time course interaction was significant ($F_{70,2455}$= 2.131, p<.001). Post-hoc analysis for 8 Hz revealed that SEI differed significantly at all time times from time 0, except for time points -4 and -3 (p< .045).

To further examine the time course of SEI (Figure 4) through sleep onset, repeated measures regression was performed and demonstrated significant main effects for time from sleep onset ($F_{1,2510}$ =25.86, p<.001), and frequency ($F_{7,1327}$=240.55, p< .001). Additionally, there was a significant interaction between time from sleep onset and frequency ($F_{7,1709}$= 5.715, p< .001) (R^2 =.346). The slopes for 8 Hz (b=-.0089, p<.001) and 12 Hz (b= -.007385, p<.001) are negative and significant.

In order to identify events that are time related to sleep onset but not explained by the linear regression model, the residuals of the repeated measures regression were examined to assess if changes in the time course of SEI values was associated with the sleep onset event. The frequency factor ($F_{1,373}$=0 , p= .988) and the interaction between frequency and time course factors ($F_{10,648}$=1.494 , p= .137) were not significant, however, the time course factor was significant ($F_{10,583}$=583.612 , p= .006) demonstrating that the mean SEI residuals differed across the sleep onset time course.

Instantaneous Phase Synchrony Distribution (IPSD)

The IPSD demonstrated significant main effects for frequency ($F_{7,5344}$= 44.445, p < .001), but not for montage and wake/sleep. Second order interactions demonstrated that frequency by montage ($F_{21,11544}$= 2.601, p < .001) and frequency by sleep/wake ($F_{7,5670}$= 3.975, p < .001) were significant, but not montage by wake/sleep. The three-way interaction frequency by montage by wake/sleep was also not significant. Post-hoc tests demonstrated that IPSD at 8 Hz increased centrally and inter-hemispheric aly (C4/A2-

C3/A1) ($p<.001$), while IPSD at 12 Hz increased intra-hemisphericaly in the occipital region (O2/A2-O1/A1) ($p=.028$) and intra-hemispherically in the occipital/central derivation (O2/A2-C4/A2) ($p=.028$).

Wake/sleep changes along the time course of sleep onset were assessed at different frequencies for the IPSD measure. The frequency dependent analysis of the time course of sleep onset demonstrated a significant effect for frequency ($F_{1,367} = 11.40$, $p=.001$) and time course ($F_{10,609} = 2.244$, $p=.014$). Additionally, the frequency by time course interaction was not significant.

Post-hoc analysis for IPSD at 8 Hz revealed that times 1 and 4 differed from time 0 (both, $p <.016$), while IPSD at 12 Hz showed no significant differences were found for any time point (Figure 5).

Repeated measures regression demonstrated significant main effects for time from sleep onset ($F_{1,547}=10.257$, $p=.001$), and frequency ($F_{1,382}=10.143$, $p=.002$), however, there was no significant interaction between time from sleep onset and frequency. The slopes for 8 Hz ($b=-.0138$, $p=.001$) and 12 Hz ($b= -.0114$, $p=.007$) are negative and significant (Figure 5).

Repeated measures ANOVA analysis of the residuals did not demonstrate any significant differences for effects of frequency, time course or time course by frequency interaction.

Amplitude Synchrony Index (ASI)

The ASI demonstrated significant main effects for frequency ($F_{7,5195}= 30.630$, $p < .001$), montage ($F_{3,5195}= 30.630$, $p < .001$), and wake/sleep ($F_{1,5687}= 10.221$, $p < .001$). Second

order interactions demonstrated that, frequency by montage ($F_{21,13536}$= 22.91, p < .001) was significant but montage by wake/sleep was not. The three way interaction frequency by montage by wake/sleep was also significant ($F_{21,13651}$= 1.834, p=.011). Post-hoc tests demonstrated that across the from wake to sleep transition, ASI at 8 and 12 Hz decreased inter-hemisphericaly (C4/A2-C3/A1) (p<.007), decreased across central-posteriorly (p<.025), and increased intra-hemisphericaly (O2/A2-C4/O2) (p=.019).

The time course of ASI during sleep onset was assessed, and significant main effects for frequency ($F_{1,625}$=20.24, p<.001) and time course ($F_{10,484}$=24.372, p=.003) were found; however, there was no significant interaction between these two factors (Figure 6). Post-Hoc tests further demonstrated the effect of time course on ASI values: at 8 Hz, 1 second before sleep onset differed from 0, 1, 2, 3, 4 seconds after sleep onset (all, p < .02); and at 12 Hz, 1 second before sleep onset differed from 1 & 2 seconds after sleep onset (both, p < .01). We followed up on this analysis by examining the linear relationship between ASI and the factor time from sleep onset at several frequencies. Repeated measures regression demonstrated significant main effects for time from sleep onset ($F_{1,3228}$=24.372, p<.001), and frequency ($F_{7,1024}$=31.461, p<.001), however, there was no significant interaction between time from sleep onset and frequency. The slopes for 8 Hz (b=-.0138, p=.001) and 12 Hz (b= -.0114, p=.007) are negative and significant (Figure 6). Repeated measures ANOVA analysis of the residuals did not demonstrate any significant differences for effects of frequency, time course or time course by frequency interaction.

Amplitude Entropy Index (AEI)

The AEI demonstrated significant main effects for frequency ($F_{1,1113}$= 30.828, p < .001), montage ($F_{3,2823}$= 66.385, p < .001), and wake/sleep ($F_{1,1240}$= 10.219, p = .001). Second order interactions demonstrated that frequency by montage ($F_{3,2837}$= 4.589, p < .001) and montage by wake/sleep ($F_{3,2865}$= 3.476, p = .015) were significant, but frequency by wake/sleep was not. The three-way interaction frequency by montage by wake/sleep was not significant. Post-hoc tests for wake/sleep differences demonstrated that at 8 and 12 Hz, AEI increased inter-hemisphericaly (C3/A1-C4/A2) (both, p <.035), while only the 12 Hz increased across the central-occipital montage (C3/C4-O1/2) (p=.016) (Figure7).

Wake/sleep changes along the time course of sleep onset were assessed at different frequencies for the AEI measure. The analysis demonstrated a significant effect for frequency ($F_{1,733}$ = 70.376, p<.001) but not for time course and the frequency by time course interaction. Post-hoc analysis for AEI at 12 Hz revealed that times -3 and -5 differed from time 0 (both, p <.027), while no significant differences were found for any time point at 8 Hz.

Repeated measures regression demonstrated significant main effects for time from sleep onset ($F_{1,631}$=11.064, p=.001), and frequency ($F_{1,273}$=8.479, p=.004), however, there was no significant interaction between time from sleep onset and frequency. The slopes for 8 Hz (b=.00272, p=.075) and 12 Hz (b= .00377, p=.014) are positive (Figure 7), but only the slope at 12Hz is significant. The repeated measures ANOVA analysis of the residuals

did not demonstrate any significant differences for effects of frequency, time course or time course by frequency interaction.

Cross-Correlation (CC)

The CC measure demonstrated significant main effects for frequency ($F_{7,5204}$= 83.749, p < .001), montage ($F_{3,1354}$= 371.157, p < .001), and wake/sleep ($F_{1,5687}$= 10.221, p < .001). Second order interactions demonstrated that, frequency by montage ($F_{21,13541}$= 29.965, p < .001) and montage by wake/sleep ($F_{3,13658}$= 71.441, p < .001) were significant, but frequency by wake/sleep was not. The three way interaction frequency by montage by wake/sleep was also significant ($F_{21,13651}$= 1.834, p=.011).

Post-hoc tests demonstrated that at 8 and 12 Hz, CC decreased from wake to sleep inter-hemisphericaly, principally in the central (C3/A1-C4/A2) and occipital montages (p<.001). However, there was a significant increase in the CC during the wake sleep transition at 8 and 12 Hz intra-hemisphericaly (O2/A2-C4/O2) (p<.04). No significant change for the central-posterior derivation at 8 and12 Hz was observed.

The time course of CC throughout sleep onset, shown in Figure 8, was examined, and significant main effects for frequency ($F_{7,2132}$= 326.030, p < .001) was found, however, there was no significant main effect for time course and the interaction between these two factors. Post-Hoc tests demonstrated that there was a time course effect on CC: at 8 Hz, times 1 and 5 seconds from sleep onset differed from sleep onset (time 0) (all, p < .035); and at 12 Hz, times 1, 3, and 5 differed from sleep onset (time 0) (all, p < .048). We

followed up on this analysis by examining the linear relationship between CC and the factor time from sleep onset at several frequencies.

Repeated measures regression demonstrated a significant main effects for frequency ($F_{1,316}$= 70.817, p < .001) and time course ($F_{1,566}$=10.638, p =.001), however, there was no significant interaction between these two factors. Time dependent slopes for CC were estimated for 8 Hz (b= -.013136, p=.004) and 12 Hz (b= -.007260, p=.113), but only the 8Hz slope was significant. The repeated measures ANOVA analysis of the residuals did not demonstrate any significant differences for effects of frequency, time course or time course by frequency interaction.

Coherence (Coh)

Coh demonstrated significant main effects for frequency ($F_{7,5440}$= 20.168, p < .001), montage ($F_{3,13552}$= 357, p < .001), and wake/sleep ($F_{21,13675}$= 1.920, p = .007). Second order interactions demonstrated that, frequency by montage ($F_{21,13554}$= 57.383, p < .001) and montage by wake/sleep ($F_{3,13676}$= 14.448, p < .001) were significant, but frequency by wake/sleep was not. The three-way interaction frequency by montage by wake/sleep was also significant ($F_{21,13675}$= 1.920, p=.007). Post-hoc tests demonstrated that at 8 and 12 Hz, Coh decreased inter-hemispherically over occipital (O2/A2 –O1/A2) and central (C3/A1-C4/A2) derivations (all, p<.004).

The time course of Coh throughout sleep onset, shown in Figure 9, was examined, and significant main effects for frequency ($F_{7,2957}$= 82.255, p < .001) and time course ($F_{10,771}$=2.09, p =.029) were found; however, there was no significant interaction between these two factors. Post-Hoc tests demonstrated that there was a time course effect on Coh: at 8 Hz , times 1 through 5 seconds from sleep onset differed from sleep onset (time 0) (all, p < .032); and at 12 Hz, time 5 differed from sleep onset (time 0) (p= .028). We followed up on this analysis by examining the linear relationship between Coh and the factor time course from sleep onset at several frequencies.

Repeated measures regression was used to assess linear changes associated with the time course of sleep onset. Significant main effects for frequency ($F_{1,316}$= 70.817, p < .001) and time course ($F_{1,566}$=10.638, p =.001) were found, however, there was no significant interaction between these two factors. Time dependent slopes for Coh were estimated for 8 Hz (b= -.013136, p=.004) and 12 Hz (b= -.007260, p=.113). The repeated measures ANOVA analysis of the residuals did not demonstrate any significant differences for effects of frequency, time course or time course by frequency interaction.

Regression and Correlation

A general mixed model was used to perform repeated measures regressions in order to predict CC values from the amplitude and phase synchrony measures. The calculated model has an estimated R^2 = .80, and incorporated many of the measures considered above: ASI (b=.33870, p< .001), AEI (b=-.315289, p<.001), SEI (b=.353485, p<.001),

IPSD (b=.001983, p=.778), SI (b=-.004630, p=.973). The phase-dependent SEI, SI, and IPSD measures are highly correlated to each other, which is why SI and IPSD were removed from the regression model and only SEI is shown to be significant. AEI and ASI are not significantly correlated to the phase-dependent measures or to each other, and therefore, both were used in the model. These results imply that the amplitude and phase synchrony measures are independent factors, and both are needed to accurately predict CC. Also, these results show that synchrony- and entropy-based measures examine different components of a signal, and may therefore carry independent information, as the lack of correlation between AEI and ASI show. Furthermore, both types of synchrony measures are predictive of CC, even though CC is comprised of both amplitude and phase synchrony: CC & SI ($r=.94$, $p<.001$), CC & SEI ($r=.95$, $p<.001$).

Discussion

The results of the analysis of the EEG power changes match the outcomes of previous studies, which have shown that the sleep onset process produces significant EEG power changes, including the increase in delta power and a decrease in beta power (Ogilvie 2001; Merica 2004). Our results further demonstrate that this decrease in beta and increase of delta can be modeled linearly in the local time course of sleep onset, comprised of an 11 second window centered precisely at the drop off of occipital alpha, suggesting that these processes occur gradually.

Additionally, time of day (TOD) effects were examined and only theta was TOD significant in both wake and sleep conditions.

Synchrony measures, which theoretically reflect changes in the temporal binding between neural assemblies between and within hemispheres, were used to examine the types of network dynamics that may be responsible for the EEG changes observed throughout the sleep onset process. The ANOVA analysis for all measures demonstrated that the time course of sleep onset for the synchrony measures was consistently modulated, and we propose that this effect may be a result of increased activity of the sleep inducing pre-optic center neurons.

The results of the analysis showed that synchrony and clustering measures were able to detect both gradual and abrupt changes in the EEG across different regions of the brain. Immediately preceding sleep onset, a peak in all synchrony and clustering measures was

observed, followed by an abrupt drop into sleep onset, which may reflect the abrupt state transition into sleep that occurs with appearance of synchronized discharges in the form of spindles. (Ogilvie 2001) This was followed with more gradual changes in the SI and SEI for 12Hz but not for 8Hz, suggesting different mechanisms are in play in the gradual regulation of the phase synchronization in the beta and theta bands throughout the sleep cycle. The ASI changed gradually in both 8 and 12Hz frequency bands, suggesting that amplitude synchronization is regulated similarly for beta and theta bands. Furthermore, our statistical analysis revealed that SEI is composed of two terms: a linear term and a temporally linked abrupt drop that lasts for two seconds. These changes may correspond to the firing rate pattern in "wake" neurons in the midbrain during sleep onset, which has been shown to decrease gradually prior to spindle onset, reach a minimum at the start of a spindle and rise again over the course of a second (Merica 2004)

We further examined the sleep onset process using repeated measures regression, and we observed that all the synchrony measures changed linearly during the time course of sleep onset. The residuals of the regression were assess for changes not linearly associated with sleep onset, but are still time locked to the sleep onset event. An examination of the mean of residuals for every time point across all measures revealed such a pattern over the time course for SEI only. From these results, we concluded that the synchrony changes during the sleep onset process can be described by a model that has two components: a gradual linear change, and another that demonstrates a large abrupt changes that lasts approximately 2 seconds and are temporally linked to the sleep onset event.

The results of the analyses of phase and amplitude synchrony (SI and ASI, respectively) during sleep onset give inverse results: phase synchrony increases with sleep onset and amplitude synchrony decreases with sleep onset. This result suggests that the phase and amplitude are independent of each other, and may contain two separate streams of information that are involved in regulating the sleep onset process. Previous studies have identified thalamocortical neurons in the lateral geniculate nucleus (LGN) that exhibit rhythmic bursting at approximately 2-13 Hz. In different combinations, these cells can generate a locally synchronized spectrum of alpha and theta oscillations, providing evidence that the thalamus can act as an independent pacemaker of alpha and theta rhythms. Pairs of thalamocortical neurons can exhibit both in-phase and out-of-phase synchrony, and will often spontaneously alternate between the two states. (Hughes 2007) These studies demonstrated that the local field oscillation amplitude is not simply linked to the extent of cell recruitment into a single synchronized neuronal assembly, but also to the degree of destructive interference between dynamic, spatially overlapping, competing anti-phase groups of continuously bursting neurons. Our results show that patterns of amplitude synchronization, as captured by the ASI measure, can affect the synchronization properties of distant neuroassemblies throughout the sleep onset process, thus providing more evidence that thalamic centers may be in control of the wake-sleep transition. It has been previously thought that the amplitude modulation of alpha and theta rhythms, described as waxing and waning, was a consequence of changes in recruitment of synchronized cells. (Ogilvie 2001) However, these results suggest that the waxing and waning of thalamic alpha/theta rhythms should not be assumed to reflect a

wholesale increase and reduction, respectively, in underlying neuronal synchrony. We argue that these network dynamics might have important consequences for relating changes in the amplitude of EEG alpha and theta rhythms to the activity of thalamic networks.

Phase synchrony has been shown to be important in long- and short-distance binding of neuroassemblies across the brain. The "temporal correlation hypothesis" has successfully used the idea that neurons can synchronize into transient oscillatory assemblies to explain the neuronal integration of processing among assemblies that are separated anatomically. (Singer 1999, Weiss & Rappelsberger, 2000). It has been demonstrated that synchronous neural activity provides a temporal code for grouping together parts of an object (Gray, 1999, Gray et al., 1989, Singer and Gray, 1995). According to this binding by synchrony (BBS) hypothesis, "spatially segregated neurons should exhibit synchronized response episodes if activated by a single stimulus or by stimuli that can be grouped together into a single perceptual object" (Singer, 1997). A good illustration of this idea is that coupling of electrical brain activity in the gamma band is considered the basic mechanism underlying transient functional coupling of neural assemblies during visual cognitive tasks (von der Malsburg, 1994). Our results demonstrate that the sleep onset process produces gradual and abrupt changes in interhemispheric phase synchrony as measured by SI, further supporting the idea that neurons can transiently, and quickly, synchronize into oscillatory assemblies.

Interestingly, ASI and AEI produce results that are independent of each other, just like SI and SEI, suggesting that the synchrony and entropy measures are focusing on different aspects of the amplitude and phase modulation patterns, and that these measures are both useful in examining the diverse and intricate EEG dynamics that occur throughout the sleep onset process. Therefore, the joint measures of phase and amplitude synchrony, such as coherence and crosscorrelation, that have been used in all previous studies to examine hemispheric synchrony during sleep onset (e.g., Corsi-Cabrera et al., 1996; Achermann and Borbely, 1998), are insufficient to quantitatively describe the detailed dynamics that are captured by the EEG.

Regression models that aim to predict CC from the all the outcome measures make it clear that phase and amplitude synchrony measures are independent predictors of CC. These results show that applying both amplitude and phase synchrony measures provides more detailed information about the types of dynamics that are not observable with CC or Coh alone, which are both joint measures of amplitude and phase synchrony. Therefore, it may be worthwhile to re-examine data previously examined with CC and Coh alone to gain more information about the types of processes responsible for generating EEG signals.

Many of the synchrony and entropy measures outlined in this study have been used in the development of a seizure prediction algorithm that is highly sensitive to subtle changes in synchrony prior to a hypersynchronous event or a seizure (Litt & Echauz 2002). A large variety of methods have been used to assess synchrony during seizures, such as cross

correlation, coherence, wavelet-based phase synchronizations, mutual information (Quiroga et al., 2002), global or local synchronization (van Putten, 2003), mean phase coherence (Mormann et al., 2000), and instantaneous phase synchrony distribution (von Gizycki et al., 2008). Furthermore, these techniques have been used in the neurocognition field to examine transient functional coupling in support of the "temporal correlation hypothesis". (Singer 1999, Weiss & Rappelsberger, 2000) Our results demonstrate that these synchrony and entropy techniques may be very useful in the study sleep onset, as well as the many other processes associated with the sleep cycle, such as the non-REM to REM-sleep transition, and pathological sleep states such as narcolepsy.

Conclusions

In conclusion, synchrony- and entropy-based EEG measures were able to extract valuable information about the sleep onset process that previously used EEG measures, such as coherence and crosscorrelation, were not. The results presented here revealed that the sleep onset process is a combination of abrupt and gradual changes in the EEG, which may be representative of the changes that occur in the thalamocortical network. These results support one of the prevailing theories of sleep onset, implicating the thalamocortical network as playing a major role in controlling the process. Furthermore, the results showed that the amplitude and phase synchrony measures are independent of each other, and yet are both predictors of the crosscorrelation, demonstrating that crosscorrelation is a mix of amplitude and phase synchronization patterns. Likewise, it was shown that the synchrony- and entropy-based measurements are independent of each

other, suggesting that they may both be useful in the analysis of EEG patterns in sleep. Taken together, these measures may be invaluable for the study of sleep onset, and the sleep cycle in general. Use of these measures may be critical in developing algorithms for detecting sleep onset, sleep phase transitions, and sleep pathologies.

Figures

Figure 1: EEG sleep epoch during selection process. Red line represents sleep onset.

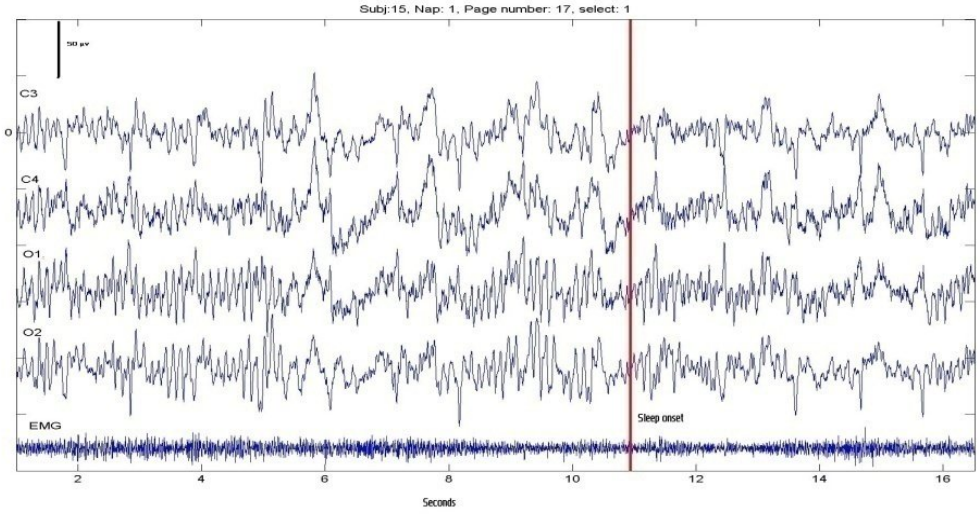

Figure 2: Delta, Theta, Alpha, Beta power in the wake-to-sleep transition.

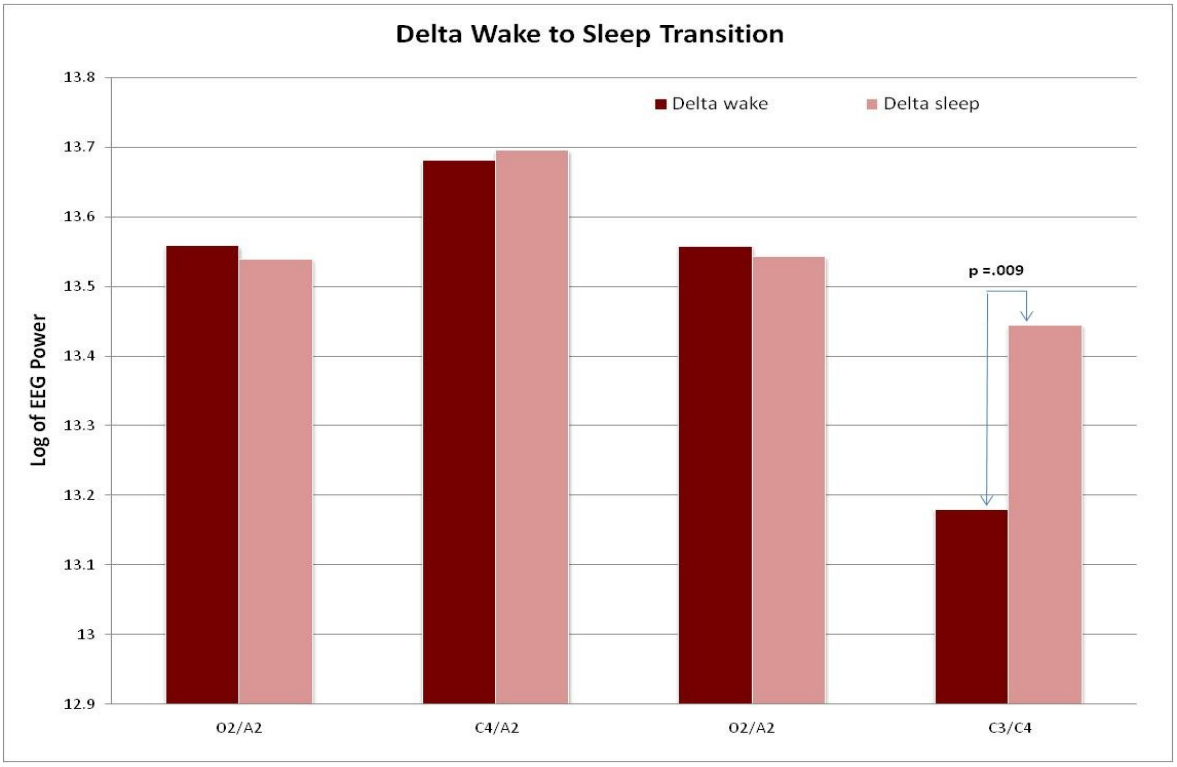

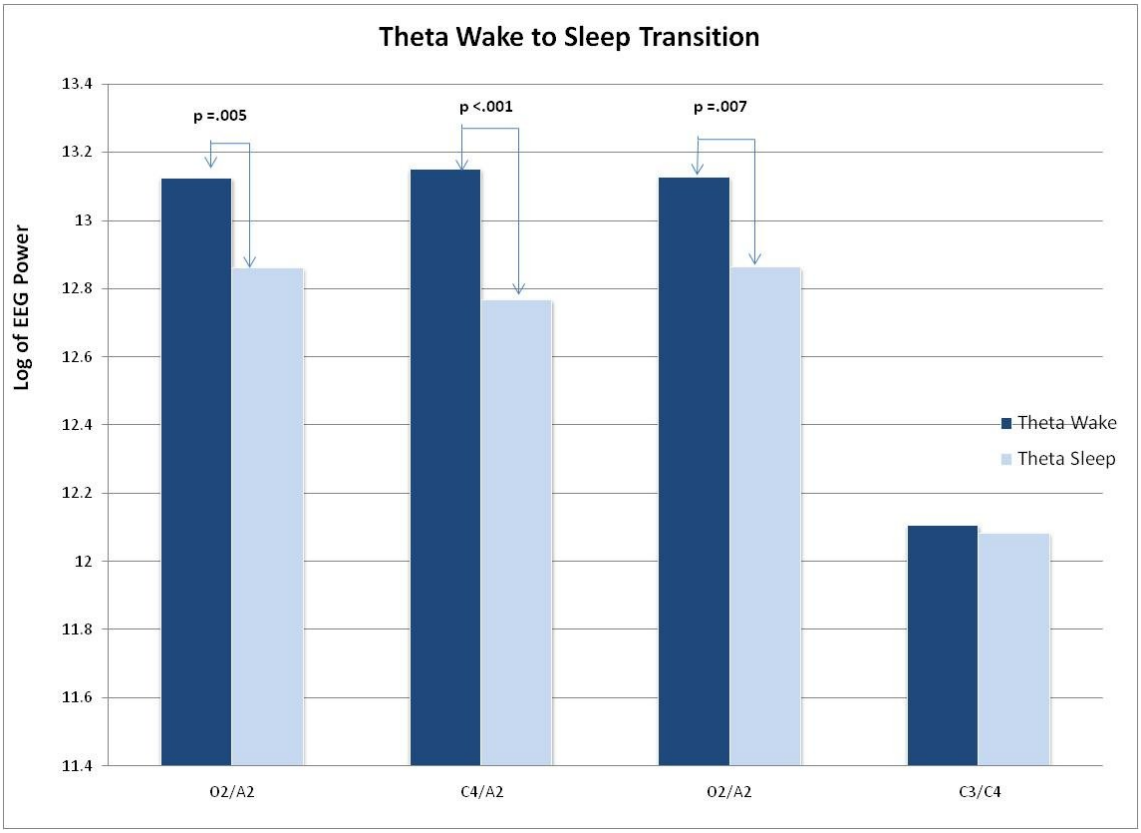
Theta Wake to Sleep Transition
Log of EEG Power
13.4
13.2
13
12.8
12.6
12.4
12.2
12
11.8
11.6
11.4
p =.005
p <.001
p =.007
O2/A2
C4/A2
O2/A2
C3/C4
Theta Wake
Theta Sleep

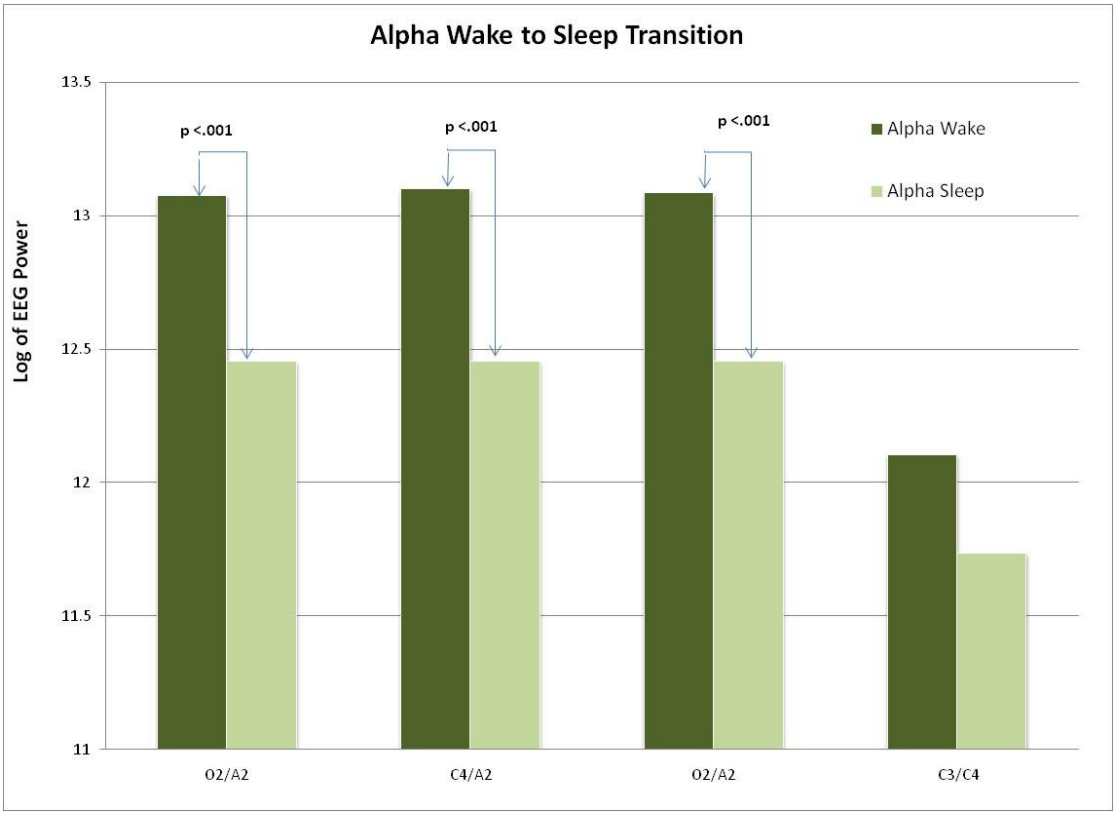
Alpha Wake to Sleep Transition
Log of EEG Power
13.5
13
12.5
12
11.5
11
p <.001
p <.001
p <.001
Alpha Wake
Alpha Sleep
O2/A2
C4/A2
O2/A2
C3/C4

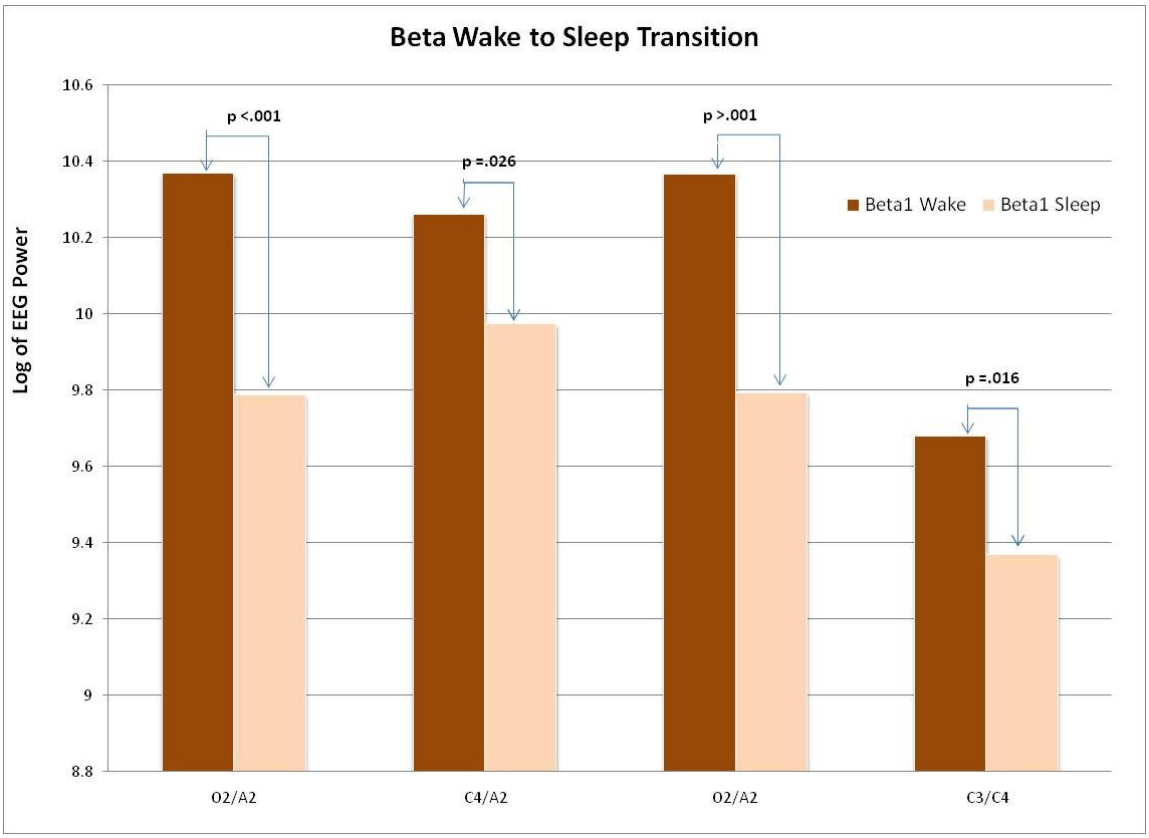
Beta Wake to Sleep Transition
Log of EEG Power
10.6
10.4
10.2
10
9.8
9.6
9.4
9.2
9
8.8
p <.001
p =.026
p >.001
p =.016
Beta1 Wake
Beta1 Sleep
O2/A2
C4/A2
O2/A2
C3/C4

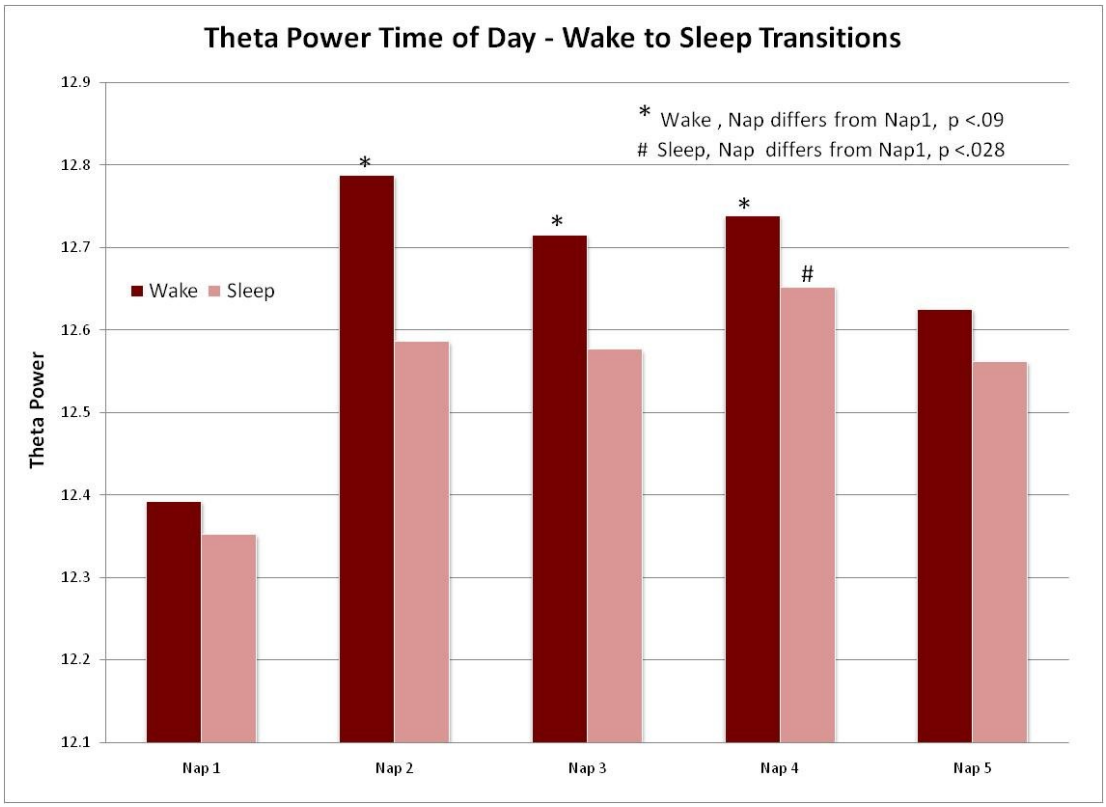
Theta Power Time of Day - Wake to Sleep Transitions
* Wake , Nap differs from Nap1, p <.09
# Sleep, Nap differs from Nap1, p <.028
Wake
Sleep
Theta Power
12.9
12.8
12.7
12.6
12.5
12.4
12.3
12.2
12.1
Nap 1
Nap 2
Nap 3
Nap 4
Nap 5

Figure 3: Changes in Synchrony Index (SI) in the wake-to-sleep transition

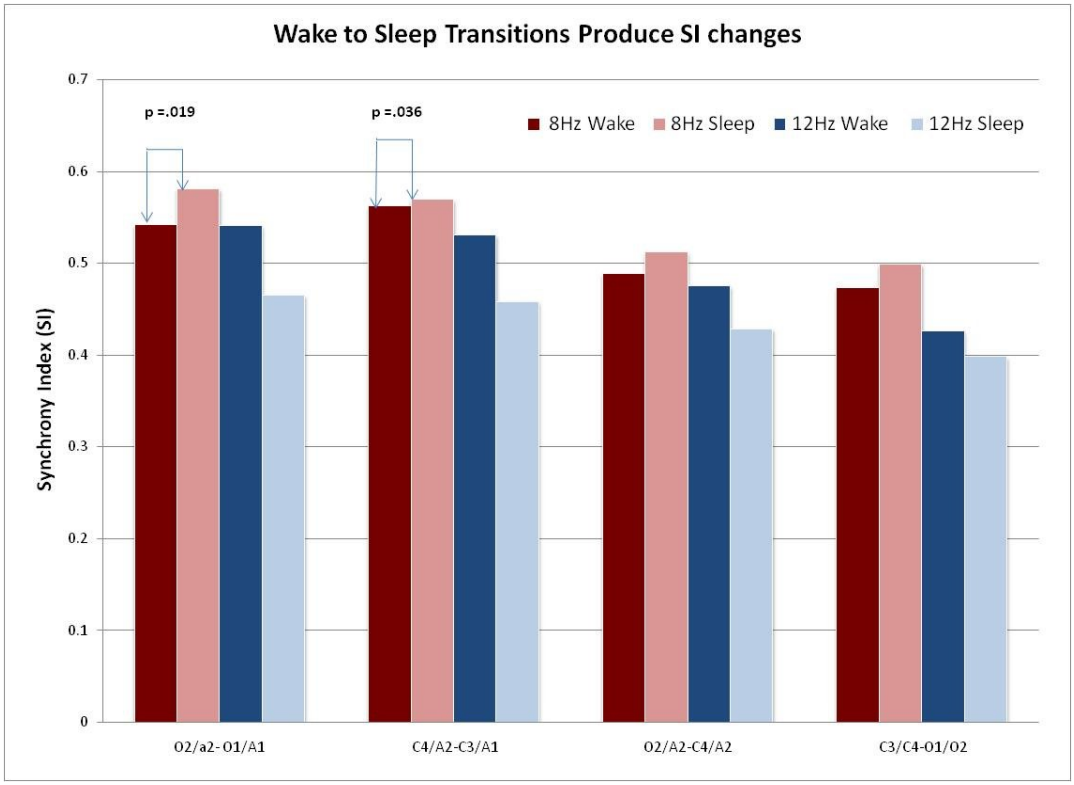

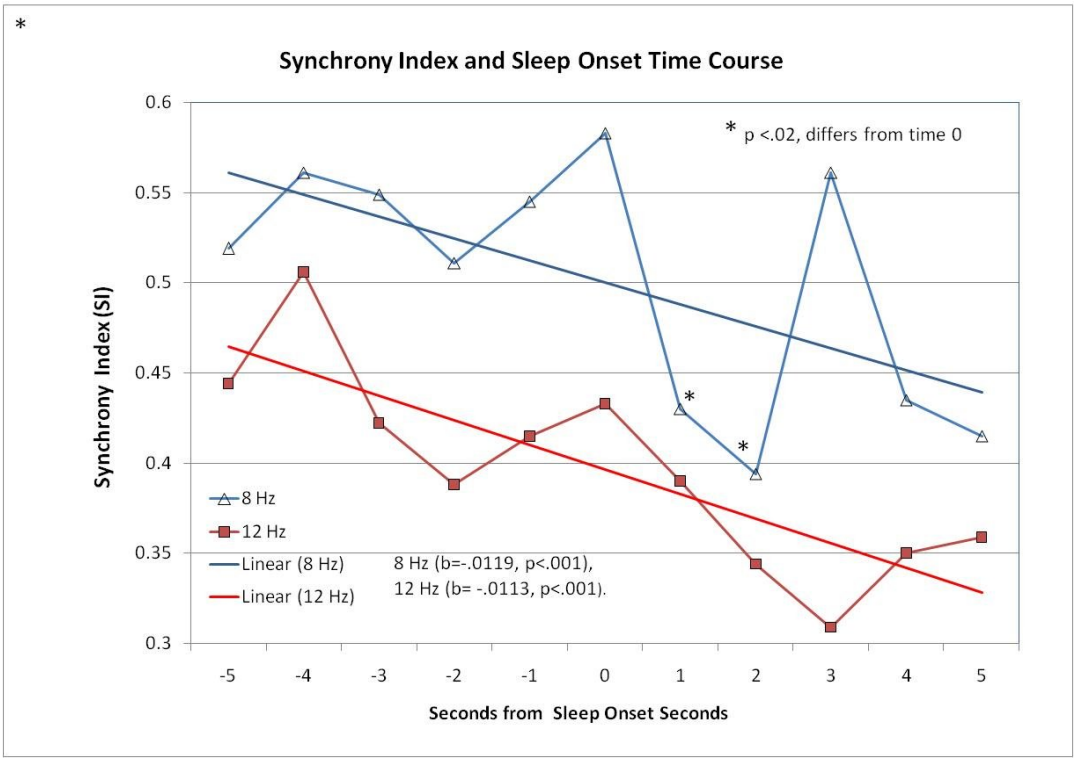

Figure 4: Changes in Synchrony Entropy Index (SEI) in the wake-to-sleep transition

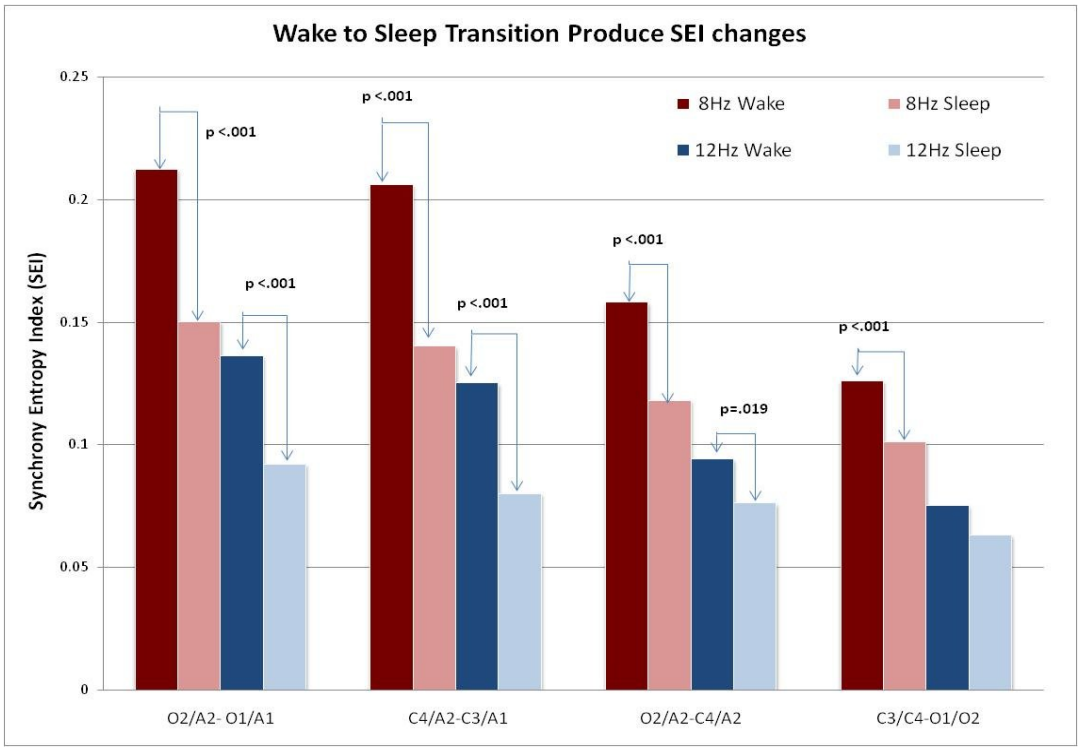

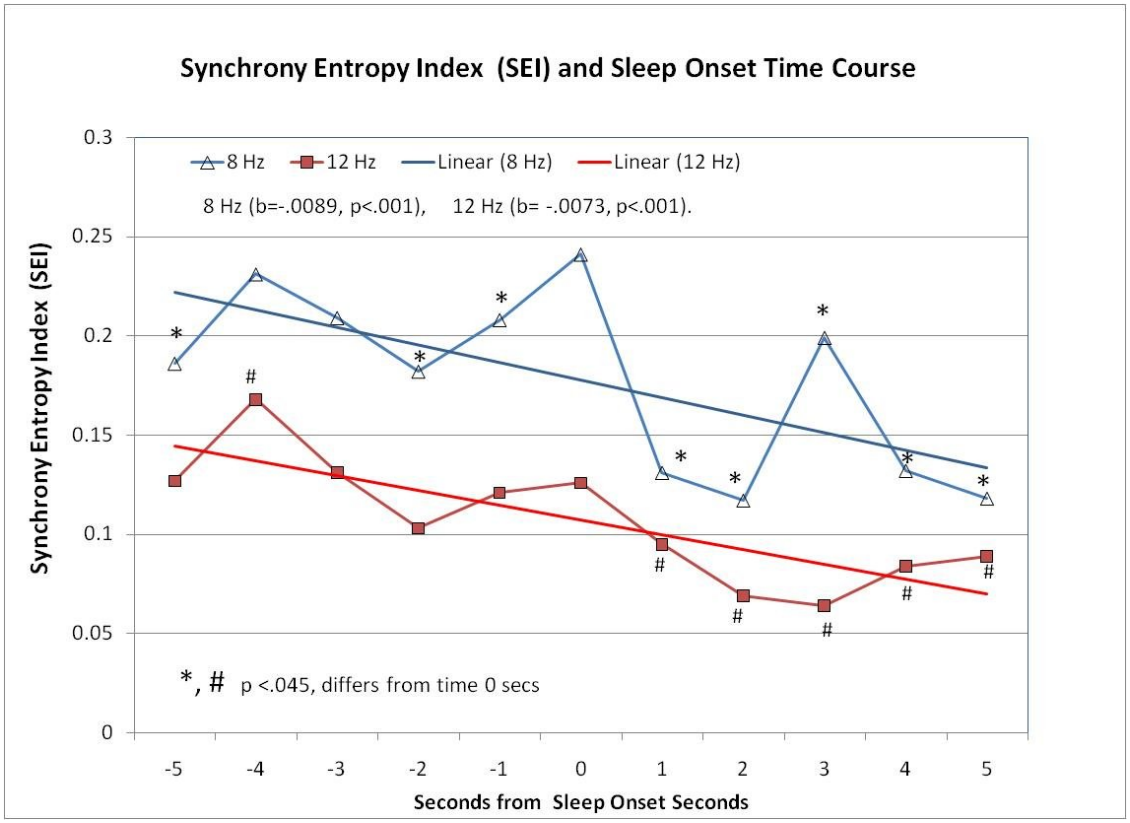

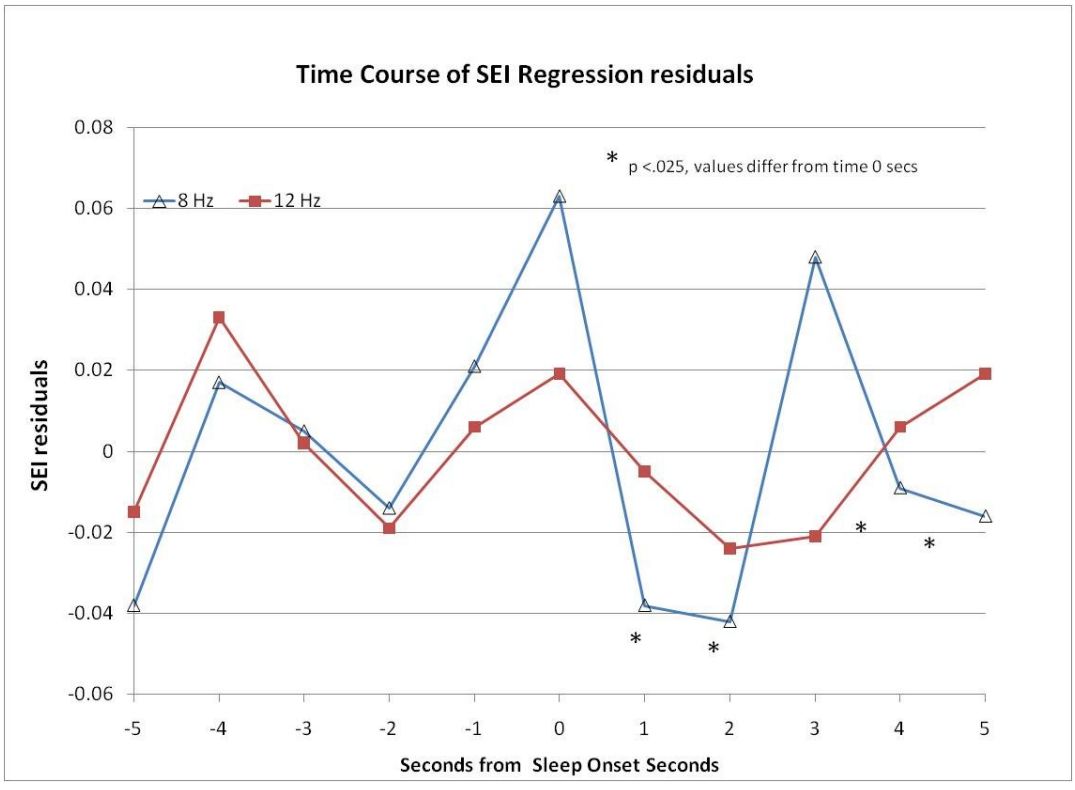
Time Course of SEI Regression residuals
* p <.025, values differ from time 0 secs
8 Hz
12 Hz
SEI residuals
0.08
0.06
0.04
0.02
0
-0.02
-0.04
-0.06
-5
-4
-3
-2
-1
0
1
2
3
4
5
Seconds from Sleep Onset Seconds

Figure 5: IPSD changes in the wake-to-sleep transition

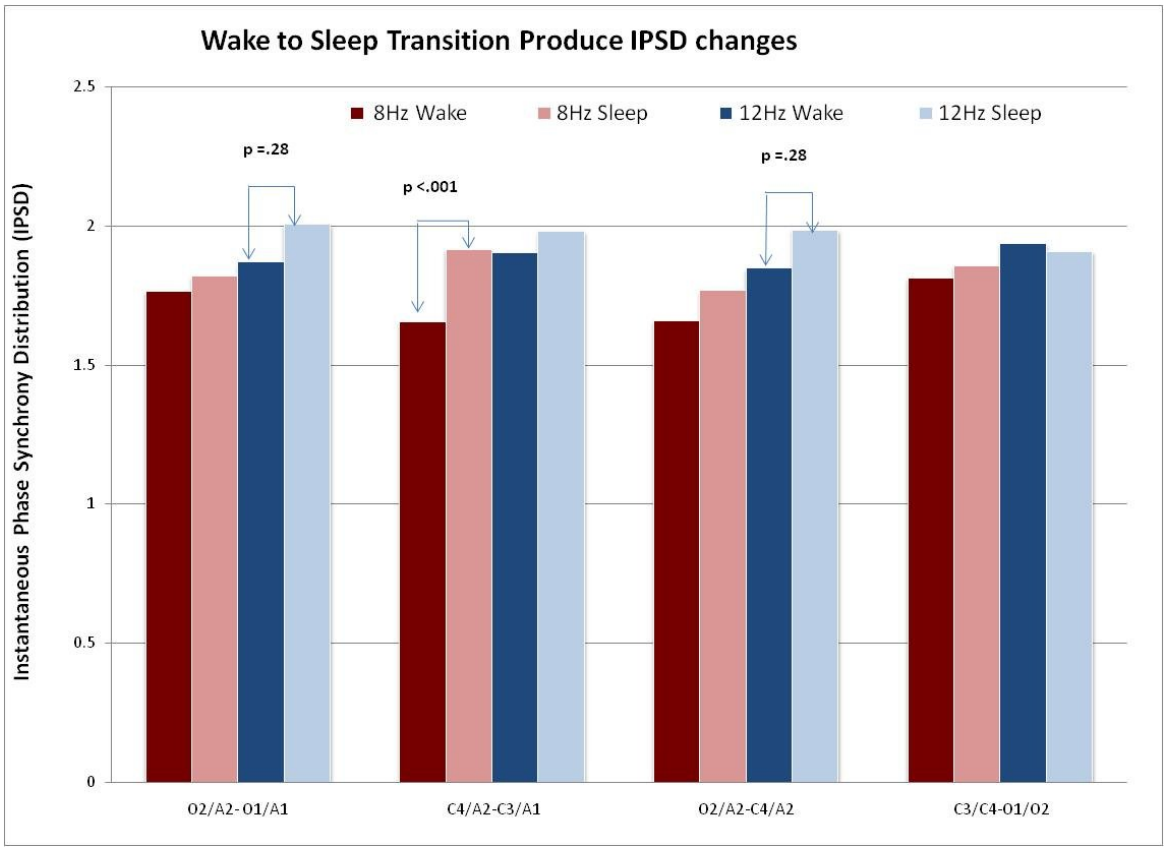

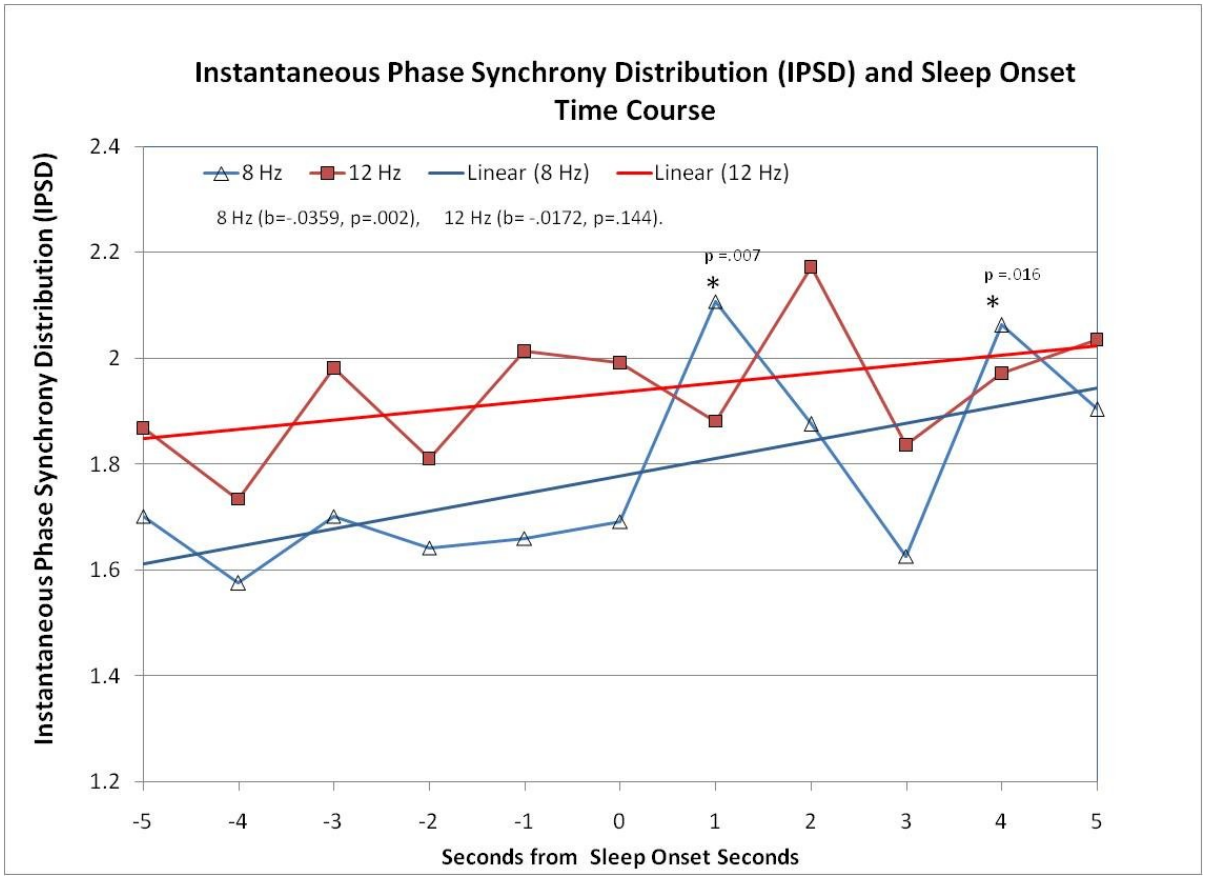

Figure 6: ASI changes in the wake-to-sleep transition

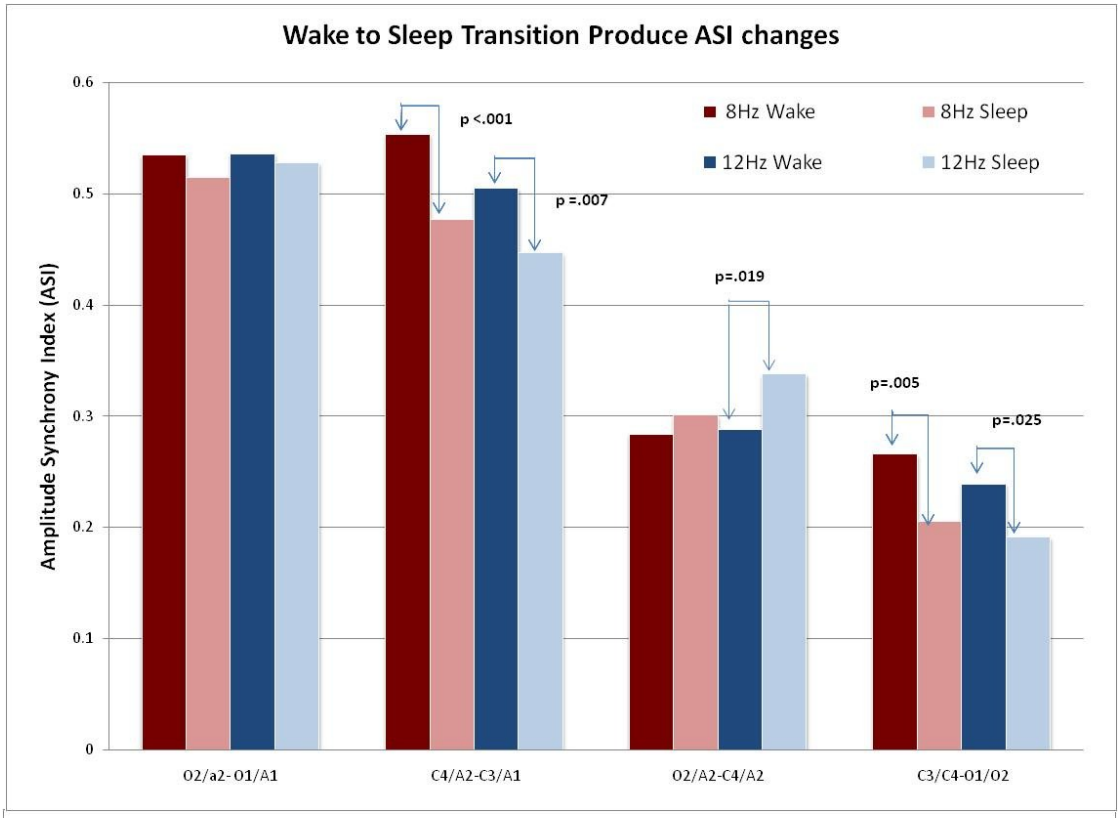

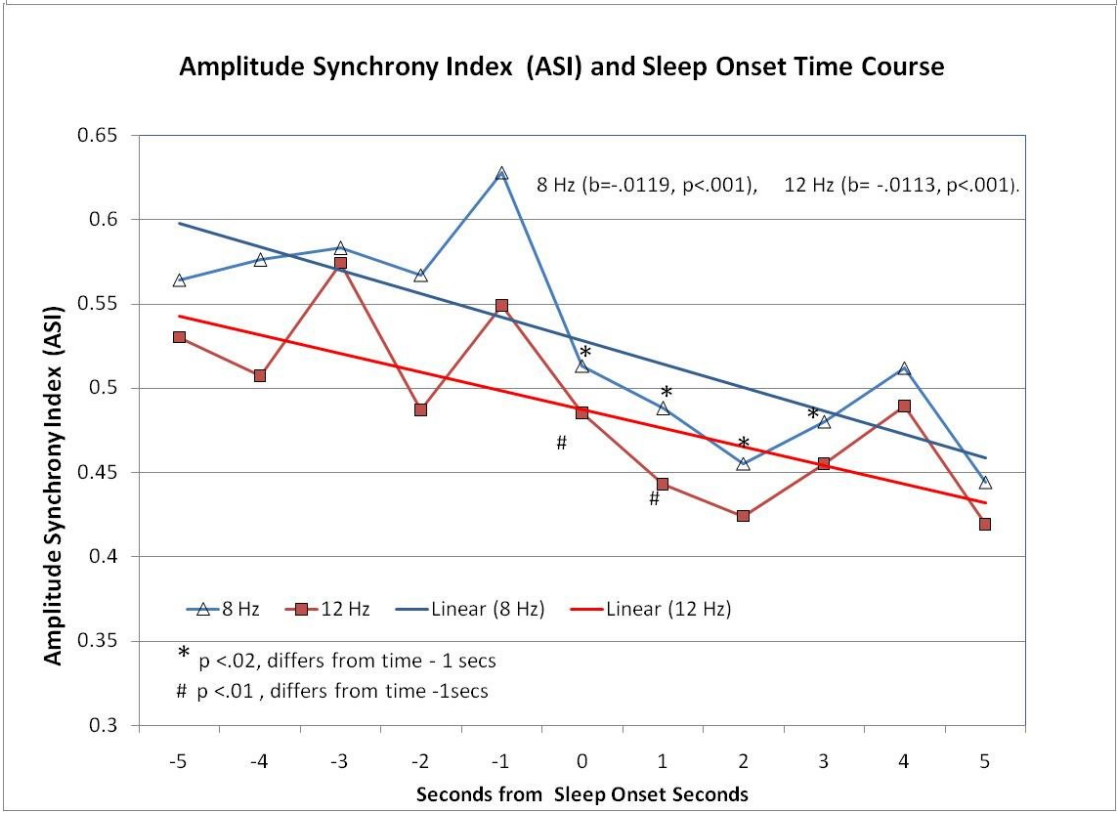

Figure 7: Amplitude Entropy Index (AEI) during the wake-to-sleep transition

Fig. 3

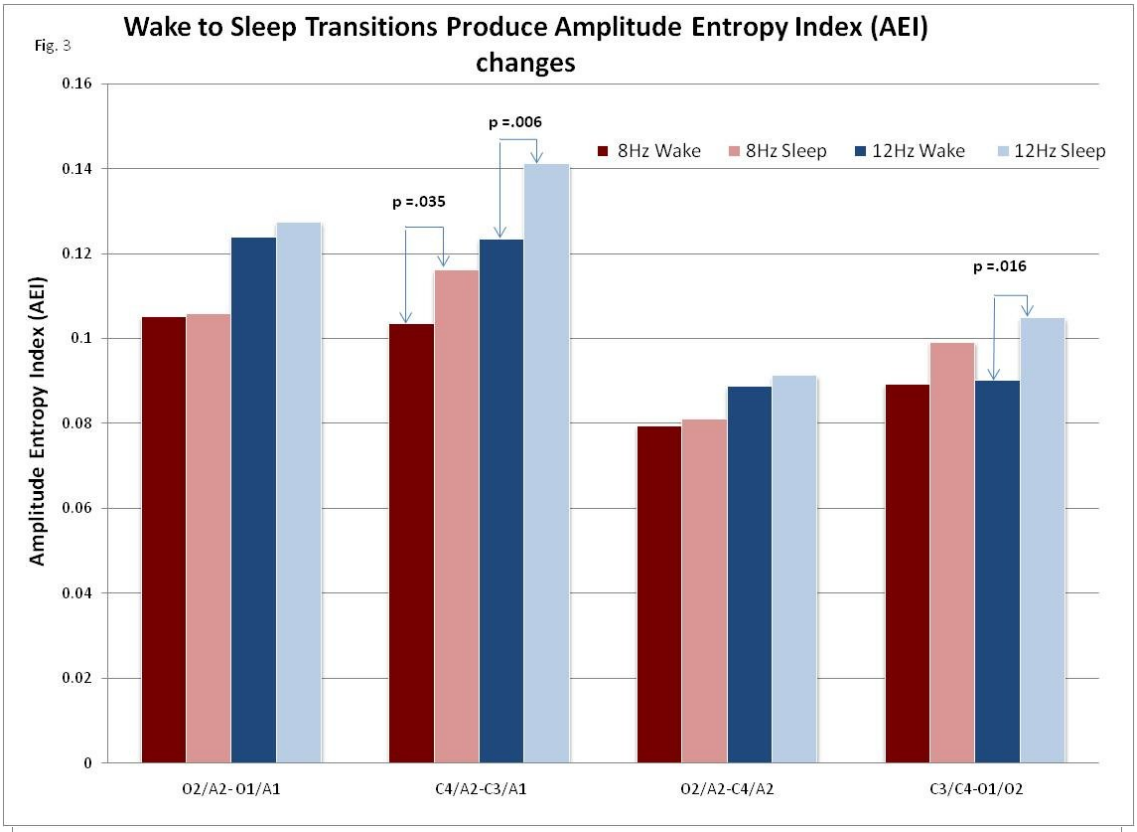
Wake to Sleep Transitions Produce Amplitude Entropy Index (AEI) changes
Amplitude Entropy Index (AEI)
0.16
0.14
0.12
0.1
0.08
0.06
0.04
0.02
0
p =.006
p =.035
p =.016
8Hz Wake
8Hz Sleep
12Hz Wake
12Hz Sleep
O2/A2-O1/A1
C4/A2-C3/A1
O2/A2-C4/A2
C3/C4-O1/O2

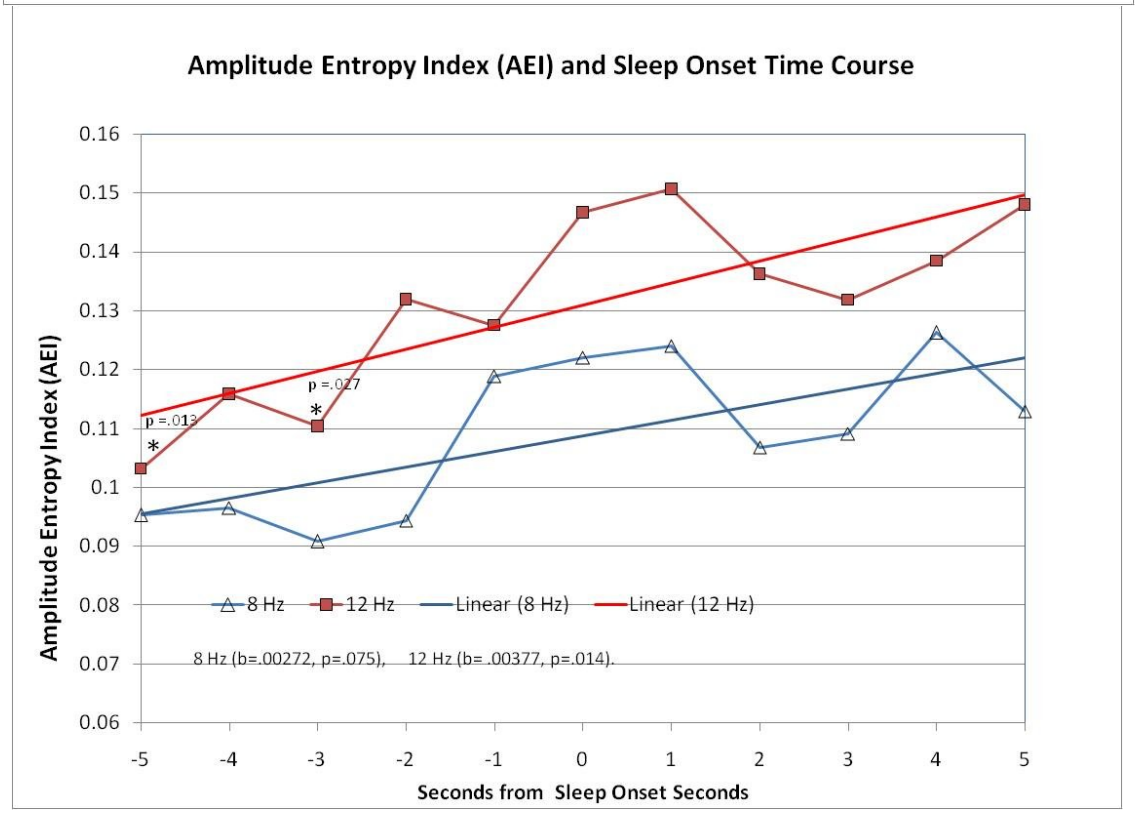
Amplitude Entropy Index (AEI) and Sleep Onset Time Course
Amplitude Entropy Index (AEI)
0.16
0.15
0.14
0.13
0.12
0.11
0.1
0.09
0.08
0.07
0.06
p =.013
*
p =.027
*
8 Hz
12 Hz
Linear (8 Hz)
Linear (12 Hz)
8 Hz (b=.00272, p=.075), 12 Hz (b= .00377, p=.014).
-5
-4
-3
-2
-1
0
1
2
3
4
5
Seconds from Sleep Onset Seconds

Figure 8: Crosscorrelation changes in the wake-to-sleep transition

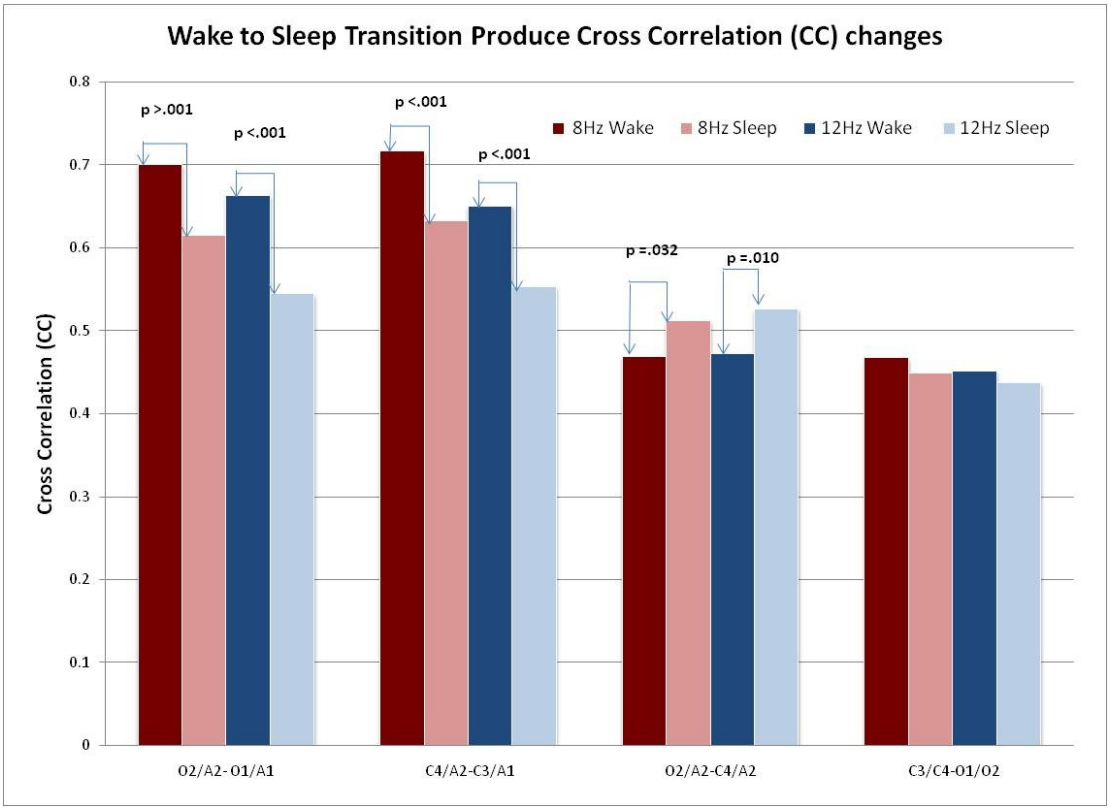

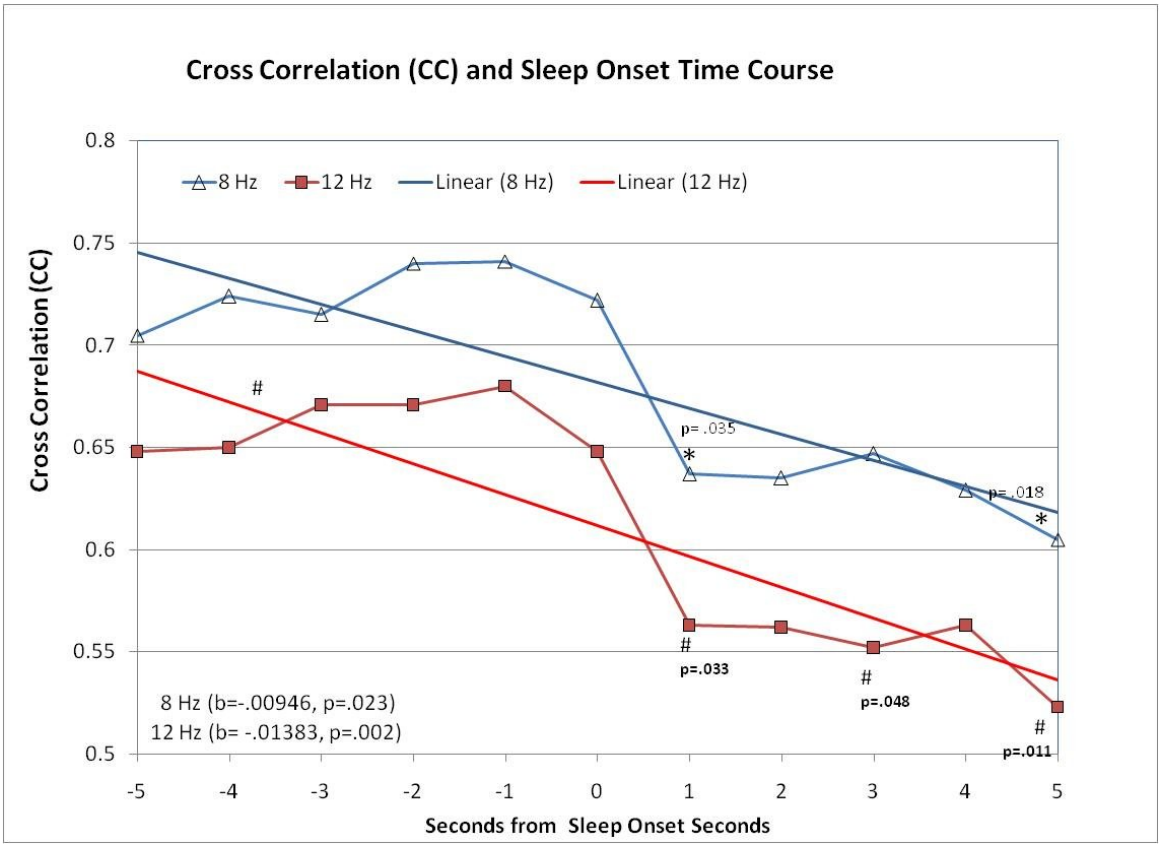

Figure 9: Coherence changes in the wake-to-sleep transition

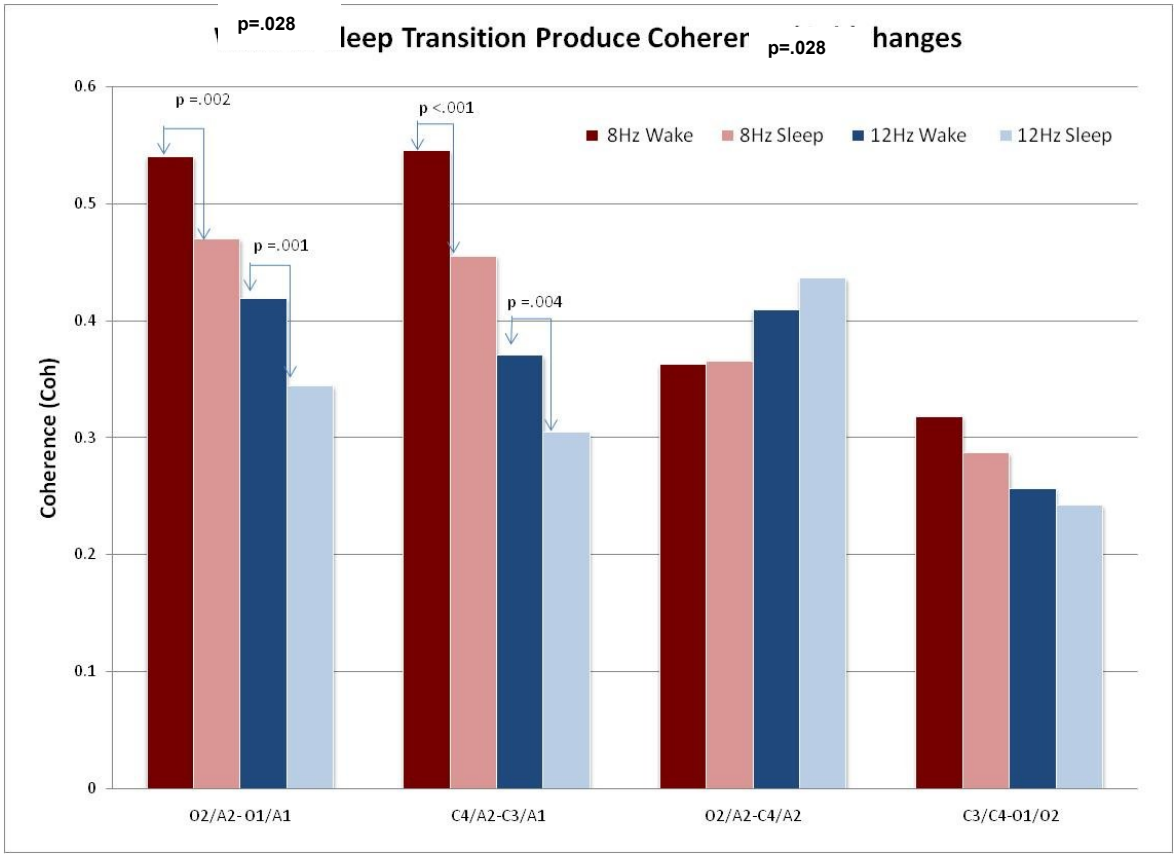

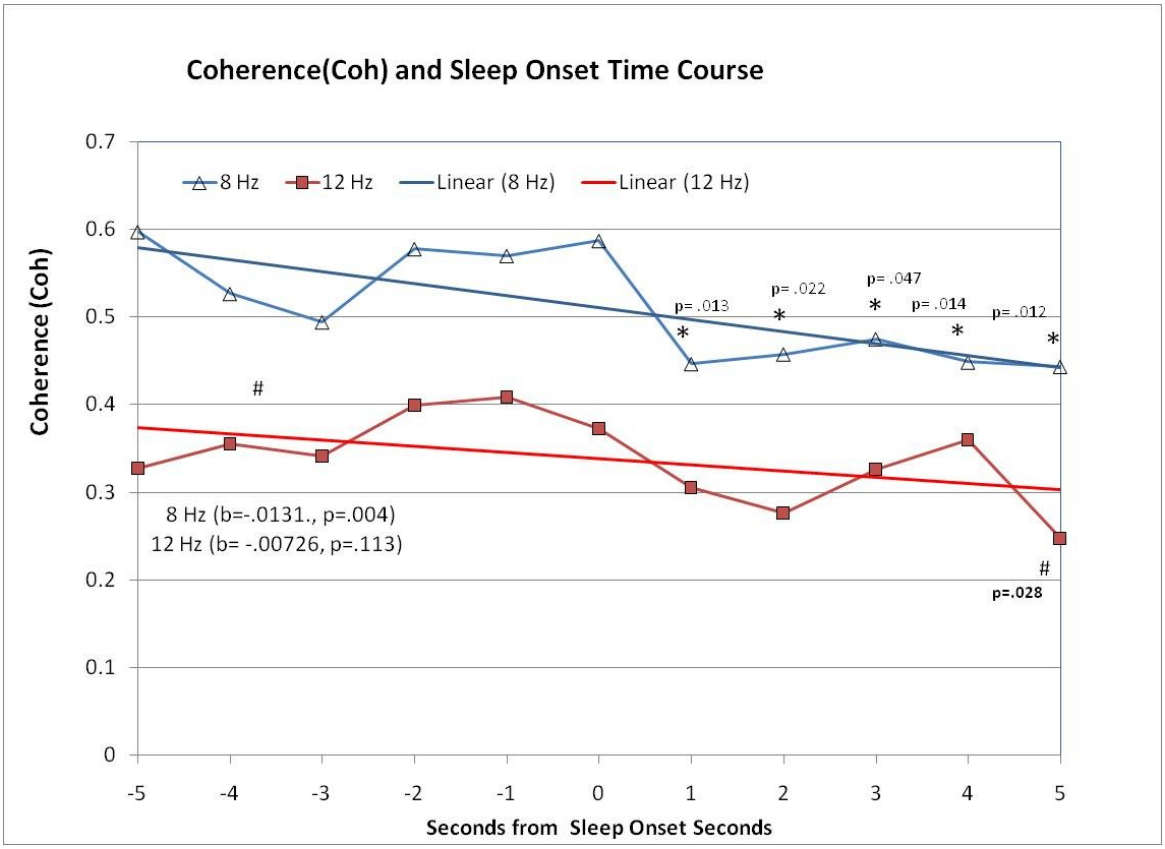

Changes in amplitude and phase synchrony distributions observed in EEG across hemispheres during sleep onset REM periods in narcolepsy

Dissertation Supervisor

Dr. Arthur J. Spielman[1]

Hans von Gizycki[1,2]

[1]The City College of the City University of New York, New York, NY

[2]Scientific Computing Center, SUNY Downstate Medical Center, Brooklyn, NY, U.S.A.

Key words: Phase Synchrony, Amplitude Synchrony, Narcolepsy, SOREMP, sleep onset, EEG activity, Analysis, Instantaneous Phase Synchrony Distribution.

Running title: Synchrony Changes Narcolepsy

Corresponding author: Hans von Gizycki, Scientific Computing Center, SUNY Downstate Medical Center, 450 Clarkson Avenue, Box 7, Brooklyn, New York, 11203, USA ; Tel.: (718) 270-7474; Fax: (718) 270-7461;

E-mail: vongizycki@downstate.edu

Abstract

Introduction: This presentation aims to analyze the evolution of sleep onset for narcoleptic subjects by examining the time course of the EEG through the wake sleep transition. This will be done in both REM and Non-REM (NREM) multiple sleep latency naps. The EEG during wakefulness and sleep will be compared between naps that contain REM and those naps that do not contain REM. We propose that the waking state prior to sleep onset is inherently different between naps that contain REM and those that don't. To obtain a high temporal resolution during the time course of sleep onset, we used continuous wavelet transform (CWT) based measures of phase and amplitude synchronization, which we have already successfully used to analyze the EEG changes associated with seizures and the normal sleep onset period.

Methods: EEG was recorded from narcolepsy patients undergoing a multiple sleep latency test (MSLT). Resultant data was visually scored in five second epochs, and then using the attenuation of occipital alpha as the sleep onset criteria it was precisely localized. This precise information was used to create an 11 second epochs of EEG data comprised of 5 seconds prior to sleep onset, 1 second of the actual sleep onset transition and 5 seconds post sleep onset. Different electrode derivations were used to assess inter- and intra-hemispheric synchrony changes in the following measures the phase synchrony measure synchrony entropy index (SEI), and the amplitude synchrony measures, amplitude synchrony index (ASI).

Results: Repeated measures factorial ANOVA and post hoc tests, with EEG frequency bands, montage, and wake/sleep transition as factors, demonstrated that it was possible to differentiate between wake and sleep in the EEG power measures, as well as in the amplitude and phase synchrony/entropy measures. The SEI and ASI measures demonstrated that the waking period before sleep onset is intrinsically different in naps that contain sleep onset REM periods (SOREMPS) and those that do not. Additionally, the SEI synchrony measure demonstrated a specific pattern across electrode sites that allows for the differentiation of REM and NREM naps.

Conclusion: The high temporal resolution CWT-based phase and synchrony measures allowed us to analyze the differences in EEG during waking SOREMPS and non-SOREMPS naps. The results of the phase synchrony analysis show that the SEI measure is able to detect the intrusion of REM into the waking state in narcoleptic patients. With further development, it will be possible to develop an algorithm to predict whether a particular nap will have a REM period or not, based on the analysis of EEG collected during sleep onset.

Introduction

Narcolepsy is a rare disorder, with a prevalence estimated to be 0.02–0.05%, characterized by excessive daytime sleepiness, abnormal appearance of REM in the context of the sleep cycle, and a history of cataplexy in the majority of patients, defined as a rapid loss of muscle tone triggered by emotion (Longstreth, et al., 2007; Billiard et al.,2006; Dauviliers et al., 2007; American Academy of Sleep Medicine, 2005). Two forms of narcolepsy are recognized: narcolepsy with cataplexy (60–70% of patients) and narcolepsy without cataplexy (Robinson & Keating, 2007).

Human and animal data indicate that narcolepsy may be caused by abnormalities in the hypocretin system. Specifically, narcolepsy with cataplexy has been linked to the loss of hypocretin neurons in the hypothalamus (Billiard et al.,2006, Dauviliers et al., 2007, Robinson & Keating, 2007). Hypocretin appears to stabilize and prevent inappropriate changes in conscious state, such as the rapid switches between wakefulness and rapid eye movement (REM) sleep. Excitatory hypocretin neurons are active during wakefulness, and have strong projections to the brainstem structures implicated in REM sleep motor regulation. Thus, it has been proposed that decreased hypocretinergic tone may be the trigger that initiates abnormal REM sleep in narcoleptic patients (Mileykovskiy et al.,2005).

REM sleep is characterized by tonic features, including cortical EEG desynchronization and muscle atonia, and phasic events, including bursts of rapid eye movements, phasic activities of both chin and limb EMG, and cardiorespiratory variability (Chase &

Morales, 1983). Neurons in the cholinergic zone of the laterodorsal tegmentum and the pedunculopontine nuclei, called REM-on neurons, show preferential discharge activity during REM sleep, and extensive data indicate a key role in production of this state (Mileykovskiy et al.,2005). Activity of these cells may be related to the complete shutdown in the release of neurotransmitters such as norepinephrine and histamine, causing REM atonia. Heart rate and breathing rate are also irregular during REM sleep, and resemble patterns observed during waking hours. The eye movements associated with REM are generated by the pontine nucleus with projections to the superior colliculus and are associated with PGO (pons, geniculate, occipital) waves.

There is a substantial body of knowledge that demonstrates that REM sleep and NREM sleep are fundamentally different. Ogilvie et al., (1998) assessed the time course of sleep onset of narcoleptics using the MSLT paradigm and he compared the onset process between non-REM naps and REM naps. In general REM had higher spectral power values for delta and theta, and lower values for alpha and sigma. However, the time course was not well defined, because the sleep onset period was divided into quartiles, and mean root mean square (RMS) amplitude within each quartile was calculated. Previous studies have also demonstrated that hemispheric coherence measures in REM sleep are significantly lower than NREM sleep (Cantero et al., 1999).

In narcoleptics, auditory evoked potentials show substantial changes in cortical reactivity in the waking state prior to a sleep onset REM period (SOREMP) that are quite different from changes that occur in the waking state prior to non-SOREMP sleep (Pressman,

Spielman , Pollak, Weitzman, 1982). This pre-SOREMP effect can be seen as an intrusion of REM into the waking state. Therefore, we propose that a decrease in synchrony is associated with the waking state EEG prior to SOREMPs, and an increase in synchrony in waking EEG is associated with the NREM condition, which is expected during normal sleep onset (Corsi-Cabrera et al., 1996; Achermann and Borbely, 1998). To examine the EEG changes associated with REM and NREM sleep onset, we will use novel synchrony and entropy measures at a high temporal resolution in the analysis of EEG patterns of narcoleptic subject population undergoing a five nap MSLT. These measures will allow for a detailed quantitative examination of the synchrony changes that occur in the transition to the SOREMP, and may provide indirect evidence for the types of mechanisms responsible for producing REM intrusion.

Methods

All subjects in this study were evaluated and formally diagnosed with narcolepsy by the New York Methodist Hospital Sleep Center during a 2007 year (N=8). Use of the clinical data for research purposes was approved by the Institutional Review Board of New York Methodist Hospital. Data will be obtained from previously collected clinical data from multiple sleep latency tests (MSLT) and it will be utilized to test the hypothesis for this study. Patients underwent a full-night diagnostic polysomnogram (NPSG) and for evaluation of hyper-somnolence prior to their MSLT. Each subject will provide data from five MSLT naps where they had an opportunity to fall asleep in an environment conducive for sleep. The MSLT naps where conducted starting at 9 am at 2-hour

intervals with each nap lasting 20 minutes (Arand et. al, 2005). Therefore, within this nap context it is possible to record one or more episodes of sleep onset.

The patients were evaluated in an accredited sleep laboratory in sound attenuated rooms, monitored by an infra-red camera. A 10-channel montage was utilized for MSLT recordings comprised of EEG, EOG, EKG, and chin EMG. Telefactor/EEG32 hardware and software were utilized for polysomnographic recordings. Standard sleep recording montage was used (C3, C4, O1, 02, referenced to contra-lateral mastoid. EEG was sampled at 200 Hz, with 12 bit precision. Amplifier settings for the EEG channels were set as follows: sensitivity = 200 μV, high pass filter = .3Hz, low pass = 70Hz, and 60Hz a notch filter.

Montages

Synchrony was measured across two channel derivations in a several montages to assess different types of brain inter-connectivity: 1) Inter-hemispheric synchrony measured across a) ipsilateral posterior derivations (O2/A2/-O1/A1), and b) across ipsilateral central derivations (C4/A2-C3/A1). 2) Intra-hemispheric synchrony a) across ipsilateral posterior to central derivations (O2/A2-C4/A2), and b) across (differential) central-posterior derivations (C3/C4-O1/ O2).

Data Selection and Visual Scoring

The EEG data was selected using Grass Telefactor PSG TWin 2.6 from the overall data set for each MSLT nap. Each nap was delimited and selected from the formal beginning

of the nap “lights out” to the formal end “lights on”. EEG was first scored in10 second epochs and then each epoch was rescored in five second epochs

In order to localize the sleep onset transition wake/sleep scoring was performed at five second intervals and defined as the attenuation of occipital alpha (Hori et al., Rechtschaffen & Kales, 1968). Additionally, the exact moment of sleep onset was visually defined, because it was precisely with proprietary software where the investigator put a cursor right at the estimated moment of sleep onset. This scoring approach will was used to create 11 second epochs of EEG data comprised of 5 seconds prior to sleep onset, 1 second of the actual sleep onset transition and 5 seconds post sleep onset.

Data Analysis

Continuous Wavelet Transform

Preliminary data transformation prior to synchrony analysis was performed as follows: First, EEG signals at 8 and 12 Hz were extracted from the EEG data using a continuous wavelet transform (CWT), applying a first order complex Gaussian wavelet (Matlab Wavelets Toolbox, Mathworks, inc). The CWT is useful for examining the time varying behavior of the frequency spectrum of a finite signal segment, and is mathematically defined as:

$$CWT_x^{\psi}(\tau, s) = \frac{1}{\sqrt{s}} \int x(t)\psi\left(\frac{t-\tau}{s}\right) dt$$

where x(t) is the signal segment, s is the scale that adjusts the wavelet to a particular frequency (higher scale corresponds to "stretched" lower frequency versions of the wavelet), τ is the window size for the wavelet, and $\psi(t)$ is the Gaussian wavelet defined as the first derivative of the Gaussian function normalized to have an area of 1:

$$\psi(t) = \frac{-t}{\sqrt{2\pi\sigma^3}} e^{\frac{-t^2}{2\sigma^2}}$$

The CWT is analogous to the Fourier Transform (FT), which identifies the frequencies present in a signal (i.e. spectrum), but resolved in the time domain such that with a CWT, one can identify the time course of the appearance and disappearance of particular frequencies present in a signal. Likewise, the real and imaginary components of a CWT are also comparable to the FT amplitude and phase. The imaginary components of the CWT results for both channels were transformed to an angular term and unwrapped, producing a phase time series for each EEG channel and allowing for the calculation of the phase differences between these channels. Additionally, the demodulated amplitude of the real component of the complex wavelet coefficients was extracted using a Hilbert transform, which involves the convolution of the signal with $h(t)=1/\pi t$. The transformed data were subjected to a series of synchrony analysis, as described below.

All the synchrony measures were computed in 1 second analysis bin

Synchrony Entropy Index

Synchrony Entropy Index (SEI) measures the deviation of phase differences from the uniform distribution. The SEI metric was quantified using an index based on Shannon's entropy (Tass et al. 1998).First, a histogram of the phase differences ϕxy is created for all the time points in the window, and divided into bins uniformly distributed around the unit circle. The entropy hN is then defined as:

$$h_N = -\sum_{j=1}^{L} p_j \log p_j$$

where pj is the probability corresponding to the jth bin, and L is the number of bins. This value can then be normalized to the maximum entropy, which is achieved with a uniform distribution where pj = 1/L for all bins j, and hNmax=log(L). This normalized entropy is the SEI, calculated as:

$$SEI = \frac{h_N^{\max} - h_N}{h_N^{\max}}$$

SEI has values between 0 and 1, and is a measurement that reflects the degree of clustering of the distribution of the phase differences. Thus, if there is are similarities between the phase difference values in particular segments of the time series (i.e. phase difference is more constant), SEI has a value closer to 1, and if the phase differences are more erratically distributed, then SEI has a value closer to 0. A similar method was used to calculate Entropy Amplitude Index (EAI), which measures the degree of clustering in

the distribution of amplitude differences. The SEI metric was developed using custom-made software written in Matlab.

Amplitude Synchrony Index

The Amplitude Synchrony Index (ASI) measures the correlation between demodulated amplitude parameters, and represents the synchronization of two EEG signals in time (Nikouline et al., 2001, Bruns et al., 2000). Thus, if the amplitude time series parameters are similar, the ASI is closer to 1, and if they are not similar, then the ASI is closer to 0. In essence, ASI represents the amplitude contribution in the coherence calculation**.** The key feature of ASI is that it is only sensitive to amplitude, and is consequently independent of signal phase. The SI metric was developed using custom-made software written in Matlab.

Statistical Analysis

The MSLT naps where performed throughout the day and time of day is usually an important consideration in this paradigm, however, in this analysis of short term changes in synchrony around sleep onset time of day was not a significant factor. Therefore, in order to present the most parsimonious and the most comprehensible model the factor time of day was removed from all the ANOVA analysis. Additionally, in order to make the analysis manageable the data was limited to synchrony analysis performed at 8 Hz, and four synchrony derivations, 2 inter-hemispheric (O2/A2-O1/A1, C4/A2-C3/A1), and 2 intra-hemispheric (O2/A2-C4/A2, C3/C4-O1/O2).

All synchrony measures were assessed across factors using repeated measures ANOVA. Sleep wake analysis initially consisted of using a General Linear Mixed Model (GLMMixed) to perform a factorial ANOVA with three factors: a) REM/NREM Nap (2 levels of nap which consisted of the presence or absence of a REM period, b) synchrony montage with 4 levels: (O2/A2-O1/A1, C4/A2-C3/A1, O2/A2-C4/A2, C3/C4-O1/O2) and, wake/sleep with two levels (wake and sleep, which consists of the average synchrony for 6 seconds for wake and sleep). After the initial wake/sleep analysis was performed on our outcome measures, further more detailed analysis with a higher temporal resolution beyond the simple categories of wake and sleep was performed at central derivation (C4/A2-C3/A1). This was done by analyzing the effect of the time course of the wake to sleep transition, which is the time course of sleep onset. Repeated measures ANOVA (GLMMixed) was used to assess the time course of the sleep onset process that was examined with a much higher resolution beyond just wake and sleep, (with 5 seconds before and after sleep onset event, with 11 levels (-5, -4, -3, -2, -1, 0, 1, 2, 3, 4, 5). Time – 5, the subject is awake and at time 0 the subject falls asleep and continues in this state until time 5. The time course of the sleep onset process was examined for all EEG synchrony and clustering variables. Additionally, post-hoc tests (Least Significant Difference) were applied to localize the source of the variance for both the averaged wake sleep and time course of sleep onset.

To further assess the time course of sleep onset, a GLMMixed model repeated measures regression was used to assess how well the synchrony and clustering measures demonstrate relatively long-term gradual linear change in the time course of sleep onset. Furthermore, using ANOVA the means of the residuals of the regression model were

assess along the time course to locate abrupt changes along the time course that are not explained by a linear term but are temporally associated with sleep onset.

Results

EEG Power

A three factor ANOVA was performed to assess log of EEG power for all frequency bands (Figure 1), with REM (REM nap type: REM, NREM), montage (O2/A2, C4/A2, O2/A2, C3/C4), and wake/sleep (wake, sleep) as factors.

For delta, the analysis demonstrated significant main effects for wake/sleep ($F_{1,919}$= 8.816, p = .003), and montage ($F_{3,2338}$= 135.299, p < .001) but not for REM ($F_{1,919}$= 3.339, p = .068). Second order interactions demonstrated that REM by montage ($F_{3,2338}$= 3.734, p=.011) was significant but wake/sleep by REM and montage by wake/sleep were not. The three-way interaction frequency by montage by wake/sleep was also not significant. Delta power differed between wake and sleep in the NREM nap condition only in the central derivation (C3/C4; p=.015). However, during the REM nap condition, wake and sleep differed for O2/A2, C4/A2, and O2/A2 (all, p<.039).Additionally, during the wake condition, REM had a higher delta power value than NREM in the C3/C4. Delta power in the sleep condition did not differ between REM & NREM in any of the derivations.

The analysis of the theta band demonstrated significant main effects for wake/sleep ($F_{1,895}$= 5.27, p = .022), and montage ($F_{3,2286}$= 295.283, p < .001) but not for REM. Second order interactions demonstrated that montage by wake/sleep ($F_{3,2286}$= 73.59, p<.001) was significant but wake/sleep by REM and REM by montage were not. The three-way interaction frequency by montage by wake/sleep was also not significant. Theta power differed between wake and sleep in the NREM nap condition only in the central derivation (C3/C4; p=.015). However, during the REM nap condition, wake and sleep differed for O2/A2, C4/A2, and O2/A2 (all, p<.039).

Alpha band analysis demonstrated significant main effects for wake/sleep ($F_{1,834}$= 108.357, p < .001), and montage ($F_{3,2355}$= 168.40, p < .001), but not for REM. Second order interactions REM by montage, wake/sleep by REM and montage by wake/sleep were not significant. The three-way interaction frequency by montage by wake/sleep was also not significant. Alpha power was greater in wake when compared to sleep in the NREM nap condition in all derivations (O2/A2, C4/A2, O2/A2, C3/C4; all p<.001). The same pattern was observed for all derivations in REM condition, where alpha power was also greater in wake when compared to sleep (p<.001). However, in the wake condition, REM and NREM did not differ for all montages, and the same situation was observed in the sleep condition.

The analysis of the beta band demonstrated significant main effects for wake/sleep ($F_{1,990}$= 60.502, p < .001), and montage ($F_{3,2286}$= 29.362, p < .001) but not for REM. Second order interactions REM by montage, and wake/sleep by REM and montage by

wake/sleep were not significant. The three-way interaction frequency by montage by wake/sleep was also not significant. Beta power was higher in wake when compared to sleep conditions in the NREM nap for all derivations (all, $p<.043$). The same was the case in the REM condition (all, $p<.001$).

Additionally, during the wake condition, REM had a higher beta power value than NREM in the C3/C4 ($p =.023$). Beta power in the sleep condition did not differ between REM & NREM in any of the derivations.

Phase Synchrony

The SEI synchrony measure at 8 Hz demonstrated significant main effects for wake/sleep ($F_{1,1374}= 36.818$, $p < .001$), REM ($F_{1,1374}= 5.512$, $p = .019$), and montage ($F_{3,2785}= 33.858$, $p < .001$). Second order interactions demonstrated that, montage by wake/sleep ($F_{3,2785}= 3.060$, $p =.027$), and REM by montage ($F_{3,2785}= 9.618$, $p < .001$) were significant but wake/sleep by REM was not. The three way interaction frequency by montage by wake/sleep was also not significant ($F_{3,2785}= 1.168$, $p=.321$). Post-hoc analysis revealed during the sleep onset process, the SEI for wake-NREM (nap type) was significantly lower than the SEI for wake REM ($p<.001$) in the occipital inter-hemispheric synchrony derivation (O2/A2-O1/A1). NREM was also significantly lower when sleep NREM and REM SEI values were compared ($p<.001$). When SEI NREM was compared between the wake and sleep conditions, it was observed that sleep SEI was significantly lower ($p=.012$). Similarly, comparisons of sleep and wake conditions for REM SEI demonstrated that the sleep condition was significantly lower than wake ($p<.001$) (Figure

2). In the central derivation (C4/A2-C3/A1), the wake condition NREM was higher than REM however, it only approached significance (p=.098).

A more refined analysis of sleep wake transition was performed, where the time course of the sleep onset period is examined with greater temporal resolution. The SEI demonstrated significant main effects for time course ($F_{10,632}$= 3.345, p <.001), and montage ($F_{3,2518}$= 34.15, p < .001) but not for REM ($F_{1,102}$= 1.490, p = .225). Second order interactions demonstrated that, time course by REM ($F_{10,632.32}$= 1.981, p = .033) and REM by montage ($F_{3,2518}$= 12.30, p < .001) were significant but montage by time course was not. The three-way interaction frequency by montage by wake/sleep was also not significant. SEI post-hoc analysis revealed differences in the effect of sleep onset for NREM and REM conditions only in the inter-hemispheric synchrony derivations C4/A2-C3/A1 and O2/A2-O1/A1 (Figure 2).

In the central derivation (C4/A2-C3/A1), wake-related times -3, -2, -1 in NREM were significantly higher than REM (p <.043). It was possible to discern this because of the high temporal resolution of the CWT-based techniques used in this study; comparisons of the averages of wake data points and sleep data points could not detect this difference. The reason is that SEI data points -5 and -1 in the NREM nap condition are below all REM values, and above in the other 3 data points (Figure 2). Additionally, these three time points for the NREM are significantly higher than sleep onset time point 0 (for all, p< .019); this effect was not observed in the REM condition.

Results similar to those obtained with the inter-hemispheric montage were obtained with the occipital derivations, however, the results are inverse, such that the REM condition is higher during wakefulness than the NREM condition, with time points -5, -2, -1, and 0 being significantly higher in the REM condition. Additionally, in the REM condition, time points -2, -1, and 0 were all significantly higher than time points 1, 2, 3, 4, and 5 (all, $p<.02$) (Figure 2). Therefore this effect is only observable inter-hemisphericaly, and in wakefulness. This appears to be a marker for sleep onset for both REM and NREM. The intra-hemispheric derivations did not show any differences between REM and NREM during the sleep onset time course.

ASI

The ASI demonstrated significant main effects for REM ($F_{1,79}= 4.98$, $p = .029$), and montage ($F_{3,2832}= 188.968$, $p < .001$), but not for time course. Second order interactions demonstrated that, montage by time course ($F_{30,2833}= 1.890$, $p =.002$), and REM by montage ($F_{3,2832}= 17.66$, $p < .001$) were significant, but time course by REM was not. The three way interaction frequency by montage by wake/sleep was also not significant ($F_{30,2833}= .880$, $p=.655$). ASI post hoc tests detected the sleep wake transition during the sleep onset time course, but unlike the SEI in the inter-hemispheric occipital derivation (O2/A2-O1/A1), there is a very large separation between the time course of NREM and REM, such that there is a significant difference between the two conditions for time points -3, -2, -1, 0, 2, 3, 4, 5 (Figure 3). Additionally, there was a time course effect especially in the REM condition, because time point 1 differed significantly from time points -3, -2, -1, 4, 5 (all, $p<.043$). The time course of the central interhemispheric

channel was a marker for sleep onset in either REM or NREM nap conditions. Additionally it was not possible to differentiate between REM and NREM at specific time points.

Discussion

SEI wake/sleep analysis demonstrated that NREM and REM naps EEG differed during the waking suggesting that the effect of an impending sleep onset REM period in the nap is already felt in the waking state. This is consistent with the earlier findings of Pressman et al., (1988) where the effects a forthcoming sleep onset REM period affects the amplitude of an auditory evoked potential during wakefulness. The same wake sleep analysis was performed during the sleep state and NREM naps were lower in synchrony than REM naps. Furthermore, there was a drop in synchrony when the transition from wake to sleep took place and this was the case in both NREM and REM nap sleep onset processes. The time course analysis further refined these results by providing fine temporal resolution for the sleep onset process.

The sleep onset time course is very different in the REM naps compared to the NREM naps. During the waking, there was higher inter-hemispheric phase synchrony (SEI) in the REM condition when compared to the NREM. Therefore, increases in occipital inter-hemispheric synchrony during the waking state can be considered as an intrusion of REM sleep during waking and can be considered as predictor of an impending narcoleptic event such as an increase hypersomnolence or the manifestation of cataplexy. This was also the case in the sleep condition, where REM sleep has a higher phase synchrony than NREM, and this approach can be used as a marker for detecting REM periods from sleep onset EEG. Additionally, this is also evident in the central channels, however, it is the inverse of the occipital, where NREM sleep episodes have higher SEI values during

waking. The amplitude synchrony measures do not detect wake to sleep transition, but provide a differentiation between REM and NREM conditions during most of the sleep onset time course. Further testing of these observations can lead to a method that can be used as a marker for REM sleep onset in the diagnostic clinical realm.

Many of the synchrony and entropy measures outlined in this study have been used in the development of a seizure prediction algorithm that is highly sensitive to subtle changes in synchrony prior to a hypersynchronous event or a seizure (Litt & Echauz 2002). A large variety of methods have been used to assess synchrony during seizures, such as cross correlation, coherence, wavelet-based phase synchronizations, mutual information (Quiroga et al., 2002), global or local synchronization (van Putten, 2003), mean phase coherence (Mormann et al., 2000), and instantaneous phase synchrony distribution (von Gizycki et al., 2008). Furthermore, these techniques have been used in the neurocognition field to examine transient functional coupling in support of the "temporal correlation hypothesis". (Singer 1999, Weiss & Rappelsberger, 2000) The novel high temporal resolution CWT-based phase and synchrony measures allowed us to separately analyze the differences in amplitude and phase synchrony in EEG during SOREMP and non-SOREMP naps. Our results demonstrate that these synchrony and entropy techniques are very useful in the study of sleep onset, and should be applicable to the many other processes that occur throughout the sleep cycle.

Figures and Captions

Figure 1: Wake/Sleep power differences between REM and NREM naps

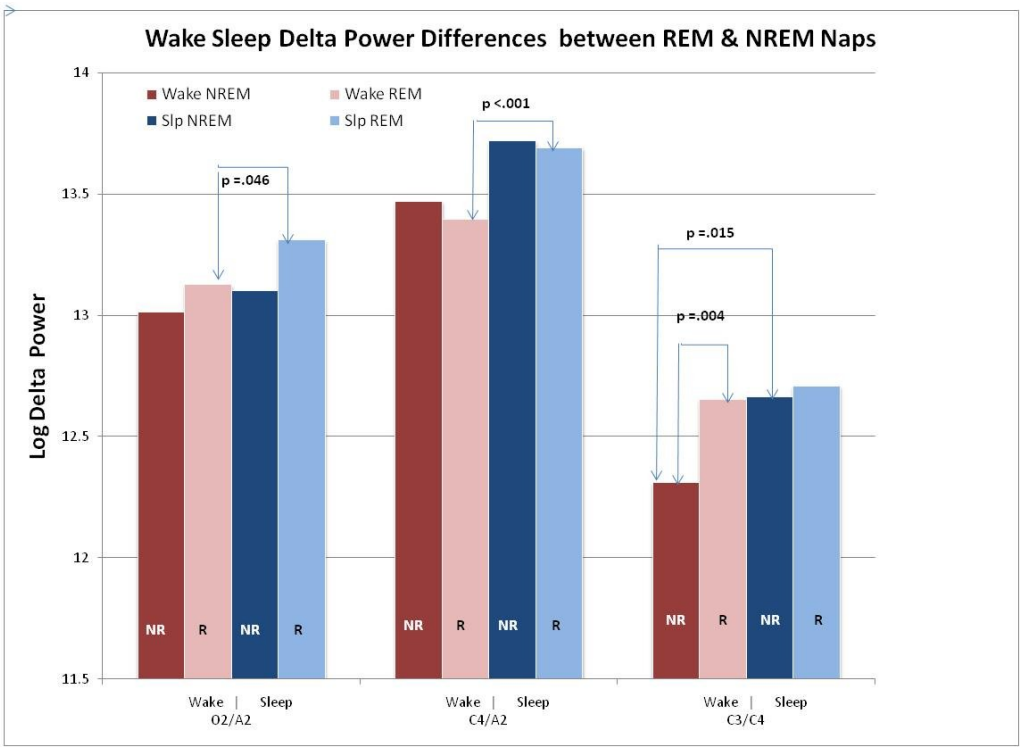

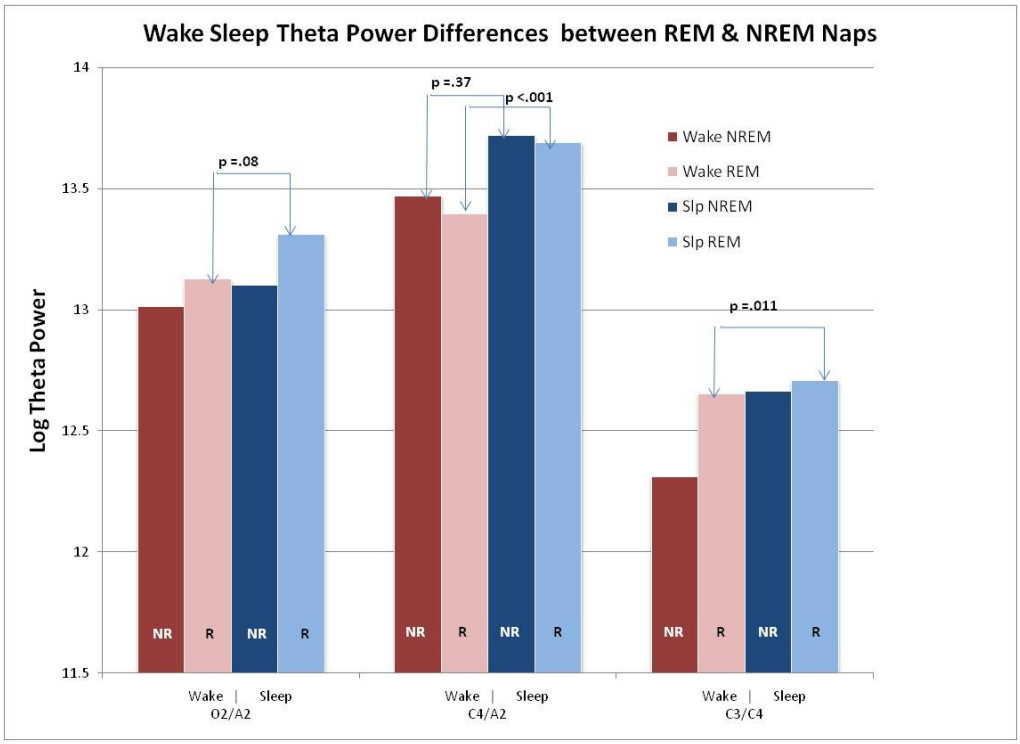

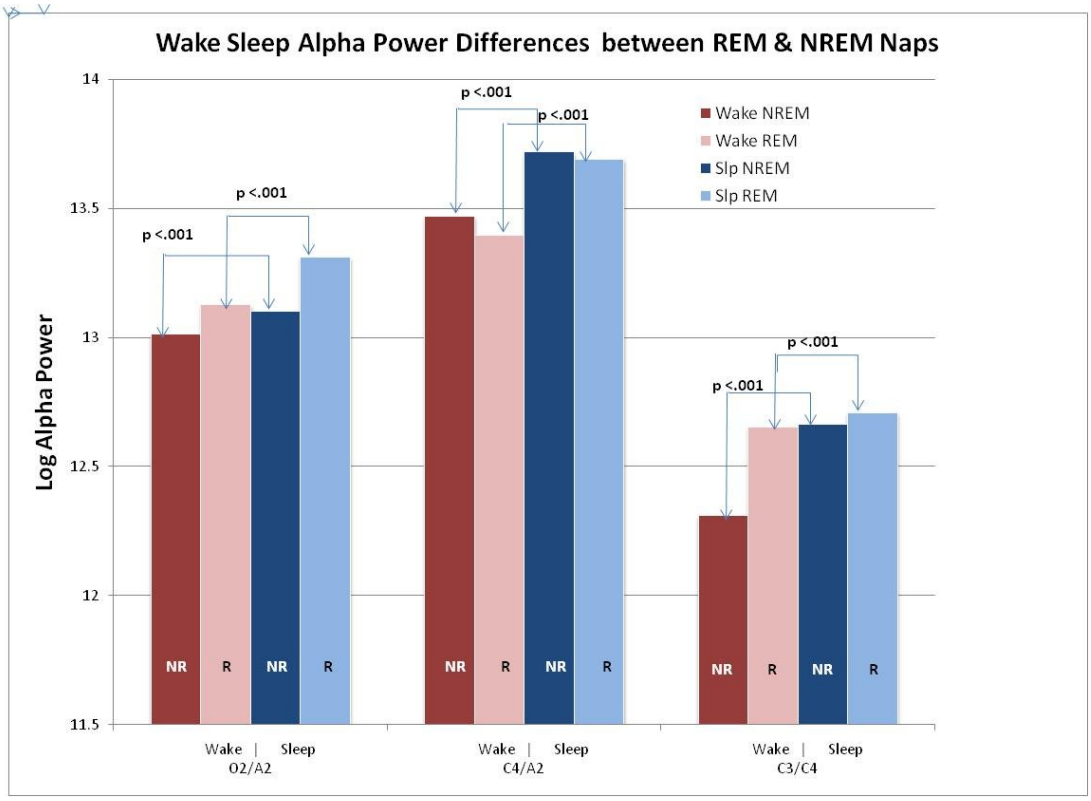
Wake Sleep Alpha Power Differences between REM & NREM Naps
Log Alpha Power
14
13.5
13
12.5
12
11.5
Wake NREM
Wake REM
Slp NREM
Slp REM
p <.001
p <.001
p <.001
p <.001
p <.001
NR
R
NR
R
Wake | Sleep
O2/A2
C4/A2
C3/C4

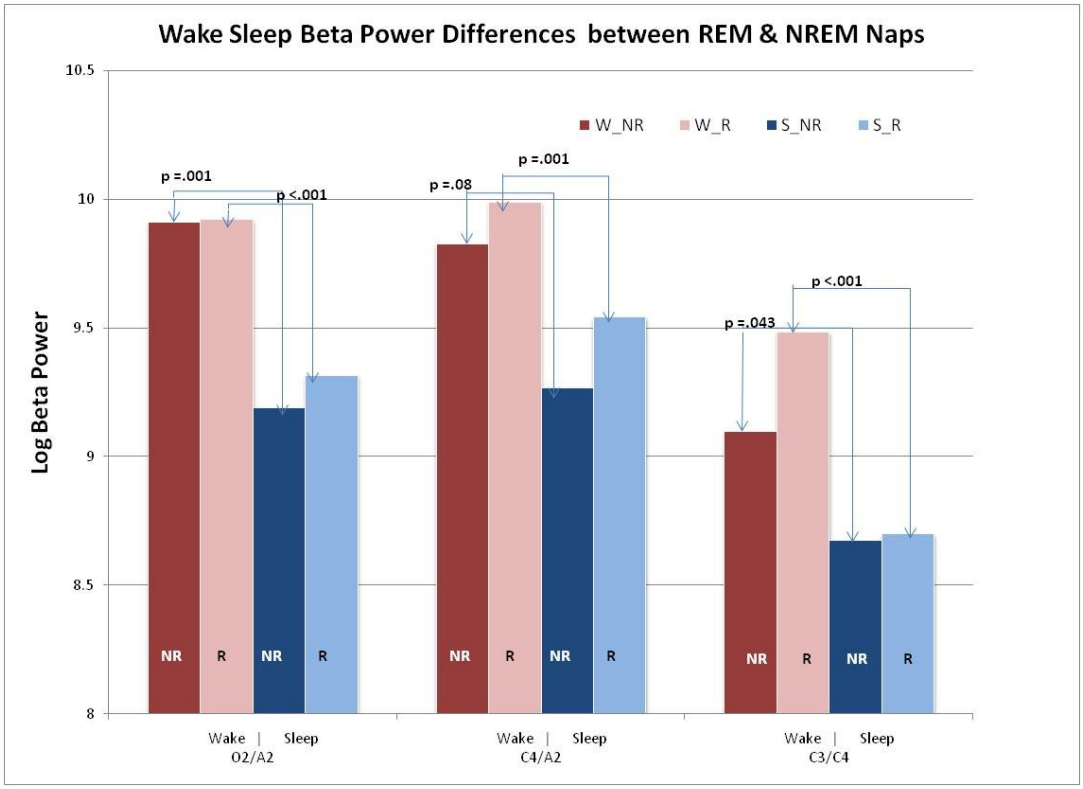
Wake Sleep Beta Power Differences between REM & NREM Naps
Log Beta Power
10.5
10
9.5
9
8.5
8
W_NR
W_R
S_NR
S_R
p =.001
p <.001
p =.08
p =.001
p =.043
p <.001
NR
R
NR
R
Wake | Sleep
O2/A2
C4/A2
C3/C4

Figure 2: Wake Sleep Changes and Time course of interhemispheric changes in SEI during REM and NREM naps

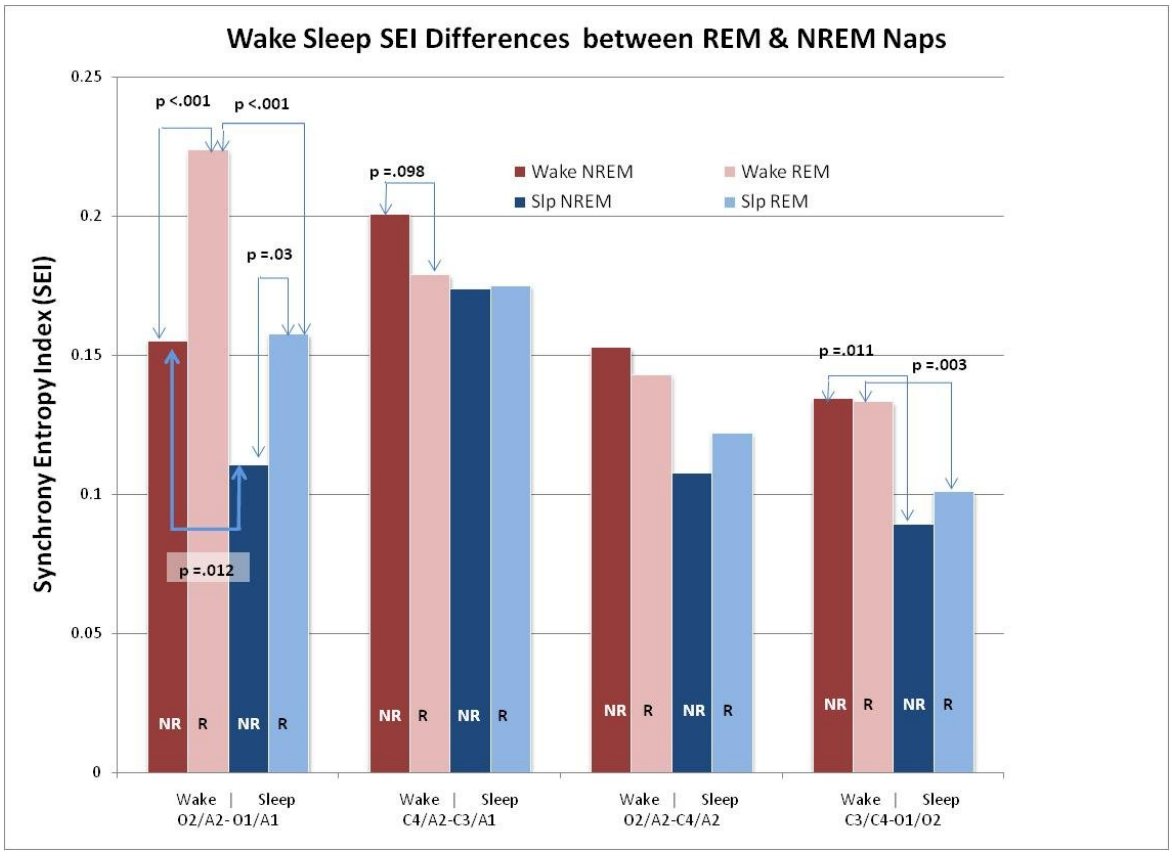

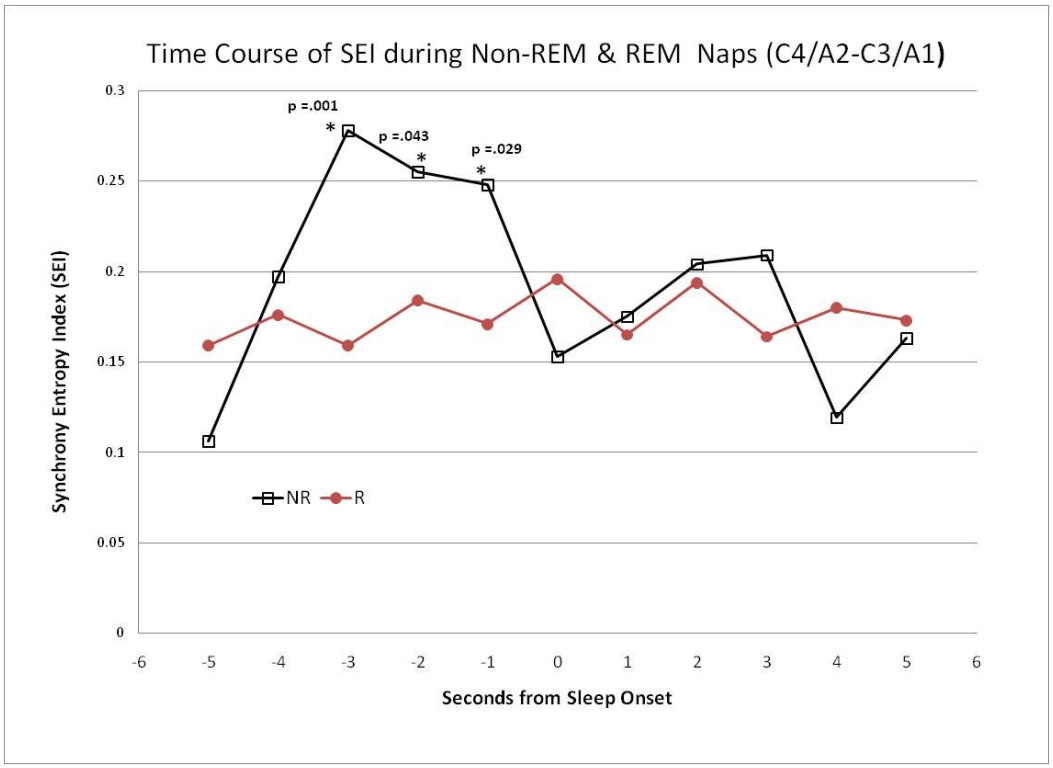
Time Course of SEI during Non-REM & REM Naps (C4/A2-C3/A1)
Synchrony Entropy Index (SEI)
Seconds from Sleep Onset
NR
R
p =.001
p =.043
p =.029
0.3
0.25
0.2
0.15
0.1
0.05
0
-6
-5
-4
-3
-2
-1
0
1
2
3
4
5
6

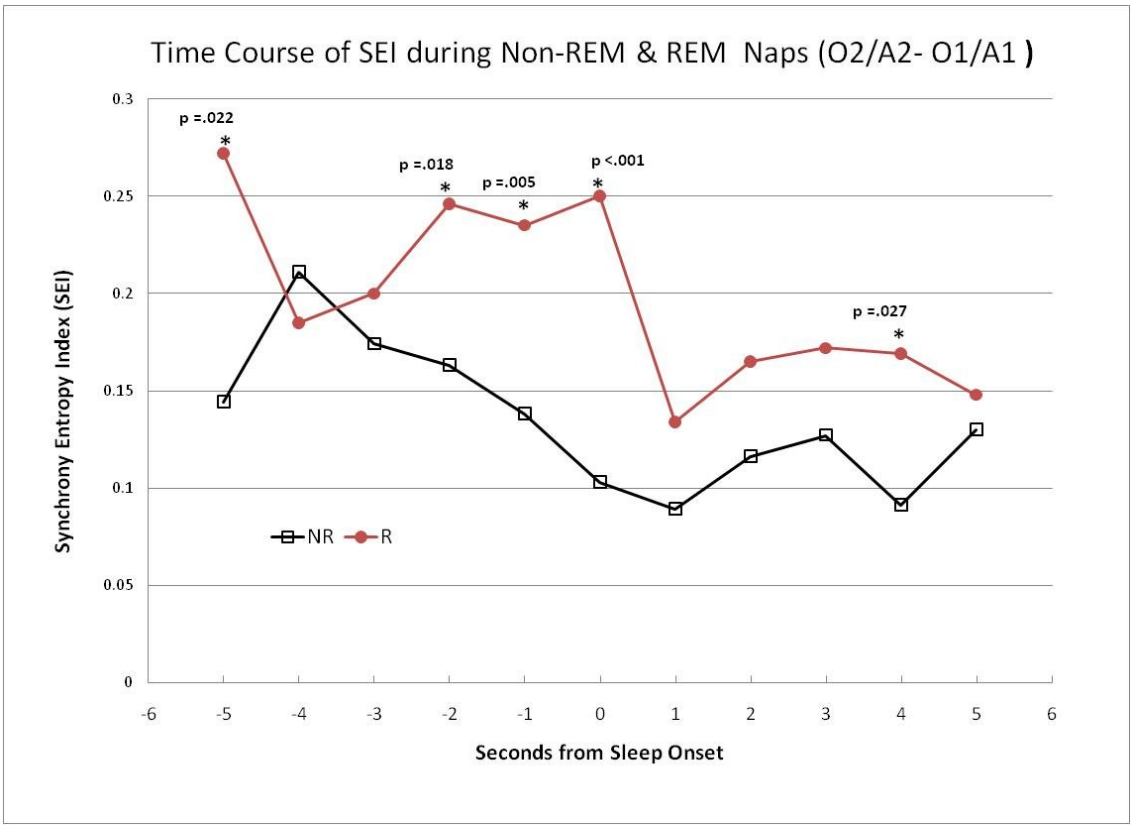
Time Course of SEI during Non-REM & REM Naps (O2/A2- O1/A1)
Synchrony Entropy Index (SEI)
Seconds from Sleep Onset
NR
R
p =.022
p =.018
p =.005
p <.001
p =.027
0.3
0.25
0.2
0.15
0.1
0.05
0
-6
-5
-4
-3
-2
-1
0
1
2
3
4
5
6

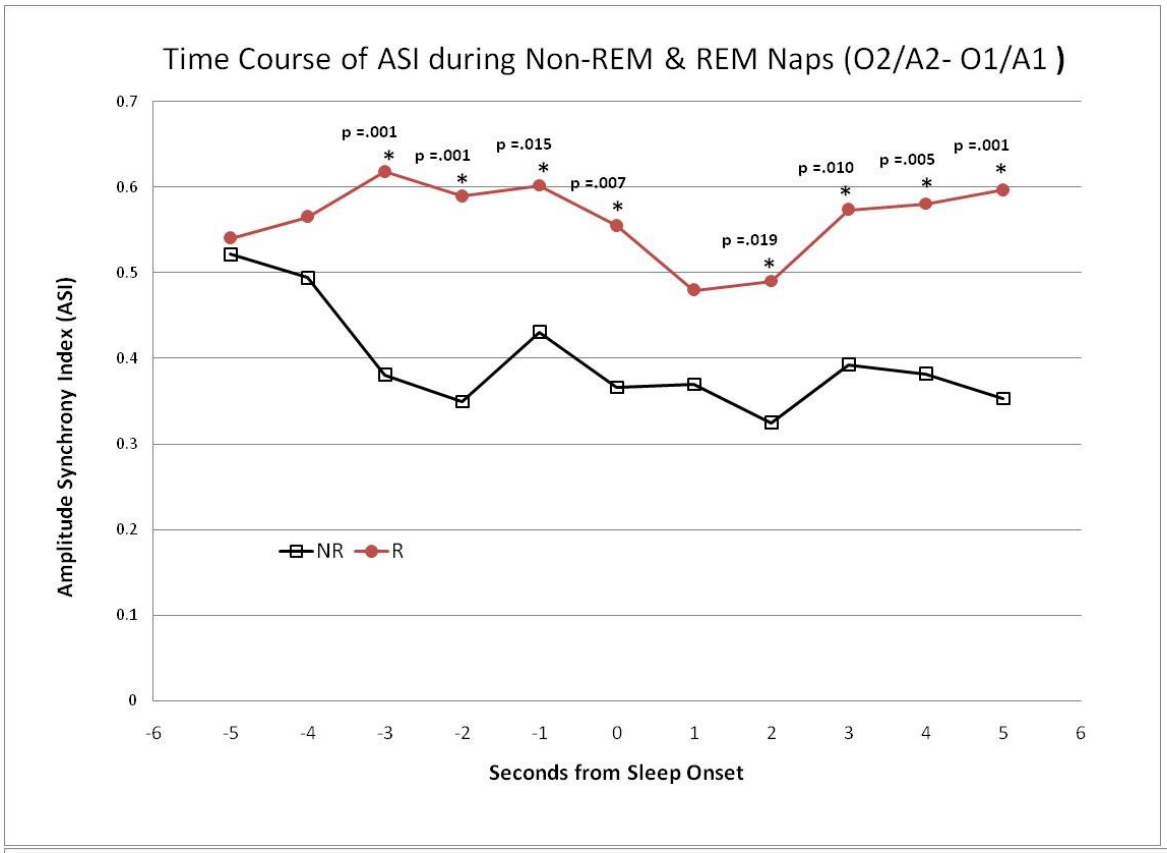

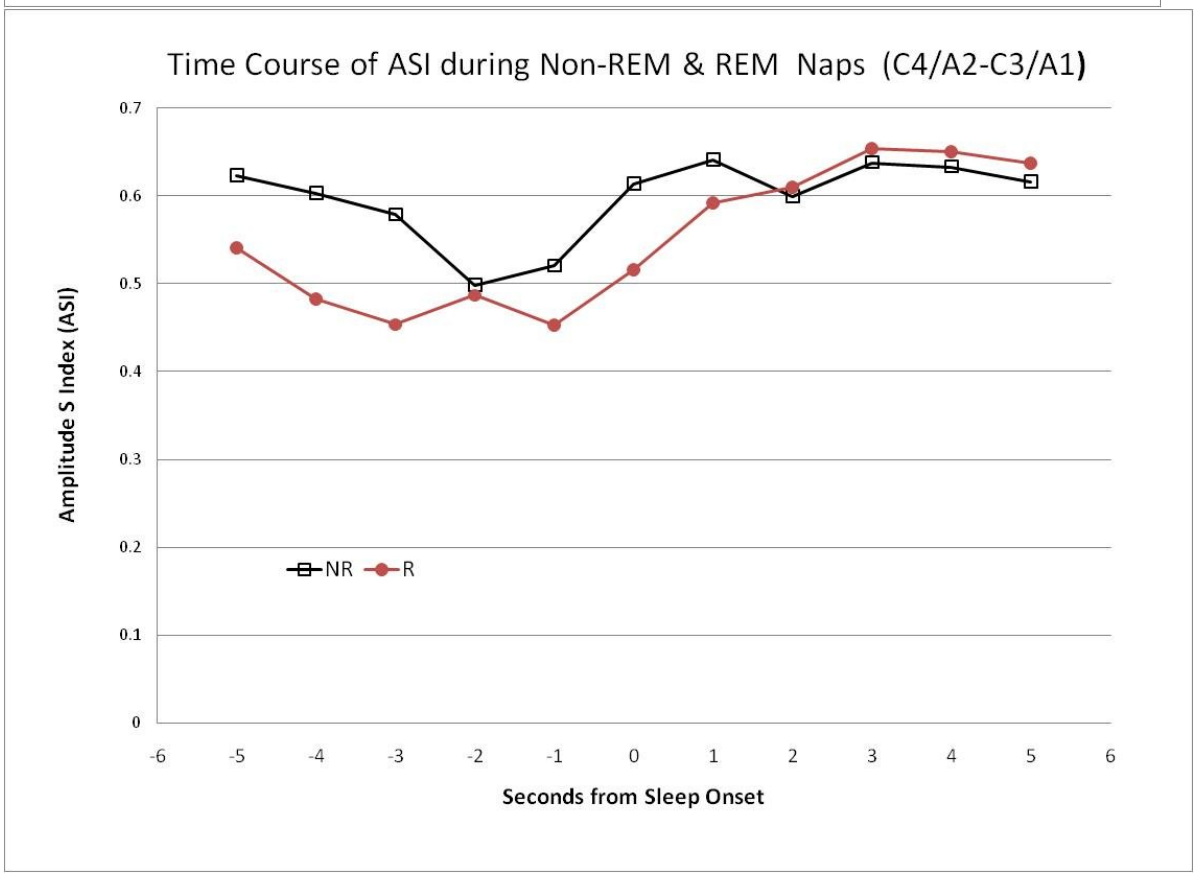

Figure 3: Time course of interhemispheric changes in ASI during REM and NREM naps

References for Introduction

Achermann P, Borbely AA (1998) Coherence analysis of the human sleep electroencephalogram. Neuroscience 85:1195–1208.

Bressler SL, Coppola R, Nakamura R.(1993) Episodic multiregional cortical coherence at multiple frequencies during visual task performance. Nature ;366(6451):153-6.

Bruns A, Eckhorn R, Jokeit H, Ebner A. Amplitude envelope correlation detects coupling among incoherent brain signals. Neuroreport. 2000 May 15;11(7):1509-14.

Bullock TH, McClune MC. (1989) Lateral coherence of the electrocorticogram: a new measure of brain synchrony. Electroencephalogr Clin Neurophysiol. 1989 Dec;73(6):479-98.

Chávez M, Le Van Quyen M; Navarro V; Baulac M; Martinerie J (2003) Spatio-Temporal Dynamics Prior to Neocortical Seizures: Amplitude Versus Phase Couplings. IEEE Transactions on Biomedical Engineering. 50(5): 571

Corsi-Cabrera M, Guevara MA, Arce C, Ramos J (1996) Inter and intrahemispheric EEG correlation as a function of sleep cycles. Prog Neuropsychopharmacol Biol Psychiatry 20:387–405.

Gray CM. (1999) The temporal correlation hypothesis of visual feature integration: still alive and well, Neuron 24: 31–47, 111–125.

Gray CM, Konig P, Engel AK, Singer AK. (1989) Oscillatory responses in cat visual cortex exhibit inter-columnar synchronization which reflects global stimulus properties. Nature, 338: 334–337.

Koeda T, Knyazeva M, Njiokiktjien C, Jonkman EJ, De Sonneville L, Vildavsky V (1995) The EEG in acallosal children: coherence values in the resting state: left hemisphere compensatory mechanism? Electroencephalogr Clin Neurophysiol 95:397–407.

Krueger JM, Oba l FJ (2003) Sleep function. Front Biosci 8:d511–d519. Kuks JB, Vos JE, O'Brien MJ (1987) Coherence patterns of the infant sleep EEG in absence of the corpus callosum. Electroencephalogr Clin Neurophysiol 66:8–14.

Kuks JB, Vos JE, O'Brien MJ. (1987) Coherence patterns of the infant sleep EEG in absence of the corpus callosum. Electroencephalogr Clin Neurophysiol. Jan;66(1):8-14.

Lachaux JP, Rodriguez E, Martinerie J, and Varela FJ. Measuring phase synchrony in brain signals. (1999) Hum Brain Mapp 8: 194–208,.

Le Van Quyen M, Foucher J, Lachaux J, Rodriguez E, Lutz A, Martinerie J, and Varela FJ. (2001) Comparison of Hilbert transform and wavelet methods for the analysis of neuronal synchrony. J Neurosci Methods 111: 83–98.

Litt B, Echauz J. (2002) Prediction of epileptic seizures. Lancet Neurology 2002; 1: 22–30

Misiti, M., Misiti, Y., Oppenheim G., Poggi J. M., Wavelet Toolbox™ 4, User's Guide, Natick, Massachusetts, The MathWorks, Inc., 2008.

Montplaisir J, Nielsen T, Cote J, Boivin D, Rouleau I, Lapierre G (1990) Interhemispheric EEG coherence before and after partial callosotomy. Clin Electroencephalogr 21:42–47.

Mormann F, Lehnertz K, David P, Elger CE (2000). Mean phase coherence as a measure for phase synchronization and its application to the EEG of epilepsy patients. Physica D; 144: 359–69.

Nielsen TA, Chenier V. Variations in EEG Coherence as an Index of the Affective Content of Dreams from REM Sleep: Relationships with Face Imagery. Brain and Cognition 41, 200–212 (1999)

Nielsen T, Montplaisir J, Lassonde M (1993) Decreased interhemispheric EEG coherence during sleep in agenesis of the corpus callosum. Eur Neurol 33:173–176.

Nikouline VV, Linkenkaer-Hansen K, Huttunen J, Ilmoniemi RJ. Interhemispheric phase synchrony and amplitude correlation of spontaneous beta oscillations in human subjects: a magnetoencephalographic study. (2001) Neuroreport.,12(11):2487-91..

Quiroga RQ, Kraskov A, Kreuz T, and Grassberger P. (2002) Performance of different synchronization measures in real data: A case study on electroencephalographic signals. Physical Review E, Vol 65, 041903

Rose M, Sommer T, Büchel C. Integration of local features to a global percept by neural coupling. Cereb Cortex. 2006 Oct;16(10):1522-8

Singer W. (1997) Time as coding space in neocortical processing: a hypothesis. In: M.S. Gazzaniga, Editor, The Cognitive Neurosciences, MIT Press, Cambridge, MA, pp. 91–104.

Singer W. (1999), Neuronal synchrony: a versatile code for the definition of relations?, Neuron 24 pp. 49–65, 111–125.

Singer W, Gray CM (1995) Visual feature integration and the temporal correlation hypothesis, Annu. Rev. Neurosci. 18 (1995), pp. 555–586.

Tass P, Rosenblum M, Weule J, Kurths J,. Pikovsky A, Volkmann J, Schnitzler A, Freund H. (1998) Detection of n:m phase locking from noisy data: Application to magnetoencephalography. Phys. Rev. Lett. 81, 3291-3294.

Timofeev I, Steriade M (1996) Low-frequency rhythms in the thalamus of intact-cortex and decorticated cats. J Neurophysiol 76:4152–4168.

van Putten MJA (2003) Nearest Neighbor Phase Synchronization as a Measure to Detect Seizure Activity from Scalp EEG Recordings. Journal of Clinical Neurophysiology 20(5):320–325.

von der Malsburg C. 1994. The correlation theory of brain function. In: Domany E, van Hemmen JL and Schulten K, editors. Models of neural networks II. Berlin: Springer. p 95--119.

von Gizycki H, Baptiste SL, Medveczky G, Kuzniecky RI, Devinsky O, Ludvig N (2006) Synchrony changes between hippocampal and neocortical EEG signals precede seizure activity induced by intrahippocampal NMDA application in freely behaving rats [Abstract] Epilepsia, 2006 SEP;47(3):47-47

von Gizycki H, Cunningham J, Spielman AJ, Lombardo G (2007) Hemispheric Phase and Amplitude Synchrony Differences Between Sleep and Wake Conditions. Submitted to the 2008 Associated Professional Sleep Societies Conference as an Poster.

Weiss S, Rappelsberger P. (2000) Long-range EEG synchronization during word encoding correlates with successful memory performance. Cognitive Brain Research 9: 299–312

References for Study 1

Aschenbrenner-Scheibe R, Maiwald T, Winterhalder M, Voss HU, Timmer J, Schulze-Bonhage A. (2003) How well can epileptic seizures be predicted? An evaluation of a nonlinear method. Brain. Dec;126(Pt 12):2616-26.

Bendat and Piersol, Engineering Applications of Correlation and Spectral Analysis, 2nd ed 1993 Wiley and Sons pg53

Bruns A, Eckhorn R, Jokeit H, Ebner A. (2000) Amplitude envelope correlation detects coupling among incoherent brain signals. Neuroreport. May 15;11(7):1509-14.

Chaovalitwongse W, Iasemidis LD, Pardalos PM, Carney PR, Shiau DS, Sackellares JC.Performance of a seizure warning algorithm based on the dynamics of intracranial EEG. Epilepsy Res. 2005 May;64(3):93-113.

Chávez M, Le Van Quyen M, Navarro V, Baulac M, Martinerie J (2003) Spatio-Temporal Dynamics Prior to Neocortical Seizures: Amplitude Versus Phase Couplings. IEEE Transactions on Biomedical Engineering. 50(5): 571

Drury I, Smith B, Li D, Savit R. (2003) Seizure prediction using scalp electroencephalogram.

Elger CE, Lehnertz K (1998) Seizure prediction by non-linear time series analysis of brain electrical activity. Eur J Neurosci. Feb;10(2):786-9.

Eriksson L, Henrik Antti H, Gottfries J, Holmes E, Johansson E, Lindgren F, Long I, Lundstedt T , Trygg J, Wold S. (2004) Using chemometrics for navigating in the large data sets of genomics, proteomics, and metabonomics (gpm). Anal Bioanal Chem 380: 419–429

Eriksson L, Johansson E, Kettaneh-Wold N, Trygg J, Wickström C, Wold S. (2006) Multi- and Megavariate Data Analysis, Basic Principles and Applications. Pub: Umetrics Academy, Umeå Sweden, 2006.

Farmer SF, Bremner FD, Halliday DM, Rosenberg JR, and Stephens JA. (1993) "The frequency content of common synaptic inputs to motoneurones studied during voluntary isometric contraction in man" *Journal of Physiology* 470:127-155

Fischell RE, Fischell DR, Adrian RM. (2000) Responsive implantable system for the treatment of neurological disorders. www.uspto.gov US Patent No.: 6,134,474.

Huxter JR, Zinyuk LE, Roloff EL, Clarke VR, Dolman NP, More JC, Jane DE, Collingridge GL, Muller RU. (2007) Inhibition of kainate receptors reduces the frequency of hippocampal theta oscillations. J Neurosci. Feb 28;27(9):2212-23.

Iasemidis LD, Shiau DS, Pardalos PM, Chaovalitwongse W, Narayanan K, Prasad A, Tsakalis K, Carney PR, Sackellares JC. (2005) Long-term prospective on on-line real-time seizure prediction. *Clin Neurophysiol* 116:532-544.

John JE, Baptiste SL, Sheffield LG, von Gizycki H, Kuzniecky RI, Devinsky O, Ludvig N. (2007) Transmeningeal delivery of GABA to control neocortical seizures in rats. Epilepsy Res. 2007 Jun;75(1):10-7.

Lachaux JP, Rodriguez E, Martinerie J, and Varela FJ. Measuring phase synchrony in brain signals. Hum Brain Mapp 8: 194–208, 1999.

Le Van Quyen M, Foucher J, Lachaux J, Rodriguez E, Lutz A, Martinerie J, and Varela FJ. Comparison of Hilbert transform and wavelet methods for the analysis of neuronal synchrony. J Neurosci Methods 111: 83–98, 2001.

Litt B, Echauz J. (2002) Prediction of epileptic seizures. Lancet Neurol. May;1(1):22-30.

Litt, B, Esteller, R, Echauz J, D'Alessanro M, Shor R, Henry T, Pannell P,Epstein C, Bakay R, Dichter M, Vachtsevanos. (2001) Epileptic seizures may begin hours in advance of clinical onset: a report of five patients. *Neuron* 30:51-64.

Ludvig N, Kovacs L, Medveczky G, Kuzniecky RI, Devinsky O. (2005) Towardthe development of a subdural hybrid neuroprosthesis for the treatment of intractable focal epilepsy. *Epilepsia* 46 (Suppl 8):270.

Ludvig N, Kovacs L. (2002) Hybrid neuroprosthesis for the treatment of brain disorders. www.uspto.gov US Patent No.: 6,497,699.

Ludvig N, Kuzniecky RI, Baptiste SL, John JE, von Gizycki H, Doyle WK, Devinsky O.(2006) Epidural pentobarbital delivery can prevent locally induced neocortical seizures in rats: the prospect of transmeningeal pharmacotherapy for intractable focal epilepsy. Epilepsia. Nov;47(11):1792-802.

Ludvig N, Tang HM. (2000) Cellular electrophysiological changes in the hippocampus of freely behaving rats during local microdialysis with epileptogenic concentration of NMDA. *Brain Res Bull* 51:233-240.

Ludvig N. (2000) Drug deliveries into the microenvironment ofelectrophysiologically monitored neurons in the brain of behaving rats and monkeys. In Chapin JK, Moxon KA (Eds) Neural Prostheses for Restoration of Sensory and Motor Function. CRC Press, New York, pp. 263-283.

Mormann F, Andrzejak RG, Elger CE, Lehnertz K. (2005) Seizure anticipation: Do mathematical measures correlate with video-EEG evaluation? Epilepsia. Aug;46(8):1335-6; 1336-7.

Mormann F, Andrzejak RG, Elger CE, Lehnertz K. (2007) Seizure prediction: the long and winding road. Brain. Feb;130(Pt 2):314-33.

Nikouline VV, Linkenkaer-Hansen K, Huttunen J, Ilmoniemi RJ. (2001) Interhemispheric phase synchrony and amplitude correlation of spontaneous beta oscillations in human subjects: a magnetoencephalographic study. Neuroreport.,12(11):2487-91.

Quiroga RQ, Kraskov A, Kreuz T, and Grassberger P.(2002) "Performance of different synchronization measures in real data: A case study on electroencephalographic signals". *Physical Review E, Vol* **65**, 041903

Quiroga RQ, Kreuz T, and Grassberger P. "Event synchronization: A simple and fast method to measure synchronicity and time delay patterns". *Physical Review E*, *Vol* **66**, 041904

Salant Y, Gath I, Henriksen O. (1998) Prediction of epileptic seizures from two-channel EEG. Med Biol Eng Comput. Sep;36(5):549-56.

Stein AG, Eder HG, Blum DE, Drachev A, Fisher RS. (2000) An automated drug delivery system for focal epilepsy. *Epilepsy Res* 39:103-14.

Tass P, Rosenblum M, Weule J, Kurths J,. Pikovsky A, Volkmann J, Schnitzler A, Freund H. (1998) Detection of n:m phase locking from noisy data: Application to magnetoencephalography. Phys. Rev. Lett. 81, 3291-3294.

Turner DA, Nicolelis MAL, Landingham K. (2005) Pre-ictal seizure detection and demand treatment strategies for epilepsy. In DA Turner (Ed) Modern Neurosurgery. Clinical Translation of Neuroscience Advances. CRC Press, New York, pp. 105-118.

Worrell G, Wharen R, Goodman R, Bergey G, Murro A, Bergen D, SmithM, Vossler D, Morrell M. (2005) Safety and evidence for efficacy of an implantable responsive neurostimulator (RNS) for the treatment of medically intractable partial onset epilepsy in adults. *Epilepsia* 46 (Suppl 8):226.

References for Study 2

Achermann P and Borbély AA (1997). "Low-frequency (<1 Hz) oscillations in the human sleep electroencephalogram." *Neuroscience* 81(1):213-222

Achermann P and Borbély AA (1998). "Coherence analysis of the human sleep electroencephalogram." *Neuroscience* 85(4):1195-1208

Arand D, Bonnet M, Hurwitz T, Mitler M, Rosa R, and Sangal RB (2005). "The clinical use of the MSLT and MWT." *Sleep* 28(1):123-44. Review.

Bruns A, Eckhorn R, Jokeit H, and Ebner A (2000). "Amplitude envelope correlation detects coupling among incoherent brain signals." *Neuroreport* 11(7):1509-14.

Corsi-Cabrera M, Guevara MA, Arce C, and Ramos J (1996). "Inter and intrahemispheric EEG correlation as a function of sleep cycles." *Prog Neuropsychopharmacol Biol Psychiatry* 20:387–405

De Gennaro L, Ferrara M, Curcio G, and Cristiani R (2001). "Antero-posterior EEG changes during the wakefulness-sleep transition." *Clinical Neurophysiology* 112:1901-1911

Destexhe A, Contreras D, and Steriade M (1999). "Spatiotemporal analysis of local field potentials and unit discharges in cat cerebral cortex during natural wake and sleep states." *J Neurosci* 19(11):4595-4608

Farmer SF, Bremner FD, Halliday DM, Rosenberg JR, and Stephens JA (1993). "The frequency content of common synaptic inputs to motoneurones studied during voluntary isometric contraction in man." *Journal of Physiology* 470:127-155

Gray CM, Konig P, Engel AK, and Singer AK (1989). "Oscillatory responses in cat visual cortex exhibit inter-columnar synchronization which reflects global stimulus properties." *Nature* 338: 334–337.

Gray CM. (1999) "The temporal correlation hypothesis of visual feature integration: still alive and well." *Neuron* 24: 31–47, 111–125.

Hori T, Hayashi M, and Morikawa T (1994). "Topographic EEG changes and the hypnagogic experience." In: Ogilvie RD, Harsh JR (eds). *Sleep Onset: Normal and Abnormal Processes*. Washington: American Psychological Association 1994

Hori T, Tanaka H, Hayashi M (1998). "Topographic mapping of EEG spectral power and coherence in the hypnagogic period" *Brain Topography Today* Proceedings of the III Pan-Pacific Conference on Brain Topography 1998:303-308

Hughes SW and Crunelli V (2007). "Just a phase they're going through: The complex interaction of intrinsic high-threshold bursting and gap junctions in the generation of thalamic α and θ rhythms." *International Journal of Psychophysiology* 64:3-7

Litt B and Echauz J (2002). "Prediction of epileptic seizures." *Lancet Neurology* 1: 22–30

Merica H and Fortune RD (2003). "A unique pattern of slep structure is found to be identical at all cortical sites: a neurobiological interpretation." *Cereb Cortex* 13:1044-50

Merica H and Fortune RD (2004). "State transitions between wake and sleep, and within the ultradian cycle, with focus on the link to neuronal activity" *Sleep Medicine Reviews* 8:473-485

Mormann F, Lehnertz K, David P, and Elger CE (2000). "Mean phase coherence as a measure for phase synchronization and its application to the EEG of epilepsy patients." *Physica D* 144: 359–69

Nikouline VV, Linkenkaer-Hansen K, Huttunen J, Ilmoniemi RJ and (2001). "Interhemispheric phase synchrony and amplitude correlation of spontaneous beta oscillations in human subjects: a magnetoencephalographic study." *Neuroreport* 12(11):2487-91

Ogilvie RD (2001). "The process of falling asleep." *Sleep Medicine Reviews* 5(3):247-270

Press WH, Flannery BP, Teukolsky SA, and Vetterling WT. "Numerical Recipes in C: The Art of Scientific Computing." Cambridge University Press. Cambridge, 1988

Quiroga RQ, Kraskov A, Kreuz T, and Grassberger P (2002). "Performance of different synchronization measures in real data: A case study on electroencephalographic signals." *Physical Review E*, Vol 65, 041903

Rechtschaffen A, Kales A, eds. A Manual of Standardized Terminology, Techniques, and Scoring System for Sleep Stages of Human Subjects. US Department of Health, Education, and Welfare Public Health Service—NIH/NIND; 1968

Singer W (1997). "Time as coding space in neocortical processing: a hypothesis." In: M.S. Gazzaniga, Editor, The Cognitive Neurosciences, MIT Press, Cambridge, MA, pp. 91–104.

Singer W (1999). "Neuronal synchrony: a versatile code for the definition of relations?" *Neuron* 24:49–65, 111–125.

Singer W and Gray CM (1995). “Visual feature integration and the temporal correlation hypothesis” *Annu. Rev. Neurosci.* 18:555–586

Steriade M and Amzica F (1998). “Slow sleep oscillation, rhythmic K-complexes, and their paroxysmal developments.” *J Sleep Res* 7 Suppl 1:30-35

Steriade M, Curró-Dossi R, and Nuñez A (1991). “Network modulation of a slow intrinsic oscillation of cat thalamocortical neurons implicated in sleep delta waves: cortically induced synchronization and brainstem cholinergic suppression.” *J Neurosci* 11(10):3200-2317

Steriade M, Timofeev I, Grenier F (2001). “Natural waking and sleep states: a view from inside neocortical neurons.” *J Neurophysiol* 85(5):1969-1985

Tass P, Rosenblum M, Weule J, Kurths J,. Pikovsky A, Volkmann J, Schnitzler A, and Freund H (1998). “Detection of n:m phase locking from noisy data: Application to magnetoencephalography.” *Phys. Rev. Lett.* 81:3291-3294.

Timofeev I and Steriade M (1996). “Low-frequency rhythms in the thalamus of intact-cortex and decorticated cats.” *J Neurophysiol* 76:4152–4168

van Putten MJA (2003). “Nearest Neighbor Phase Synchronization as a Measure to Detect Seizure Activity from Scalp EEG Recordings.” *Journal of Clinical Neurophysiology* 20(5):320–325.

von der Malsburg (1994). “The correlation theory of brain function.” In: Domany E, van Hemmen JL and Schulten K, editors. Models of neural networks II. Berlin: Springer. p 95--119.

Von Gizycki (2008). “Hippocampal-Neocortical phase and amplitude synchrony changes precede seizure events in freely behaving rats.” *Submitted*

Weiss S, Rappelsberger P. (2000) Long-range EEG synchronization during word encoding correlates with successful memory performance. Cognitive Brain Research 9: 299–312

References for Study 3

Achermann P and Borbély AA (1997). "Low-frequency (<1 Hz) oscillations in the human sleep electroencephalogram." *Neuroscience* 81(1):213-222

Achermann P and Borbély AA (1998). "Coherence analysis of the human sleep electroencephalogram." *Neuroscience* 85(4):1195-1208

Alloway CE, Ogilvie RD, Shapiro CM (1999). "EEG spectral analysis of the sleep-onset period in narcoleptics and normal sleepers." *Sleep* 22(2):191-203.

American Academy of Sleep Medicine (2005). ICSD-2-International Classification of Sleep Disorders, 2nd edn. Diagnostic and Coding Manual. Westchester, IL; 2005.

Arand D, Bonnet M, Hurwitz T, Mitler M, Rosa R, and Sangal RB (2005). "The clinical use of the MSLT and MWT." *Sleep* 28(1):123-44. Review.

Billiard M, Bassetti C, Dauvilliers Y, et al (2006). "EFNS guidelines on management of narcolepsy." *European Journal of Neurology* 13:1035–1048.

Bruns A, Eckhorn R, Jokeit H, and Ebner A (2000). "Amplitude envelope correlation detects coupling among incoherent brain signals." *Neuroreport* 11(7):1509-14.

Chase MH and Morales FR (1983). "Subthreshold excitatory activity and motoneuron discharge during REM periods of active sleep." *Science* 221:1195-98

Corsi-Cabrera M, Guevara MA, Arce C, and Ramos J (1996). "Inter and intrahemispheric EEG correlation as a function of sleep cycles." *Prog Neuropsychopharmacol Biol Psychiatry* 20:387–405

Dauvilliers Y, Arnulf I and Mignot E (2007). "Narcolepsy with cataplexy." *Lancet* 369:499–511.

De Gennaro L, Ferrara M, Curcio G, and Cristiani R (2001). "Antero-posterior EEG changes during the wakefulness-sleep transition." *Clinical Neurophysiology* 112:1901-1911

Destexhe A, Contreras D, and Steriade M (1999). "Spatiotemporal analysis of local field potentials and unit discharges in cat cerebral cortex during natural wake and sleep states." *J Neurosci* 19(11):4595-4608

Farmer SF, Bremner FD, Halliday DM, Rosenberg JR, and Stephens JA (1993). "The frequency content of common synaptic inputs to motoneurones studied during voluntary isometric contraction in man." *Journal of Physiology* 470:127-155

Gray CM, Konig P, Engel AK, and Singer AK (1989). "Oscillatory responses in cat visual cortex exhibit inter-columnar synchronization which reflects global stimulus properties." *Nature* 338: 334–337.

Gray CM. (1999) "The temporal correlation hypothesis of visual feature integration: still alive and well." *Neuron* 24: 31–47, 111–125.

Hori T, Hayashi M, and Morikawa T (1994). "Topographic EEG changes and the hypnagogic experience." In: Ogilvie RD, Harsh JR (eds). *Sleep Onset: Normal and Abnormal Processes*. Washington: American Psychological Association 1994

Hori T, Tanaka H, Hayashi M (1998). "Topographic mapping of EEG spectral power and coherence in the hypnagogic period" *Brain Topography Today* Proceedings of the III Pan-Pacific Conference on Brain Topography 1998:303-308

Hughes SW and Crunelli V (2007). "Just a phase they're going through: The complex interaction of intrinsic high-threshold bursting and gap junctions in the generation of thalamic α and θ rhythms." *International Journal of Psychophysiology* 64:3-7

Litt B and Echauz J (2002). "Prediction of epileptic seizures." *Lancet Neurology* 1: 22–30

Longstreth WT Jr, Koepsell TD, Ton TG, et al (2007). "The epidemiology of narcolepsy." *Sleep* 30:13–26.

Merica H and Fortune RD (2003). "A unique pattern of slep structure is found to be identical at all cortical sites: a neurobiological interpretation." *Cereb Cortex* 13:1044-50

Merica H and Fortune RD (2004). "State transitions between wake and sleep, and within the ultradian cycle, with focus on the link to neuronal activity" *Sleep Medicine Reviews* 8:473-485

Mileykovskiy BY, Kiyashchenko LI and Siegel JM (2005). "Behavioral correlates of activity in identified hypocretin/orexin neurons." *Neuron* 46:787-98.

Mormann F, Lehnertz K, David P, and Elger CE (2000). "Mean phase coherence as a measure for phase synchronization and its application to the EEG of epilepsy patients." *Physica D* 144: 359–69

Nikouline VV, Linkenkaer-Hansen K, Huttunen J, Ilmoniemi RJ and (2001). "Interhemispheric phase synchrony and amplitude correlation of spontaneous beta oscillations in human subjects: a magnetoencephalographic study." *Neuroreport* 12(11):2487-91

Ogilvie RD (2001). "The process of falling asleep." *Sleep Medicine Reviews* 5(3):247-270

Press WH, Flannery BP, Teukolsky SA, and Vetterling WT. "Numerical Recipes in C: The Art of Scientific Computing." Cambridge University Press. Cambridge, 1988

Quiroga RQ, Kraskov A, Kreuz T, and Grassberger P (2002). "Performance of different synchronization measures in real data: A case study on electroencephalographic signals." *Physical Review E*, Vol 65, 041903

Rechtschaffen A, Kales A, eds. A Manual of Standardized Terminology, Techniques, and Scoring System for Sleep Stages of Human Subjects. US Department of Health, Education, and Welfare Public Health Service—NIH/NIND; 1968

Robinson DM and Keating GM (2007). "Sodium oxybate: a review of its use in the management of narcolepsy." *CNS Drugs* 21:337–354.

Singer W (1997). "Time as coding space in neocortical processing: a hypothesis." In: M.S. Gazzaniga, Editor, The Cognitive Neurosciences, MIT Press, Cambridge, MA, pp. 91–104.

Singer W (1999). "Neuronal synchrony: a versatile code for the definition of relations?" *Neuron* 24:49–65, 111–125.

Singer W and Gray CM (1995). "Visual feature integration and the temporal correlation hypothesis" *Annu. Rev. Neurosci.* 18:555–586

Steriade M and Amzica F (1998). "Slow sleep oscillation, rhythmic K-complexes, and their paroxysmal developments." *J Sleep Res* 7 Suppl 1:30-35

Steriade M, Curró-Dossi R, and Nuñez A (1991). "Network modulation of a slow intrinsic oscillation of cat thalamocortical neurons implicated in sleep delta waves: cortically induced synchronization and brainstem cholinergic suppression." *J Neurosci* 11(10):3200-2317

Steriade M, Timofeev I, Grenier F (2001). "Natural waking and sleep states: a view from inside neocortical neurons." *J Neurophysiol* 85(5):1969-1985

Tass P, Rosenblum M, Weule J, Kurths J,. Pikovsky A, Volkmann J, Schnitzler A, and Freund H (1998). "Detection of n:m phase locking from noisy data: Application to magnetoencephalography." *Phys. Rev. Lett.* 81:3291-3294.

Timofeev I and Steriade M (1996). "Low-frequency rhythms in the thalamus of intact-cortex and decorticated cats." *J Neurophysiol* 76:4152–4168

van Putten MJA (2003). “Nearest Neighbor Phase Synchronization as a Measure to Detect Seizure Activity from Scalp EEG Recordings.” *Journal of Clinical Neurophysiology* 20(5):320–325.

von der Malsburg (1994). “The correlation theory of brain function.” In: Domany E, van Hemmen JL and Schulten K, editors. Models of neural networks II. Berlin: Springer. p 95--119.

von Gizycki (2008). “Hippocampal-Neocortical phaes and amplitude synchrony changes precede seizure events in freely behaving rats.” *Submitted*

Weiss S, Rappelsberger P. (2000) Long-range EEG synchronization during word encoding correlates with successful memory performance. Cognitive Brain Research 9: 299–312.